Brain Infiltration of Leukocytes Contributes to the Pathophysiology of Temporal Lobe Epilepsy

Dissertation

zur

Erlangung der naturwissenschaftlichen Doktorwürde
(Dr. sc. nat.)

vorgelegt der

Mathematisch-naturwissenschaftlichen Fakultät

der

Universität Zürich

von

Michela Zattoni

aus
Italien

Promotionskomitee

Prof. Dr. Jean-Marc Fritschy (Vorsitz)
Prof. Dr. Karl Frei
Prof. Dr. François Verrey

Zürich, 2010

Table of contents

ZUSAMMENFASSUNG

Temporallappen-Epilepsie (TLE) ist eine chronische neurologische Erkrankung mit einer weltweit globalen Inzidenz von 0,5-2%. Trotz zahlreicher Studien über funktionelle und morphologische Veränderungen, die in TLE auftreten, bleiben die pathophysiologischen Vorgänge dieser Erkrankung weitgehend unbekannt. In den letzten Jahren entstand ein Paradigmenwechsel auf Grund experimenteller und klinischer Evidenz, dass entzündliche Prozesse direkt zur Pathogenese der TLE beitragen. Das Ziel der vorliegenden Arbeit basiert auf Befunden von unserem Labor, dass mehrere pro-inflammatorische Mediatoren sowohl im Hirngewebe als auch in mikrovaskulären Endothelzellen von Patienten mit therapie-resistenter Epilepsie hochreguliert sind, und dass $CD45^+$ Immunzellen in das epileptische Hirngewebe eindringen können. Um die Bedeutung dieser Beobachtungen zu entschlüsseln, habe ich an einem experimentellen Modell der fokalen Epilepsie untersucht, ob Wechselwirkungen zwischen angeborener („innate“) und erworbener („adaptive“) Immunität der Neurodegeneration und Epileptogenese im Hippocampus zugrunde liegen. Obwohl mehrere Tiermodelle der TLE zur Verfügung stehen, sind die meisten mit generalisierten Anfällen und bilateralen Läsionen gekennzeichnet, wie zum Beispiel dem "Pilocarpin-Modell" der Ratte. Um diese wesentliche Unterschiede zur Pathologie der TLE zu überwinden, wurde ein Maus-Modell entwickelt, in dem ein epileptischer Fokus durch eine einseitige Injektion einer niedrigen Dosis von Kainatsäure (KA) in den dorsalen Hippocampus von adulten Mäusen ausgelöst wird. Der epileptische Herd entwickelt sich schrittweise in diesem Modell, einhergehend mit einer ausgeprägten Neurodegeneration im CA1 Bereich und eine starke Dispersion der Körnerzellen im Gyrus dentatus. Nach einer Latenzphase von etwa 2 Wochen treten chronisch wiederkehrende epileptische Anfälle auf, die mittels implantierten EEG-Elektroden registriert werden können. Um den direkten Vergleich mit mutierten, immungeschwächten Mäusen zu ermöglichen, habe ich diese Ergebnisse zunächst in C57BL/6J Mäusen repliziert. Darüber hinaus konnte ich zeigen, dass die KA-induzierte Läsion im dorsalen Hippocampus eine dauerhafte Aktivierung von $CD68^+$ Mikroglia-Zellen verursachte. Die regionale Verteilung dieser Zellen spiegelte genau das Muster der Neurodegeneration wieder. Mittels weiterer immunhistochemischer Analysen konnte ich eine graduelle Akkumulation von $CD3^+$ T-Lymphozyten im epileptischen Hippocampus feststellen, die mit dem Beginn der chronischen Anfälle zusammenfielen. Diese Ergebnisse zeigten folglich, dass mehrere Komponenten der erworbenen und angeborenen Immunität in diesem TLE Modell aktiviert werden, mit spezifischen räumlich-zeitlichen Mustern während der Epileptogenese.

Um kausale Zusammenhänge zwischen diesen Phänomenen zu ermitteln, habe ich die Auswirkungen der KA-Injektion in RAG1-Knockout (KO) Mäusen, welche keine B-und T-Zellen produzieren können, untersucht. Auffallend war, dass das Fehlen der adaptiven Immunität die langfristige Degeneration und Mikroglia-Aktivierung im epileptischen Hippocampus deutlich verstärkte, aufgrund der Infiltration von Gr-1^+ neutrophilen Granulozyten in das verletzte Gewebe. Ferner zeigte eine Doppel-Immunfluoreszenz-Analyse, dass Mikrogliazellen diese Neutrophilen umgeben und einhüllen, was auf Phagozytose im entzündeten Gewebe hinweist. Demzufolge sind Mikroglia-Zellen möglicherweise schützend durch die Bekämpfung der Neutrophilen-Invasion in RAG1-KO-Mäusen. Zusammenfassend zeigen diese Resultate, dass die Integrität der erworbenen Immunität entscheidend ist für die Begrenzung der Neurodegeneration in einem KA-induzierten epileptischen Fokus. In der Tat war eine Depletion der neutrophilen Granulozyten in der Peripherie durch systemische Behandlung mit anti-Gr-1 monoklonalen Antikörpern ausreichend, um die verstärkte Neurodegeneration in RAG1-KO-Mäusen zu verhindern, wohingegen die selbe Behandlung in Wildtyp-Mäusen keine Auswirkungen auf die KA-Läsion hatte.

Mittels Immunhistochemie und eines Antikörpers gegen F4/80, einem Marker für Makrophagen/Mikroglia, habe ich in beiden Genotypen das Auftreten von großen, Makrophagen-ähnlichen Zellen nach der KA-Injektion beobachtet, selektiv in der molekularen Schicht des Gyrus dentatus. Um zu ermitteln, ob diese Zellen aus dem hämatopoetischen und lymphoiden System stammen, und um ihre Funktion zu untersuchen, habe ich zwei therapeutische Eingriffe angewandt: (1) Verhinderung des Eintritts von mononukleären Zellen aus dem Blut in das Gehirn durch die Behandlung mit monoklonalen anti-α_4 Integrin Antikörpern, (2) Elimination von peripheren Monozyten/Makrophagen durch die Behandlung mit Clodronat-Liposomen. Beide Eingriffe verringerten deutlich die Zahl von Makrophagen im Gyrus dentatus; sie zeigten aber unerwarteter Weise, dass das Überleben und die Dispersion der Körnerzellen beeinträchtigt waren. Diese Befunde zeigen, dass eindringende periphere Makrophagen eine neurotrophische Funktion an Körnerzellen ausüben. Überraschenderweise reduzierten beide Behandlungen ebenfalls die Granulozyten Infiltration in den epileptischen Herd bei RAG1-KO-Mäusen. Folglich war die Neurodegeneration drastisch reduziert, was das Resultat der Anti-Gr-1-Behandlung bestätigte.

Danach habe ich die funktionelle Bedeutung der Leukozyten-Infiltration mittels EEG-Analyse untersucht. EEG Ableitungen wurden mit chronisch-implantierten Elektroden in KA-behandelten Mäusen registriert und ausgewertet. Verschiedene Linien von immundefizienten Mäusen einschließlich RAG1-KO, RAG2-KO, β2-microglobulin-KO

(keine $CD8^+$ Zellen) und MHC II-KO (keine $CD4^+$ Zellen) wurden untersucht um die Beteiligung von $CD4^+$ und $CD8^+$ Zellen an der Epileptogenese zu charakterisieren. Schon am zweiten Tag nach der KA-Injektion wurden charakteristische epileptische Anfälle in allen mutanten Genotypen nachgewiesen, was auf eine dramatische Verkürzung der latenten Phase hinweist. Zudem waren die Frequenz und der Zeitpunkt des Beginns der Anfälle unabhängig vom Schweregrad der KA-induzierte Läsion. Dennoch wies die Mehrheit der MHC II-KO-Mäusen keine wiederkehrenden Anfälle bis 16 Tage nach der KA-Injektion auf, trotz der Entstehung einer typischen Läsion. Folglich löst das Fehlen von T-Zellen einen frühzeitigen Anfallbeginn aus, was darauf hinweist, dass keine synaptische Reorganisation im verletzten Hippocampus für das Auftreten von hippocampal paroxysmalen Entladungen notwendig ist.

Abschliessend, um besser zu verstehen welche löslichen Faktoren (Zytokine und Chemokine) für die Infiltration von Leukozyten und Makrophagen in den KA-injizierten Hippocampus, wie auch Neutrophile im RAG1-KO-Mäusen, verantwortlich sind, habe ich das Luminex 100-System verwendet und den Zytokin und Chemokin Spiegel im dorsalen Hippocampus von Kontrol- und KA-behandelten Wildtyp und RAG1-KO-Mäusen bestimmt. Obwohl die Luminex xMAP-Technologie sehr empfindlich ist und die Detektion von mehreren Analyten in einer einzigen Probe ermöglicht, erwies sich dieser biochemischen Ansatz als wenig geeignet in meinen Experimenten und brachte nur begrenzten Einblick in die Rolle von Zytokinen, welche an den verschiedenen pathologischen Veränderungen in diesem TLE-Modell beteiligt sind.

Insgesamt unterstreichen diese Resultate eine bedeutende Rolle der angeborenen und adaptiven Immunzellen im KA-Mausmodell der TLE für die Steuerung der Epileptogenese und der Neurodegeneration. Wider Erwarten erbringt die Aktivierung der angeborenen Immunantwort trophischen Support durch Makrophagen und Schutz gegen die Neutrophilen-Invasion durch Mikrogliazellen. Darüber hinaus schränkt das Fehlen von T-Zellen die epileptische latente Phase massgebend ein und führt zu Neutrophil-vermittelter Neurodegeneration in immungeschwächten Mäusen. Demzufolge scheint eine koordinierte Regulierung des Immunsystems in verschiedenen Entwicklungsstadien eines epileptischen Fokus der Pathophysiologie des TLE zu unterliegen. Aus therapeutischer Sicht bedeuten diese Ergebnisse, dass Behandlungsstrategien der TLE darauf hinzielen sollten, schützende immunomodulierende Wirkungen durch gezielte Regulierung der Immunantworten zu unterstützen.

SUMMARY

Temporal lobe epilepsy (TLE) is a chronic neurological disorder with a world-wide global incidence of 0.5-2%. Despite the wealth of studies on the functional and morphological alterations occurring in TLE, the pathophysiology of this disorder remains poorly understood. A paradigm shift was introduced by recent experimental and clinical data suggesting that inflammation directly contributes to the pathogenesis of epilepsy. The aim of this project is based on our own observations that several pro-inflammatory genes are upregulated both in brain tissue and microvascular endothelial cells obtained from patients with intractable TLE, and that $CD45^+$ leukocytes can infiltrate the epileptic brain parenchyma. To understand the relevance of these findings, we investigated whether interactions between innate and adaptive immunity underlie neurodegeneration of the hippocampal formation and epileptogenesis in an experimental model of focal epilepsy. While several animal models of TLE are available, they often present with bilateral lesions underlying generalized seizures, as seen in the "pilocarpine model", for instance.

To overcome these major differences with the human pathology, a mouse model has been developed, based on a unilateral injection of a low dose kainic acid (KA) into the dorsal hippocampus of adult mice. In this model, an epileptic focus develops gradually, accompanied by severe degeneration of the CA1 region and a pronounced dispersion of granule cells in the dentate gyrus. Chronic recurrent seizures appear after a latent phase of about two weeks. Here, we first replicated these findings in C57BL/6J mice to provide a baseline for comparison with mutant, immunodeficient mice. The KA-induced lesion in the dorsal hippocampus caused enduring activation of $CD68^+$ microglial cells that mirrored precisely the pattern of neurodegeneration. Furthermore, immunohistochemical analysis revealed a gradual accumulation of $CD3^+$ T cells in the epileptic hippocampus, with a plateau coinciding with the onset of recurrent seizures, as determined by EEG recordings. These results revealed that multiple components of acquired and innate immunity are activated in this model of TLE, with specific spatio-temporal patterns during epileptogenesis.

To establish causal relationships between these phenomena, we next investigated the effects of KA injection in RAG1-knockout (KO) mice, lacking B and T cells. Strikingly, the absence of adaptive immunity markedly aggravated long-term degeneration and microglia activation in the epileptic hippocampus, due to infiltration of $Gr\text{-}1^+$ neutrophils in the lesioned tissue. Moreover, double immunofluorescence analysis revealed that

microglial cells surround neutrophils and engulf them, suggesting phagocytosis in the inflamed tissue. Therefore, microglial cells might be protective by fighting the neutrophil invasion in RAG1-KO mice. Taken together, these results demonstrated that the integrity of adaptive immunity is crucial for limiting neurodegeneration in a KA-induced epileptic focus. Indeed, depleting neutrophils in the periphery by systemic treatment with anti-Gr-1 monoclonal antibodies was sufficient to prevent the aggravated neurodegeneration in RAG1-KO mice, whereas the same treatment in wild-type mice had no effect on the KA-induced lesion.

Using an antibody against F4/80, a marker of macrophage/microglia, we observed in both genotypes the appearance of large, macrophage-like, cells selectively in molecular layer of the dentate gyrus after KA injection. To determine whether these cells arise from the hematopoietic and lymphoid system and to investigate their role we used two therapeutic interventions: (1) preventing entry of blood mononuclear cells into the brain (anti-α_4 integrin monoclonal antibodies); (2) depletion of peripheral monocytes/ macrophages (clodronate liposomes). Both treatments markedly reduced macrophages in the dentate gyrus; unexpectedly, they were deleterious for granule cell survival and dispersion, suggesting that peripheral macrophages invading the brain provide neurotrophic support. Surprisingly, both treatments interfered with neutrophil recruitment in RAG1-KO mice as well. As a result, neurodegeneration was strongly reduced confirming the effects of the anti-Gr-1 treatment.

Next, the functional relevance of leukocyte infiltration was evaluated by EEG analysis using chronically implanted electrodes in KA-treated mice. To distinguish the role of $CD4^+$ and $CD8^+$ cells, various lines of immunodeficient mice were investigated, including RAG1-KO, RAG2-KO, β2-microglobulin-KO (lacking $CD8^+$ cells), and MHC II-KO (lacking $CD4^+$ cells) mice. In all genotypes, characteristic hippocampal paroxysmal discharges were detected already at day 2 post-KA, indicating a dramatic shortening of the latent phase. Moreover, in any given genotype, the frequency and time of onset of seizures did not depend on the severity of the KA-induced lesion. However, the majority of MHC II-KO mice did not exhibit any recurrent seizures, at least up to 16 days post-KA, despite formation of a typical lesion. Therefore, absence of T cells can trigger rapid seizure onset, suggesting that synaptic reorganization in the lesioned hippocampus is not necessary for the occurrence of hippocampal paroxysmal discharges.

Finally, to better understand which soluble factors (chemokines and cytokines) might be responsible for the infiltration of lymphocytes into the KA-injected hippocampus, as well

as neutrophils in RAG1-KO mice, we employed the Luminex 100 platform and determined the cytokine/chemokine protein level in the lesioned and control dorsal hippocampus of wild-type and RAG1-KO mice. Despite the fact that the Luminex xMap technology is very sensitive and allows detection of multiple analytes in a single sample, this biochemical approach proved limited in our experiments and provided little insight into the role of cytokines in the differential pathological changes observed in this TLE model.

Taken together, the present results underscore the preeminent role played by innate and adaptive immunity in the KA mouse model of epilepsy for the control of epileptogenesis and neurodegeneration. Against expectations, activation of innate immune responses provides trophic support by macrophages and microglial cell-mediated protection against neutrophils. Furthermore, absence of T cells curtails the latent phase of epileptogenesis and leads to neutrophil-mediated neurodegeneration in immunodeficient mice. Therefore, concerted regulation of immune responses at different stages of development of an epileptic focus likely underlies the pathophysiology of TLE. From a therapeutic perspective, these findings imply that treatment strategies should aim to support the beneficial effects produced by this concerted regulation of the immune system.

Introduction

Epilepsy is a chronic neurological disorder that affects people of all ages with a global incidence of 0.5-2% (around 50 million people worldwide have epilepsy) demanding a very high priority among central nervous system (CNS) diseases (Browne and Holmes, 2001). It results from an imbalance between neuronal excitation and inhibition, giving rise to clinical manifestations of abnormally hyper-synchronized, rhythmic neuronal discharges (Colmers and El Bahh, 2003). Epilepsy is a chronic and progressive brain disorder, characterized by the periodic and unpredictable occurrence of seizures. A seizure is a stereotyped episode, with a defined start and finish, involving altered sensory, motor, autonomic function, consciousness, and due to abnormal electrical discharge in the brain. Some seizures result from an acute insult, such as head trauma. Others result from metabolic derangements or structural abnormalities, such as tumors. However, the majority of seizures have no clear etiology, yet.

Epilepsies can be classified in many different ways:

- By etiology (first cause)
- By semiology (the observable manifestations of the seizures)
- By the location in the brain where the seizures originate.
- As a part of discrete, identifiable medical syndromes.
- By the event that triggers the seizures, as in primary reading epilepsy or musicogenic epilepsy.

Based on etiology, epilepsies can be classified in three groups. 1) Idiopathic: with a genetic predisposition but without a known CNS damage. 2) Symptomatic (structural/metabolic) caused by a known disorder of the CNS including preceding brain damage through tumor, trauma, or trough drugs of abuse and endotoxins. 3) cryptogenic: where the cause remains elusive. Nevertheless, the boundaries between these forms are not strict and sometimes difficult to define.

The “International Classification of Seizures” (1993) divides seizures into two groups:

- “partial” seizures that start focally; they are subclassified as simple partial seizures, which involve no alteration in cognitive state, and complex seizures, which are associated with loss of consciousness or memory.

- “generalized” seizures that begin in widespread regions of the brain and are further divided into absence (“petit mal”), tonic-clonic (“grand mal”), atonic (drop seizures), myoclonic (brief jerks), and a few less common types.

Among the various different kinds of epilepsy, temporal lobe epilepsies are a group of disorders in which humans and animals experience recurrent epileptic seizures arising from one or both temporal lobes of the brain. Two main types are internationally recognized:

Mesial temporal lobe epilepsy (MTLE) arises in the hippocampus, parahippocampal gyrus and amygdala which are located in the inner aspect of the temporal lobe.

Lateral temporal lobe epilepsy (LTLE) arises in the neocortex on the outer surface of the temporal lobe of the brain.

Because of strong neuronal interconnections, seizures beginning in either the medial or lateral areas of the temporal lobe often involve neighboring areas of the brain. The causes or etiology of different TLEs vary.

Typically, patients who develop MTLE have experienced a febrile seizure during early childhood. Histological analysis of surgical specimens from patients with MTLE have revealed common occurrence of hippocampal sclerosis (HS) (Loup et al., 2000) and focal lesion. HS is characterized by a selective neuronal cell loss and extensive astrogliosis in the cornu ammonis (CA) region 1 (CA1) and in the hilus of the dentate gyrus, occasional dispersion of the granule cell layer as well as mossy fiber sprouting, a mode of synaptic reorganization leading to abnormal recurrent circuits in the dentate gyrus (Thom, 2004). In contrast to CA1, neuronal loss in the CA3 area is variable and sometimes negligible.

Despite considerable progress in understanding the pathogenesis of seizures and epilepsy, for many seizure types and epilepsy syndromes we still have little information about their pathophysiological basis (Loscher, 2002). In the absence of a specific etiological understanding, approaches to drug therapy of epilepsy must necessarily be directed at the control of symptoms, i.e., the suppression of seizures. Chronic administration of antiepileptic (anticonvulsant) drugs (AEDs) is

the treatment of choice in epilepsy. The selection of an AED is based mainly on its efficacy for specific types of seizures, tolerability, and safety. The goal of therapy is to keep the patient free of seizures without interfering with normal brain function. However, although the prognosis for seizures control is good in at least 60% of patients, up to 40% of individuals suffer from intractable pharmacoresistant epilepsy. Although the terms "pharmacoresistant" or "medically refractory" lack a precise definition, most clinicians would consider an epilepsy pharmacoresistant when it is not controlled by any of two to three first-line AEDs (notably carbamazepine, oxcarbamazepine, and phenytoin), alone or in combination with a second-line drug.

In MTLE, 49-80% of adult and 67-90% of juvenile patients have incomplete seizure control, and 65-80% of these become seizure-free after surgical resection of the epileptic focus by selective amygdalohippocampectomy (sAHE) (Deckers et al., 2003). Amygalohippocampectomy is indicated when the focal point of the seizures can be localized anatomo-functionally to the hippocampus and amygdala, and the contralateral hippocampal formation is not affected, for preserving memory functions upon resection of the epileptic focus. In addition, to be considered for this procedure, one must have failed all first-line treatments.

The main obstacle for developing new strategies for treatment of pharmacoresistant epilepsy is that mechanisms of pharmacoresistance and pathogenesis are only poorly understood. Some clinical features are associated with resistance, including early onset of seizures (before 1 year of age), high seizure frequency prior the onset of treatment, a history of febrile seizures, the type of seizure or epilepsy, structural brain lesions, and malformation of cortical lamination. The mechanisms of drug resistance in epilepsy are undoubtedly multifactorial, and, at least in part, dependent on genetic polymorphisms. The latter factor probably plays a key role in two currently favored resistance mechanisms, the 'target' and the 'transporter' hypotheses (Sisodiya, 2003). Additional genetic and epigenetic factors may be important to explain why patients with the same type of epilepsy or seizures may differ in their response to AEDs.

Other mechanisms contributing to pharmacoresistance and pathogenesis to be considered include inflammatory processes and dysfunctions of the blood-brain barrier (BBB) (Soranzo et al., 2005). The integrity of the BBB is essential to protect the brain, notably from entry of immunocompetent cells and antibodies. The highly specialized tight endothelium of brain microvessels isolates the CNS from immune surveillance and allows only a few mononuclear cells to migrate into the brain parenchyma (Silverman et al., 2000). When inflammation does occur, there is extensive leukocyte migration into the brain. The vascular endothelium forming the BBB plays an active role in the mediation of this neuroimmune response, either by the production of inflammatory mediators (cytokines) or by expression of adhesion molecules. This response potentially links intravascular inflammatory events to pro-epileptogenic events in the brain. In addition, in intractable MTLE, glial cells are thought to play an important contribution to hippocampal hyper-excitability. For instance, astrocytes may influence excitability through altered water homeostasis and K^+-buffering by redistribution of aquaporin-4 on their plasma membrane. In this way, they contribute to a high extracellular glutamate level, which in turn enhances excitatory neurotransmission and further Ca^{2+}-dependent glutamate release. Furthermore, such a focal pool of glutamate may diffuse to surrounding neuron-rich areas, generating seizure activity in TLE (de Lanerolle and Lee, 2005).

Evidence of inflammatory processes in the clinical manifestations and neuropathological consequences of epilepsy has accumulated in the past 10 years (Vezzani et al., 2002; Vezzani, 2004). For instance, Vezzani et al. showed that manipulation of pro- and anti-inflammatory cytokines can modify the outcome, as well as the neuropathological sequelae, of experimentally induced seizures (Vezzani et al., 2002).

Ravizza et al. (Ravizza et al., 2008) demonstrated that IL-1-dependent inflammatory pathways are chronically activated during epileptogenesis. These authors could demonstrate that microglial cells and astrocytes are the main source of IL-1β, whereas IL-1R is expressed by neurons. Other studies reported that IL-1β and IL-1R are rapidly up-regulated in brain following seizures (Jankowsky and Patterson, 2001; Vezzani and Granata, 2005; Ravizza and Vezzani,

2006). It has been shown that BBB permeability, neuronal cell loss and increased neuronal excitability are influenced by activation of IL-1β/IL-1R system (Ravizza et al., 2008).

In addition, the study by Fabene et al. (Fabene et al., 2008) established that brain inflammation and BBB disruption are key triggers of seizures in a mouse model of status epilepticus (SE), based on systemic administration of pilocarpine. Recent data support the concept that intravascular and CNS inflammation are pro-epileptogenic. Moreover, Marchi et al. demonstrated that BBB damage can directly cause seizures (Marchi et al., 2007b). Shedding light on the mechanisms by which BBB leakage may occur in TLE, Fabene et al. (Fabene et al., 2008) demonstrated that leukocyte-endothelial cell interactions are altered by seizures and, in turn, contribute to BBB leakage, seizure pathogenesis, and chronic epilepsy. This seminal study supports previous findings (Marchi et al., 2007b) showing that microvasculature modification induced by SE and leading to BBB breakdown, significantly contribute to hyperexcitability underlying spontaneous seizures.

Key concepts in Neuroimmunity

The CNS has long been considered as an immuno-privileged site because of the presence of the BBB, graft acceptance, lack of conventional lymphatic drainage, and an apparently low level of leukocyte trafficking. This dogma began to break down with the realization that immune cell infiltration into the CNS may be more common than previously believed. Indeed, the immune system and the nervous system both are remarkable ensembles that are at once sensors of impeding danger and responders to those dangers. Many acute diseases of the CNS, such as stroke, brain tumors, or traumatic injury typically are accompanied by disruption of the BBB, promoting extensive interactions between the brain and the immune system. Furthermore, immune surveillance and inflammatory reaction are activated in the brain in various neurodegenerative diseases, including multiple sclerosis, Alzheimer's and Parkinson's diseases, as well as in epilepsy. Diverse fields of research show convincing results regarding the bidirectional

communication between the nervous and immune systems. The neural-immune cross-talk may even occur in non-disease condition.

It is more appropriate to define the CNS as an immunologically specialized site (Ransohoff et al., 2003), because it is becoming evident that immune and inflammatory reactions occur in the CNS. The origin of immune cells in the brain could be either intrinsically, thus constituting part of the innate immunity, or in the periphery and through specific soluble factors like cytokines/chemokines imported by immuno-competent cells into the CNS (adaptive immunity) (Vezzani and Granata, 2005). These two components involve many molecules that are known to have dual roles in the immune system and in normal brain physiology.

Adaptive and innate immunity

The adaptive immune system is composed of highly specialized cells that comprise: i) antigen presenting cells (APC); ii) T-lymphocytes and iii) B-lymphocytes. It relies on the capacity of immune cells to distinguish between the body's own cells and unwanted invaders. The host's cells express "self" antigens. These antigens are different from those on the surface of bacteria ("non-self" antigens) or on the surface of virally-infected host cells (“missing-self”). The adaptive response is triggered by recognizing non-self and missing-self antigens. With the exception of non-nucleated cells, all cells are capable of presenting antigens and of activating the adaptive response. Some cells are specially equipped to present antigens, and to prime naive T cells. Several T cells subgroups can be activated by professional antigen presenting cells (dendritic cells), and each type of T cell is specially equipped to deal with each unique toxin or bacterial and viral pathogens.

The vertebrate immune system functions due to the ability of B cells and T cells to recognize antigens and mount the necessary response to neutralize the pathogen. Antigens are recognized in the body through highly specific interactions with the variable immnoglobulin domains on B cells and the T cell receptor region of T cells.

The regulation of gene expression and gene assembly is determined by site-specific recombination process and is fundamental in the life cell cycle of a variety of organisms (Chun et al., 1991). The site-specific recombination system, also known as somatic recombination is a mechanism of genetic recombination that occurs in developing lymphocytes of vertebrates which randomly selects and assembles the variable portions of the genes that encode immunoglobulin and T cell receptor molecules using component V (variable), D (diversity), and J (joining) gene segments. This somatic recombination is largely responsible for generating the highly diverse array of immunoglobulins and T cell receptors that is characteristic of the vertebrate immune system.

The recombination activating proteins RAG -1 and RAG-2 act together as a heterodimer in the initiation of the process of antigen receptor gene segment assembly (Spanopoulou et al., 1995). These proteins are essential for proper formation and function of B cell and T cell receptors. Rag1 and Rag2 genes are fundamental in the V (D) J recombination for the establishment of a functional immune system with diverse antigen receptors. These proteins are active only in the very early stages of lymphoid development as part of the V (D) J recombinase. The RAG complex is responsible for initiating the recombination process.

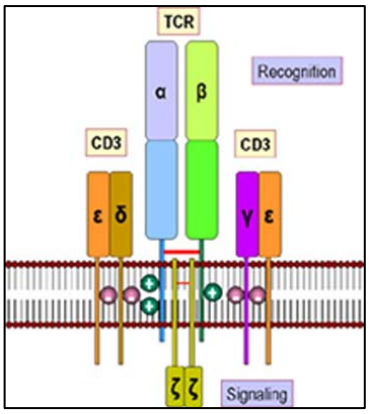

Panel A: *Structure of the T-cell receptor complex (Roitt, Immunology, 7th Ed.)*

Therefore, T cells can be distinguished by their different antigen receptors. The definitive T-cell lineage marker is the T-cell antigen receptor (TCR). There are two defined types of TCR: one is a heterodimer of two disulphide-linked polypeptides (α and β); the other is structurally similar but consists of γ and δ polypeptides. Both receptors are associated with a set of 5 polypeptides, the CD3 complex, and together form the T-cell receptor complex (panel A). Approximately 90-95% of blood T cells are αβ T cells and the remaining 5-10% is γδ T cells. Aβ T cells are further distinguished in two distinct non-overlapping populations; a subset carrying the CD4 marker, which mainly “helps”

immune response (T helper cells), and a subset carrying the CD8 marker and being predominantly cytotoxic T cell (CTL).

$CD4^+$ T cells recognize their specific antigens in association with major histocompatibility complex (MHC) class II molecules, whereas $CD8^+$ cells recognize antigens in association with MHC class I (panel B). MHC class I molecules are found on every nucleated cell of the body and consist of two polypeptide chains, α and β2-microglobulin. The two chains are associated non-covalently. Only the α chain is polymorphic and encoded by MHC gene, while β2-microglobulin is not polymorphic and is encoded by other genes. The transmembrane α3 chain is where CD8 binds. The α1 and α2 domains fold to make up a groove for peptides to bind. MHC class II molecules are found only on a few specialized cell types, including macrophages, dendritic cells, and B cells, all of which are professional antigen-presenting cells (APCs). Like MHC class I molecules, MHC class II molecules also are heterodimers, but in this case consist of two homologous peptides, an α and β chain, both of which are encoded in the MHC gene.

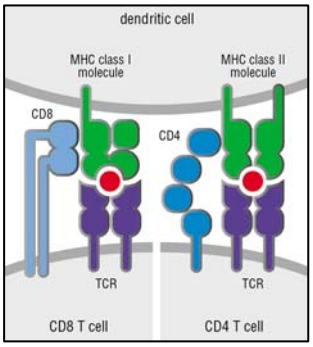

Panel B: *Structure of MHC class I and II (Roitt, Immunology, 6th Ed.)*

About 5-15% of the circulating lymphoid pool are B cells defined by the presence of surface immunoglobulins (mainly IgM and IgG). These are constitutively produced and are inserted into the plasma membrane, where they act as specific antigen receptor. The majority of B cells carry MHC class II antigens, which are important for cooperative interactions with T cells. B cells are lymphocytes that play a large role in the humoral immune response (as opposed to the cell-mediated immune response, which is governed by T cells). The principal functions of B cells are to make antibodies against antigens, perform the role of APCs, and eventually develop into memory B cells after activation by antigen interaction. B cells are an essential component of the adaptive immune system. Every day, the human body makes millions of different types of B cells that circulate in the blood and lymphatic system performing the role of immune surveillance. They do not produce antibodies until they become fully activated. Each B cell has a unique receptor protein (referred to as the B cell receptor (BCR)) on its surface that will

bind to one particular antigen. The BCR is a membrane-bound immunoglobulin, and it is this molecule that allows the distinction of B cells from other types of lymphocyte, as well as being the main protein involved in B cell activation. Once a B cell encounters its cognate antigen and receives an additional signal from a T helper cell, it can further differentiate into one of the two types of B cells listed below (plasma B cells and memory B cells). The B cell may either become one of these cell types directly or it may undergo an intermediate differentiation step, the germinal center reaction, where the B cell will hyper mutate the variable region of its immunoglobulin gene ("somatic hyper mutation") and possibly undergo class switching. CD19, CD20, and CD22 are the main markers currently used to identify B cells, together with B220 (in the mouse only).

The innate immune system is characterized by a more rapid response to danger and does not involve antibodies or antigen-specific receptors on T lymphocytes. It is mediated by a variety of cells, and by the soluble molecules which they secrete (see panel C). One important group of leukocytes is the phagocytic cells. Phagocytes belong to two major lineages: monocytes/macrophages and polymorphonuclear granulocytes. The latter have a lobulated, irregularly shaped (polymorphic) nucleus. The polymorphonuclear cell family (PMNs) is subdivided into neutrophils, basophils and eosinophils, on the basis of how their cytoplasmic granules stain with acid and basic dyes. Neutrophils are most abundant type of white blood cells in mammals and form an essential part of the innate immune system. They have a characteristic multilobulated nucleus and are 10-20 μm in diameter. They have a large arsenal of antibiotic proteins stored in two main types of granules. The primary (azurophilic) granules are lysosomes containing hydrolases, myeloperoxidase and muramidase (lysozyme). The secondary (specific) granules contain lactoferrin and lysozyme. Neutrophils undergo a process called chemotaxis, which allows them to migrate toward sites of inflammation or injury. Cell surface receptors allow neutrophils to detect chemical gradients of specific molecules used to direct the path of their migration.

The mononuclear phagocyte system has two main functions, which result from the activities of two different types of bone marrow-derived cells: i) professional

phagocytic macrophages and ii) APCs, whose role is to take up, process and present antigenic peptides to T cells. APCs are, therefore, components of both adaptive and innate immunity. Phagocytic macrophages are found in many organs (e.g., Kupffer cells in the liver, microglia in the brain). The mononuclear phagocyte lineage is derived from bone marrow stem cells, and their function is to engulf particles, including infectious agents. Blood cells belonging to this lineage are called monocytes. In time, they migrate from the blood into various organs, where they develop into tissue macrophages. These cells are very effective in presenting antigens to T lymphocytes.

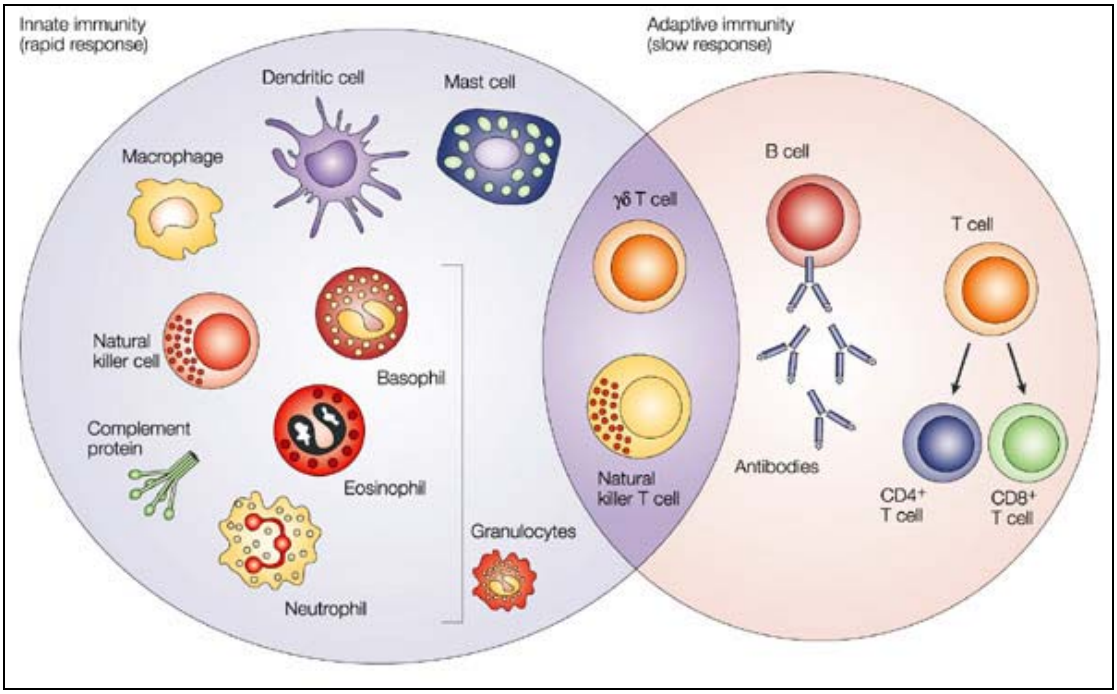

Panel C: *The principal component of the innate and adaptive immunity are shown (Glenn Dranoff, 2004)*

Several populations of macrophages are found in the CNS, some of which are long term residents while others are more transient (Williams and Hickey, 2002). Macrophages of the choroid plexus, macrophages of the meninges, microglia (the resident brain macrophages), and perivascular cells (a CNS resident monocyte-like cells found around small parenchymal vessels, outside of the BBB) belong to the so called monocyte/macrophage population of the CNS. It has been proposed that members of this family regulate T cell responses in the CNS (Aloisi et al., 2000)

and may govern the ability of T cells to enter the neural parenchyma itself (Owens et al., 1998). All the cells mentioned above are of bone marrow origin and therefore share common myeloid markers; however, their biology, surface marker expression, turnover and location within the CNS are different.

The development of appropriate immunological, physiological, and behavioral responses to immune stimulation in the CNS strictly depends on a highly regulated bi-directional communication between the immune system and the CNS. Innate immune cells in the CNS, notably microglia and perivascular macrophages, play integral roles in receiving and propagating inflammatory signals that are initiated at the periphery. In particular, antigen presentation in the CNS has to be considered separately at the level of the BBB and within the CNS parenchyma. At each site, the cells need to express both the requisite MHC and costimulatory molecules for a competent antigen presentation. At the BBB, the perivascular macrophages are implicated as the central APC, whereas in the brain parenchyma, this task is devoted to microglia cells, as well as to dendritic cells (Bulloch et al., 2008), whose presence in healthy brain has been demonstrated recently.

Microglial cells constitute the resident macrophage population of the CNS, therefore named the CNS-specific tissue macrophage. They are of myeloid-monocytic origin and colonize the brain at two different “developmental windows” pre- and perinatally (Kettenmann and Verkhratsky, 2008; Tambuyzer et al., 2009). Therefore, microglial cells are essential components of the innate and adaptive immune responses in the CNS, similar to macrophages in the peripheral tissue (Yang et al., 2009). Microglia steadily survey their environment to phagocytose debris and to present antigens to lymphocytes; they can migrate and adopt different phenotypes in response to a multitude of stimuli. However, they are not considered as being very competent APCs. Microglial cells usually are beneficial and favor neuronal survival by secreting growth factors and anti-inflammatory cytokines, but, as seen in several pathological conditions, they can be detrimental due to exaggerated pro-inflammatory activity (Kim and de Vellis, 2005; Block et al., 2007).

Microglial cells are furnished with receptors for a plethora of molecules; in normal conditions they are in a ″resting state″ (better termed surveying, because of their continuous scanning of the surrounding area to sense any signs of changes) and are characterized by long branching processes and a small cellular body. Upon detection of homeostatic disturbances microglial cells become alerted with shorter processes; if the stimuli are excessive and microglial cells are not able to restore the normal homeostasis, they become reactive and activated and in some conditions can contribute to damaging cascades.

Finally, activation of peripheral innate immune cells elicits the secretion of inflammatory cytokines, including interleukin (IL)-1, IL-6, and tumor necrosis factor-α (TNFα), that use neural and humoral pathways to relay this signal across the BBB to the CNS (Henry et al., 2008).

Immune and inflammatory responses in neurological diseases

Multiple sclerosis

Immune cells can infiltrate the CNS in the presence of systemic inflammation and modulate neural activities. The best example is the human autoimmune disease, multiple sclerosis (MS), where the imprimatur of an adaptive immune response is very strong. Within the CNS, CD4, CD8, and natural killer (NK) T cells are found along with B cells (Goverman, 2009) and disrupted myelin. Moreover, the responses of macrophages and microglial cells are very important for the clinical outcome. Their depletion or blockade can prevent disease progression (Jack et al., 2005); however suppression of macrophages and microglia can impair remyelination in toxin-induced models of de- and remyelination (Kotter et al., 2005). In MS, microglial cells activation can have opposite functions: 1) exacerbate damage or 2) protect by delivering trophic factors, clearance of tissue damage and supporting myelin regeneration (Hanisch and Kettenmann, 2007). Moreover, microglial cells play a central role in the initiation of the acute inflammatory reactions within the CNS.

Brain inflammation

To model brain inflammation as occurring in bacterial meningitis, for instance, lipopolysaccharide (LPS), a cell-surface component of Gram-negative bacteria, is often used to mimic infection (Alexander and Rietschel, 2001). LPS administration is associated with behavioral and cognitive complications, underlying the relevance of neuroimmune interactions for normal CNS function. Stimulation of the peripheral immune system in rodents evokes exacerbated neuroinflammation that is associated by prolonged sickness, impaired working memory, and depressive like behaviors (Henry et al., 2008). Activation of the peripheral innate immune system stimulates the secretion of cytokines and chemokines in the CNS that are able to modulate the behavioral symptoms of sickness (Henry et al., 2008). However, excessive production of pro-inflammatory cytokines, such as interleukin-1β (IL-1β) by microglia may contribute to the long lasting behavioral and cognitive complications induced by LPS.

Cerebral ischemia

There is substantial evidence that an inflammatory response is mounted within the CNS after cerebral ischemia. Post-ischemic inflammation is characterized by infiltration of neutrophils and monocytes/macrophages into the injured brain parenchyma, along with activation of microglial cells, and expression of pro-inflammatory cytokines, cell adhesion molecules, and other inflammatory mediators (Neumann et al., 2008). Abundant evidence exists that activation of microglial cells and infiltration of neutrophils into the injured parenchyma are playing an crucial role in the pathology of cerebral ischemia (Neumann et al., 2008). However, considerable lines of evidence suggest that accumulation of microglial cells correlates with a reduction of neuronal damage, depicting microglial cells a neuroprotective factor (Hanisch and Kettenmann, 2007). Accordingly, while neutrophils contribute to tissue damage by releasing oxygen radicals, proteases, and proinflammatory cytokines, activated microglial cells are

neuroprotective because they are able to engulf and destroy neutrophils, as shown in an *in vitro* model of cerebral ischemia (Neumann et al., 2008).

Spinal cord injury

Similar to other injured tissues, an inflammatory response arises after spinal cord injury (SCI), denoting the beginning of wound healing and scarring processes (Stirling et al., 2009). These early responses to injury include the activation of microglial cells and astrocytes that release pro-inflammatory mediators, such as cytokines, chemokines, and lipid mediators and lead to leukocyte recruitment to the injured tissue (Stirling et al., 2009). Thus, SCI is followed by rapid and marked mobilization of circulating neutrophils and their entry into the injured spinal cord; subsequently monocytes are mobilized and recruited, followed by lymphocytes. The firm adhesion to the endothelial cells is a prerequisite for neutrophils diapedesis (Engelhardt, 2008; Muller, 2009).

Epilepsy

In experimental models and in clinical cases of epilepsy pro-inflammatory and anti-inflammatory cytokines have been described in brain and plasma after seizure induction (Vezzani, 2005; Vezzani and Granata, 2005; Ravizza et al., 2008). Experimental findings demonstrated that pro-inflammatory cytokines IL-1β, IL-6 and tumor necrosis factor (TNF)-α in microglia and astrocytes are increased and followed by a cascade of downstream inflammatory events which may recruit cells of the adaptive immune system (Nguyen et al., 2002; Vezzani and Granata, 2005; Cacheaux et al., 2009). In addition to inflammatory disease, recent evidence shows the activation of innate immune system and associated inflammatory reactions in epilepsy may modulate some of the molecular and structural changes occurring during and after seizure activity (Vezzani and Granata, 2005). Moreover, experimental strategies aiming to block CNS or systemic inflammatory pathways reduces SE duration and seizure frequency (van Vliet et al., 2007).

Recently, van Gassen et al. (van Gassen et al., 2008) investigated the involvement of the immune system in human MTLE by microarray gene expression analysis and observed that CCL3 and CCL4 were highly (>10fold) upregulated in hippocampal specimen from TLE patients in compare to autopsy controls. Moreover, glial cells, neurons, and endothelial cells express cytokines following seizures in experimental models (Ravizza et al., 2008) and in human epileptogenic tissue. Therefore microglial cells may direct innate responses to the CNS injury and chemokines/cytokines emerge as important mediators of microglial response. These findings revealed a prominent role of chemokines and cytokines in the pathogenesis of seizures.

Fabene et al. (Fabene et al., 2008) demonstrated that inflammation, BBB leakage, and seizures are etiologically linked. In human patients and animal models, it was already shown that cerebrovascular alterations or inflammatory reactions can actually cause seizures (Vezzani and Granata, 2005; Oby and Janigro, 2006). These authors provided compelling evidence that the epileptogenic process may actually begin in the vasculature. Accordingly, the study by Fabene et al. provided strong evidences that brain inflammation and BBB disruption are effective triggers of seizures in the pilocarpine mouse model of epilepsy. In particular, after the pilocarpine administration, endothelial cell activation was examined. Under physiological conditions the expression of vascular cell adhesion molecules is very low; however after pilocarpine administration the results showed vascular induction of leukocyte cell adhesion molecules (in particular VCAM-1) with consequent induction of adhesion of circulating lymphocytes. Treatment with an anti-α_4 integrin antibody, which hampers adhesion of leukocytes to VCAM-1 on endothelium, was able to prevent SE and reduce chronic recurrent seizures. Furthermore, α_4 integrin is also important for neutrophil adhesion and trans-migration in experimental models of inflammation or in human disease. Fabene et al. (Fabene et al., 2008) demonstrated that neutrophils depletion by treatment with a neutralizing antibody also inhibits seizures activity. Altogether, these results support previous findings showing that microvascular changes induced by SE and contributing to BBB disruption are significantly involved in sustained hyperexcitability underlying spontaneous seizures (Marchi et al., 2007b; Fabene

et al., 2008). How inflammatory reactions intrinsic to the brain compared with those mediated by peripheral immune cells can contribute to epileptogenesis, is poorly understood (Vezzani and Janigro, 2009). Clearly, BBB failure is the link between these two mechanisms.

We have studied by microarray analysis the content of cytokines and chemokines (CCL3, CCL4, MIP-1α and β, CXCL2, CXCR4) in hippocampal tissue resected from pharmacoresistant MTLE patients and we have seen that they are strongly up-regulated (Lachos et al., under revision).

Therefore, we analyzed by immunohistochemistry hippocampal sections from patients with MTLE in order to determine whether these pro-inflammatory factors reflect an inflammatory response in the brain. Unexpectedly, we observed an accumulation of granulocytes ($CD15^+$), T cells ($CD3^+$), as well as $CD68^+$ microglia/macrophages in these tissue sections, but not in control post-mortem tissue. These findings suggested a role for leukocyte recruitment in the pathogenesis of MTLE. The presence of granulocytes and activated microglia in areas of neuronal loss is in line with their known contribution to neuronal injury by releasing cytotoxic mediators and/or cytokines.

In addition, alterations in BBB permeability were assessed by fibrinogen immunochemistry. In control sections, fibrinogen staining was invariably intraluminal, but in epileptic tissue, fibrinogen immunoreactivity was evident in the parenchyma of the hippocampus, as well as in astrocytes and in neurons, suggesting enduring leakage across the BBB and fibrinogen uptake into brain cells.

Panel D: *Fibrinogen staining in the hippocampus of TLE patients. Fibrinogen-IR is evident in the brain parenchyma of the hippocampus (A, C), outside the layer, as well as in astrocytes and in neurons (B). Figures show transverse sections outside the layer from TLE patients. Magnifications: A, B and C, 10X.*

These findings provided the foundation of the present work, in which we aimed to study in an experimental model of TLE the relevance of lymphocyte and neutrophil accumulation in epileptic brain tissue. The model used was based on a chronic lesion made in adult mice to have access to mutant models for manipulating adaptive immunity.

Transgenic mouse models for studies of neuroinflammation in CNS disorders

Considering these broad interaction between the CNS and the immune system, it is perhaps not surprising to see accumulation of immune cells in almost every CNS disease. In order to understand these interactions and the role of these cells, a large number of mice with targeted mutations for components of the immune system has been generated, including CD antigens, surface receptors, histocompatibility markers, endothelial adhesion molecules, and microglial cells. For instance, genetically modified mice deficient in adhesion molecules like PSGL-1 (Selplg$^{-/-}$) or in a 1,3-fucosyltransferase (FuTs) FucT-VII and FucT-IV, enzymes required to generate functional selectin-binding carhohydrates (Fut4$^{-/-}$ and Fut7$^{-/-}$ mice) have been used by Fabene et al. (Fabene et al., 2008) to demonstrate the role for leukocyte adhesion in seizure generation in the pilocarpine model of epilepsy.

Another relevant example includes CXCR2-KO mice. This chemokine receptor is essential for efficient neutrophil extravasation and intraparenchymal migration. Therefore, the blockade of the CXCR2 receptor is an efficient tool of limiting neutrophil infiltration into the sites of CNS inflammation (Shaftel et al., 2007) and of providing insight into inflammatory mechanisms underlying leukocyte recruitment to the CNS.

In addition, immunodeficient mice lacking cells of the adaptive immune system are widely used in the study of the autoimmune diseases in order to understand the role of a specific T cell population in the pathogenesis of a certain neurological disease.

Of particular interest are mice lacking the components of the adaptive immunity (B and T lymphocytes) due to targeted deletion of the RAG1 or RAG2 genes, which

are essential for the maturation of these cells, as well as mice lacking either $CD8^+$ T cells or $CD4^+$ cells. The former mice are based on the fact that the β2-microglobulin chain is required for the normal surface expression of MHC class I molecules. Thus, mice carrying a deletion in the gene encoding for β2-microglobulin chain fail to express MHC class I products and therefore unable to produce mature $CD8^+$ lymphocytes (see panel C). Similarly, the α and β chain constituting MHC class II (panel B) are required for the normal surface expression of MHC class II; therefore, mice carrying a deletion in the gene encoding for these chains fail to produce mature $CD4^+$ lymphocytes.

While these mice have been extensively used for studies of neuroimmune diseases and brain injury, they also represent a promising model for investigating experimentally the significance of the leukocyte invasion that we have observed in hippocampal tissue from MTLE patients.

The kainate mouse model of TLE

In the last decade, experimental evidence supported by clinical observations highlighted the possibility that brain inflammation is a common factor contributing, or predisposing, to the occurrence of seizures and cell death, in various forms of epilepsy of different etiologies. TLE is the most common epileptic syndrome in adult humans; for this reason, the neurobiological bases of TLE have been extensively studied in preclinical research and adequate animal models resembling the human pathology are required.

Several animal models of TLE are available for elucidating the pathophysiology of MTLE. In particular, most of the experimental data discussed above regarding the role of the immune system and inflammatory processes in epilepsy were performed in the pilocarpine model of epilepsy. In rodents, systemic administration of single dose of pilocarpine (a muscarinic cholinergic agonist) leads to SE and after a seizure-free period, to a chronic condition characterized by spontaneous recurrent seizures (SRS). This model has been proposed as sufficiently isomorphic with the human disease but several aspects differ significantly from the human pathology. Thus, the extent of brain damage is

considerable, pilocarpine treated animals having bilateral lesions in the brain underlying generalized seizures (Cavalheiro et al., 1991).

To overcome this major difference with the human pathology, a mouse model has been developed, based on a unilateral injection of a low dose kainic acid (KA) into the dorsal hippocampus (Suzuki et al., 1995). In this model, an epileptic focus develops gradually, accompanied by severe degeneration of the CA1 region and a pronounced dispersion of granule cells in the dentate gyrus, accompanied by massive mossy fiber sprouting with relative sparing of the CA3 region (Bouilleret et al., 1999). These histopathological changes are unilateral, restricted to the dorsal hippocampus, and develop over a period of several weeks. Furthermore, intrahippocampal injection of KA in adult mice results in profound, progressive, and long-term modifications of hippocampal EEG activity. Using intrahippocampal recordings, different phases could be distinguished in this model: a) a transient non-convulsive SE initiated immediately after KA-injection and persisting up to 10 hours; b) a seizure-free latent period of about 2 weeks characterized by sporadic low voltage spikes or spike-and-waves; c) a chronic phase characterized by recurrent high voltage sharp waves and hippocampal paroxysmal discharges, lasting for the life of the animal (Riban et al., 2002). The latent phase likely corresponds to a phase of epileptogenesis and the recurrent seizures are resistant to classical antiepileptic drugs, mimicking two major features of MTLE.

The mouse KA model has been extensively used to investigate morphological and functional adaptations underlying seizures (Straessle et al., 2003; Ledergerber et al., 2006; Antonucci et al., 2008; Le Duigou et al., 2008). Likewise, the model has enabled studies of the mechanisms of pharmacoresistance, in particular the significance of altered adenosine metabolism due to the severe astrogliosis, leading to enhanced activity of adenosine kinase, the main adenosine metabolizing enzyme (Gouder et al., 2003; Gouder et al., 2004; Fedele et al., 2005; Boison, 2006). The presence of a well-defined latent phase prior to recurrent seizure onset allows separating events contributing to epileptogenesis from those underlying seizure activity. However, despite extensive analysis (Le Duigou et al., 2005; Dugladze et al., 2007; Antonucci et al., 2008; Le Duigou et al., 2008; Antonucci et al., 2009), the mechanisms underlying the transition from the

latent to the chronic phase remain unidentified. So far, the potential role of immune and inflammatory responses in the KA-lesioned hippocampus has not been investigated.

Aims of the study

Traditionally, epilepsy is viewed as a disease of the brain, with seizures resulting from alterations in neuronal circuits, synaptic function, and physiological properties of neurons. However, despite the wealth of studies on the functional and morphological alterations occurring in epilepsy, notably in temporal lobe epilepsy, the pathophysiology of this disorder remains not understood. A paradigm shift was produced by recent experimental and clinical data suggesting that inflammation directly contributes to the pathogenesis of epilepsy. In particular, the demonstration that interactions between leukocytes and vascular endothelial cells are particularly important for seizure generation (Fabene et al., 2008), along with the identification of numerous genes associated with altered BBB function or systemic inflammation (Vezzani and Granata, 2005; Oby and Janigro, 2006) strongly support the notion that neuroimmune interactions play a key role in epileptogenesis and seizure disorders. However, owing to the lack of temporal perspective of neurological studies, the question remains unresolved whether inflammation is the cause or the consequence of seizures or neuronal cell loss.

The overall aim of this project is based on our own observations that a large array of pro-inflammatory genes are upregulated in both brain tissue and microvascular endothelial cells derived from patients with intractable epilepsy, and that immune cells, in particular CD45 and CD3 cells, infiltrate the epileptic brain parenchyma. Our goals are to investigate the interactions between innate and adaptive immunity during epileptogenesis and determine their role for functional and histopathological reorganization of the hippocampal formation in an experimental model of focal epilepsy. Using the intrahippocampal KA mouse model of TLE, we specifically addressed the following issues:

1. We investigated the time-course and pattern of hippocampal lesion caused by KA injection into C57BL/6J mice and monitored the activation and potential recruitment of immune cells derived from the monocyte/macrophage lineage. We observed that C57BL/6J mice, which are resistant to the systemic effects of KA (Bouilleret et al., 1999), develop the same lesion than Swiss and NMRI mice upon intrahippocampal KA injection. The lesion caused enduring microglial cell activation that

mirrored precisely the pattern of neurodegeneration, providing an index for indirectly quantifying the extent of neuronal loss in this model. Furthermore, we observed the appearance of macrophage-like cells, selectively in the ipsilateral, KA-lesioned dentate gyrus.

2. We determined whether leukocyte recruitment seen in human tissue also occurs in KA-lesioned mice and established their spatio-temporal distribution pattern during the latent and chronic phase of epileptogenesis; $CD3^+$ T cells, but no $B220^+$ B cells were observed selectively within the lesioned hippocampal formation, increasing during the latent phase to reach a plateau at the expected time of seizure-onset (about 14 days post-KA injection).
3. To determine the role of these lymphocytes for mediating or protecting against KA-induced lesions and epileptogenesis, we investigated the effects of KA injection in RAG1-KO mice (lacking T and B cells, components of the adaptive immunity); neuronal cell loss was markedly aggravated in immunodeficient mice as seen 2-4 weeks after KA injection. The activation of microglial cells was more severe and widespread mirroring precisely the pattern of neurodegeneration and was accompanied by infiltration of Gr-1^+ neutrophils in the lesioned hippocampus. The latter feature was never seen in wild-type mice.
4. To determine the role of Gr-1^+ neutrophils for mediating the severe cytoarchitectural changes observed in RAG1-KO mice, we investigated the effect of neutrophil depletion in RAG1-KO and wild-type mice. Neutrophil depletion was sufficient to prevent the delayed neuronal cell loss. By contrast, neutrophil depletion in wild-type mice did not influence the pattern of KA-induced neurodegeneration.
5. To investigate the origin of macrophage-like cells found in the molecular layer of the dentate gyrus, whether from resident microglia or peripheral monocytes, we performed two pharmacological interventions in wild-type and RAG1-KO mice aiming at preventing lymphocyte and monocyte diapedesis into the brain parenchyma, and at depleting mononuclear phagocytes in the blood and lymphoid organs. The results suggest that

granule cell survival and dispersion depend on macrophage infiltration in both genotypes. Surprisingly, both treatments interfered with neutrophil recruitment in the RAG1-KO mice as well, thus causing a reduced KA-induced neurodegeneration.

6. To determine the functional relevance of leukocyte infiltration into the KA-treated hippocampus in wild-type mice and the specific role played by $CD4^+$ and $CD8^+$ T cells, we used EEG analysis during the latent and the chronic phase in this model in various lines of immunodeficient mice. Unexpectedly, RAG1-KO mice showed a dramatic shortening of the latent phase prior to SRS onset, suggesting that synaptic reorganization in the lesioned hippocampus is not necessary for the onset and expression of hippocampal paroxysmal discharges. In addition, $\beta_2$microglobulin-KO (lacking $CD8^+$ T cells) and MHC II-KO mice (lacking $CD4^+$ cells) likewise exhibited a curtailed latent phase along with a reduced lesion severity compared to wild-type mice. Surprisingly, a cohort of MHC II-KO mice showed no hippocampal paroxysmal discharges over the entire period analyzed; furthermore, the absence of seizures was again not related to lesion severity.
7. To understand which soluble factors might be responsible for the infiltration of lymphocytes into the KA-lesioned hippocampus, as well as neutrophils in RAG1-KO mice, we employed the Luminex X100 platform to determine the cytokines/chemokines protein level in KA- and saline-injected hippocampus. It is known that cells of the innate immunity are crucial to first line defense against injury but which are chemokines important to carry signals between cells and exert chemotaxis to the site of injury is not still fully understood.

This work will contribute to unravel the contribution of the various facets of the immune system (including T cell, neutrophil, and macrophage recruitment, microglial cell activation and production of soluble factors, like cytokines and chemokines) to neuronal damage and morphological reorganization, epileptogenesis, and timing of seizure onset in the KA-treated hippocampal formation by targeting specific mediators during both the acute and chronic

phases of epilepsy in this mouse model of TLE. The identification of inflammatory pathways activated in epileptic brain may point to novel pharmacological strategies to prevent epileptogenesis and control recurrent seizures refractory to classical antiepileptic drugs.

Materials and methods

Materials and Methods

An overview of all experiments performed is given in Table 1.

Animals

Experiments were performed on 12- to 14-weeks old male wild-type and knockout (KO) mice weighing 25-35g (see Table 2). The mice were housed and bred in the "OHB" animal facility of the Institute of Pharmacology and Toxicology on a 12 h light/dark cycle (lights on at 7 a.m.) with food and water provided ad libitum. They were transferred to the conventional facility shortly before experiments. After KA or vehicle injection they were housed in individual cages for two-three weeks, depending on the duration of the experiment under the same conditions as above.

Table 2: List of mice used for experiments

Short name	***Genetic background***	***Supplier***	***Experiments***
B6, wild-type	C57BL/6J	LTK (RCC, Füllinsdorf, Switzerland)	Morphology, EEG, Neurochemistry
RAG1-KO	C57BL/6-CD45.1/T x B6.129S7-Rag^{1tmMom}/J	Jackson Laboratory (Bar Harbor, ME, USA) Prof. B. Becher, UZH	Morphology, EEG, Neurochemistry
B6-RAG2-KO	B6.129S6-Rag2^{tm1Fwa} N12	Taconics Farm (Lille Skensved, DK)	EEG
Cg-RAG2-KO	Balb/c-IL2rg^{tm1} B6.129S6-Rag2^{tm1Fwa}	Prof. A. Aguzzi, UZH	EEG
β_2-microglobulin-KO	B6;129P2-B2m^{tm1Jae}	Prof. B. Becher, UZH	EEG
MHC II-KO	B6-I-A^{tm1Blt}	Prof. B. Becher, UZH	EEG

Mice homozygous for the *Rag1^{tm1Mom}* and Rag2^{tm1Fwa} mutation were used because they lack T cells and B cells. RAG-1 and RAG-2 are essential to the generation of

mature B and T lymphocytes. Either homozygous mutants exhibit total inability to initiate V (D) J rearrangement and fail to generate T or B lymphocytes.

β_2-microglobulin knockout and MHC class II knockout (MCH II-KO) mice were used because they lack $CD8^+$ T cells and $CD4^+$ T cells, respectively. β_2-microglobulin is a polypeptide chain belonging to the MHC class I complex and $CD8^+$ T cells maturation is strictly dependent on their interaction with MHC I. In the absence of β_2-microglobulin $CD8^+$ T cells are not viable. MHC class II molecules are found only on a few specialized cell types, including macrophages, dendritic cells and B cells, all of which are professional APCs. Mice missing MHC class II molecules fail to produce $CD4^+$ T cells.

Animal procedures were approved by the Cantonal Veterinary Office of Zurich. All efforts were made to minimize animal suffering and to reduce the number of animals used.

Kainic acid injection and electrodes implantation

Mice were treated with KA (Tocris, Lucerna Chem AG, Lucerne, Switzerland) or with vehicle only (0.9% NaCl). Under anesthesia by inhalation of 2.5-3% isoflurane (Baxter, Volketswil, Switzerland) in conjunction with oxygen, mice received a unilateral stereotaxic injection of 70 nl of a 5 mM solution of KA in saline into the right CA1 area of the dorsal hippocampus [coordinates with Bregma as reference: anteroposterior (AP) = −1.8 mm, mediolateral (ML) = −1.6 mm, dorsoventral (DV) = −1.9 mm] as described (Bouilleret et al., 1999). Control mice were treated identically but were injected with vehicle only.

For EEG recordings, mice were implanted under anesthesia with bipolar electrodes aimed at the right dorsal hippocampus, using the same coordinates (AP=-1.8 mm, ML=-1.6 mm, DV=-1.9 mm) immediately after KA injection. A monopolar reference electrode was inserted over the cerebellum. All electrodes were fixed to the skull with cyanoacrylate and dental acrylic cement. Following surgery, the mice were allowed to recover from anesthesia on a warm pad, injected with 1 mg/kg buprenorphine (Temgesic, Essex Chemicals, Lucerne,

Table 3: Design of the experiments performed (except Luminex assay)

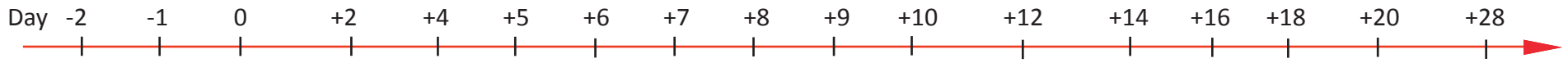

C57BL/6J		Saline-ipsi (control); perfusion-fixation after 7 (n=3), 10 (n=3), 14 (n=6), and 28 (n=3) days														
		KA-ipsi; perfusion-fixation after 7 (n=8), 10 (n=10), 14 (n=11), and 28 (n=6) days														
RAG1-KO		Saline-ipsi (control); perfusion-fixation after 7 (n=2), 10 (n=2), and 14 (n=2) days														
		KA-ipsi; perfusion-fixation after 7 (n=6), 10 (n=4), 14 (n=11) and 28 (n=6) days														
anti-Gr1 treatment (*)																
C57BL/6J	*	KA-ipsi			*			*			† n=6					
RAG1-KO		KA-ipsi				*			*			*	† n=6			
anti-α_4-integr. treatment (§)																
C57BL/6J	§	KA-ipsi		§				§				§	† n=6			
RAG1-KO	§	KA-ipsi		§				§				§	† n=6			
Clodrolip treatment (□)																
C57BL/6J	□	KA-ipsi	□		□			□			† n=8					
RAG1-KO	□	KA-ipsi	□		□			□			† n=8					
EEG recordings (o)																
C57BL/6J		KA-ipsi	o	o		o		o		o	o	o	o	o	o	o † n=6
RAG1-KO		KA-ipsi	o	o		o		o		o	o	o	o	o	o	o † n=10
RAG2-KO-B6		KA-ipsi	o	o		o		o		o	o	o	o	o	o	o † n=4
RAG2-KO-Balb/c		KA-ipsi	o	o		o		o		o	o	o	o	o	o	o † n=6
$\beta_2$microglobulin-KO		KA-ipsi	o	o		o		o		o	o	o	o	o	o	o † n=10
MHC II-KO		KA-ipsi	o	o		o		o		o	o	o	o	o	o	o † n=11

Switzerland) and then returned to their home cage with daily monitoring of wellbeing until termination of the experiment.

Electroencephalographic recordings

EEGs were recorded in freely moving KA-treated mice using a digital acquisition system (AcqKnowledge MP100, Biopac Systems Inc, Santa Barbara, CA, USA; sampling rate, 200 Hz). Recordings were performed during 3-4 hours following habituation to the test cage (about 30 minutes), around midday to minimize potential circadian variations. To assess the frequency and duration of recurrent seizures, mice were recorded every other day starting from day 2 post-SE until maximum day 20 post-KA injection. EEG recordings were analyzed off-line and artifacts due to animal movements were discarded. Paroxysmal events were defined as seizures when they lasted more than 20 seconds (s) and were separated from each other by intervals of at least 3s. For each animal, the average number of seizures per hour and seizure duration was calculated.

Pharmacological treatments

Three different pharmacological interventions were used to interfere with innate and acquired immune responses in KA-treated mice.

Neutrophil depletion

Aim:

KA-injection in RAG1-KO mice induced a robust neutrophil response in the hippocampus. Therefore, we applied the RB6-8C5 anti-Ly6G/Gr-1 antibody to deplete neutrophils and study their role in the pathophysiology of TLE.

The RB6-8C5 clone recognizes an epitope on the myeloid differentiation antigen Gr-1, a glycosylphosphatydil inositide-linked protein. Ly6G is the major antigen on mature neutrophils identified by the RB6-8C5 clone. The antibody depletes neutrophils in both blood and spleen for up to 2-3 days after i.v. injection (Stirling et al., 2009).

Protocol:

C57BL/6J mice were pre-treated with 100 µg purified anti-Gr-1 mAb (clone RB6-8C5, 16-5931, eBioscience) intravenously one day before KA injection and then received 3 additional doses of 100 µg mAb, given at 3 day intervals. The animals were killed at day 10 post-KA injection and the tissue analyzed.

RAG1-KO mice were injected with KA at day 0 and then treated with 100 µg anti-Gr-1 mAb at day 6, 9 and 12 post KA-injection. They were sacrificed at day 14 post-KA injection. Neutrophil depletion was confirmed by analysis of the spleen in all treated mice.

Blockade of leukocyte infiltration

Aim:

The α_4 integrin supports leukocyte rolling and adhesion (first transient and later firm) to the vessel wall. Therefore, administration of mAb to α_4 integrin was used to interfere with the rolling or firm adhesion of leukocytes to the vascular wall (Fabene et al., 2008). The aim of this treatment was to determine the role of leukocyte transmigration across the vessel wall into brain parenchyma for mediating histopathological alterations in TLE.

Protocol:

Experiments were performed in C57BL/6J and RAG1-KO mice (Table 1). The mice received an i.v. injection of α_4 integrin-specific mAb (400 µg) (PS/2 clone, affinity purified; kindly provided by Prof. Dr. B. Engelhardt (University of Bern, Switzerland) 1 day before the unilateral injection of KA; treatment was repeated every 3-4 days intraperitoneally (200 µg) until day 12 post-KA injection. The mice were killed at 14 days post-KA injection and the tissue was analyzed for different immunological and glial markers.

Macrophage depletion

Aim:

Clodronate Liposomes (Clodrolip) are artificially-prepared lipid vesicles, consisting of concentric phospholipid bilayers entrapping an aqueous compartment. They can be used to encapsulate strongly hydrophilic molecules, such as clodronate, a toxic bisphosphonate. After systemic injection, liposomes are selectively phagocytosed and digested by macrophages, followed by intracellular release and accumulation of clodronate. Above a certain concentration, clodronate induces apoptosis of the macrophage.

Clodrolip contains approximately 18±2 mg clodronate (0.5 micromoles, clodronic acid disodium salt tetrahydrate, $CH_2Cl_2Na_2O_6P_2$ x$4H_2O$) per ml. To assess the role of macrophages in TLE we therefore used Clodrolip. i.p. administration of Clodrolip depletes macrophages within 24-36 hours by >90%.

Protocol:

Macrophage depletion was performed by i.p. administration of Clodrolip (1.5 mg in C57BL/6J and 0.5 mg in RAG1-KO mice) per/20g body weight. The first administration was given one day before KA injection. To maintain the depletion over a longer time period, the treatment was repeated twice at 3-4 days interval and the mice were euthanized at day 10 post-KA for immunohistochemical analysis (see Table 1). After KA injection, the cages with the mice were put on a warm pad to facilitate the recovery. Clodrolip was kindly provided by Dr. Reto Schwendener (University of Zurich).

Immunohistochemistry

Mice were deeply anaesthetized with pentobarbital (Nembutal®, 60 mg/kg, i.p.) and perfused transcardially with 10 ml phosphate-buffered saline (PBS; pH 7.4) followed with 60 ml ice-cold fixative (0.15 M sodium phosphate buffer, 4% paraformaldehyde, 15% saturated picric acid solution, pH 7.4), as described (Fritschy and Mohler, 1995). Brains were removed immediately after perfusion, postfixed for 3 h at 4°C, and impregnated overnight with 30% sucrose in PBS for

cryoprotection. Transverse 40 µm-thick sections were cut from frozen blocks with a sliding microtome and collected in ice-cold PBS. Sections were then stored in anti-freeze solution (50mM phosphate buffer, 15% glucose, 30% v/v ethylene glycol, sodium azide; pH 7.4) at -20°C. One series of section was Nissl-stained with Cresyl violet to verify the location of the KA injection, the pattern of neuronal loss, and the dispersion of the dentate gyrus granule cells, as reported previously (Bouilleret et al., 2000). Additional sections were processed for immunohistochemistry, as described below.

Immunological and glial markers

Primary antibodies were used against cluster of differentiation (CD)3^+ T cells (purified hamster anti-mouse CD3e, CD3 ε chain, 553058; BD Pharmingen), T helper cells (purified rat anti-mouse CD4, 553727), cytotoxic T cells (purified rat anti-mouse CD8a, 553027, BD Pharmingen), B cells (rat anti-mouse CD45R/B220, 550286, BD Pharmingen) (see Table 3), neutrophils (Gr-1, purified rat anti-mouse Ly-6G and Ly-6C, 553123, BD Pharmingen), activated microglial cells (rat anti-mouse CD68, MCA1957GA, AbD Serotec and purified rat anti-mouse CD11b, 550282 clone M1/70, BD Pharmingen), microglial cells (rabbit anti-mouse Iba-1, 019-19741, Wako) and macrophage-like cells (rat anti-mouse F4/80, ab6640, Abcam).

Table 3: Description of the cluster of differentiation (CD) markers

Cluster of differentiation	*Description*	*Cell types*
CD3	T-cell receptor-associated CD3 complex	Thymocytes, mature T lymphocytes, NK (natural killer) T cells
CD4	Co-receptor for the T cell receptor (TCR)	T helper cells, regulatory T cells, subset of NK-T cells
CD8	Co-receptor for the T cell receptor (TCR)	Cytotoxic T cells
CD11b	Integrin α_M, Mac-1α chain, also known as complement receptor 3 (CR3)	Granulocytes, NK cells, B-1 cells, macrophages, dendritic cells, activated microglial cells
CD45R (B220)	Transmembrane glycoprotein	B lymphocytes

Immunoperoxidase staining

Immunoperoxidase staining was performed to visualize the regional distribution of cellular markers (notably CD3, CD68, Gr-1, F4/80) and assess their changes in KA-treated mice (Table 4). Sections from KA and vehicle-treated mice were incubated overnight at 4°C with continuous agitation (100 rpm) with primary antibodies diluted in Tris-Triton pH 7.4 containing 2% normal goat serum (CD3/CD4/CD8 1:1000, CD11b 1:1000, B220 1:1000, Gr-1 1:1000, CD68 1:2000, Iba-1 1:3000, F4/80 1:1000) and 0.2% Triton X-100. The sections used for CD3, CD4, CD8 and Gr-1 staining were pre-incubated at room temperature for 15 min in 1.5% H_2O_2 in PBS to block endogenous peroxidase prior the incubation with the primary antibody. This step was necessary to avoid non-specific labeling of erythrocytes, which might have confounded the analysis. The next day sections were washed in Tris-Triton pH7.4 and incubated for 30 min at room temperature in biotinylated secondary antibodies (1:300; Jackson Immunoresearch, West Grove, PA). After washing, sections were incubated in ABC complex for 30 min (Vectastain Elite Kit; Vector Laboratories, Burlingame, CA), washed again and finally reacted with diaminobenzidine tetrahydrochloride (DAB; Sigma, St. Louis, MO) in Tris-triton (pH 7.7) containing 0.05% Triton X-100 and 0.015% hydrogen

peroxide. The color reaction was stopped after 5-15 minutes by transferring the sections into ice-cold PBS. The sections were mounted in gelatin-coated slides and air-dried overnight. Finally, they were dehydrated with an ascending series of ethanol, cleared in xylene, and coverslipped with Eukitt (Erne Chemie, Dällikon, Switzerland).

Immunofluorescence staining

Immunofluorescence staining was perform to compare the cellular distribution of two (or three) markers in the same tissue section (Table 4). Multiple labeling requires primary antibodies raised in different species. The identity of $CD3^+$ T cells was determined by double immunofluorescence staining for either CD4 or CD8. The spatial interactions between microglial cells and neutrophils were determined by triple labeling for Gr-1, Iba-1 and the nucleic acid stain Sytox Green (Molecular Probes) or DAPI. Comparative morphological analysis of microglia and macrophage-like cells was determined by double labeling for Iba-1 and F4/80.
Free-floating sections were incubated overnight in a mixture of antibodies diluted in Tris pH 7.4 containing 2% normal goat serum and 0.2% Triton X-100. Sections were then washed in Tris-Triton and incubated for 30 min at room temperature in a mixture of affinity-purified secondary antibodies raised in goat (Jackson Immunoresearch) coupled to Alexa 488 (1:1000); Alexa 647 (1:1000) or Cy3 (1:500) diluted in Tris pH 7.4 containing 2% normal goat serum and 0.2% Triton X-100. After washing in Tris-Triton, sections were mounted onto gelatin-coated slides, air-dried and coverslipped with fluorescent mounting medium (DAKO, Carpinteria, CA).

Table 4: Immunohistochemical staining performed in each experiment

CD3, CD3/CD4; CD3/CD8	*Peroxidase* *Fluorescence*	Chapter 1 Chapter 1
Gr-1 **Gr-1/Iba-1**	*Peroxidase* *Fluorescence*	Chapter 2 Chapter 2
CD68	*Peroxidase*	Chapters 1-3
F4/80 **Iba-1/F4/80**	*Peroxidase* *Fluorescence*	Chapters 1, 3 Chapters 1, 3

Data Analysis

Sections stained with Cresyl violet or processed for immunoperoxidase staining were analyzed with bright-field microscopy (Zeiss AxioCam, Jena; Germany). Digital images were acquired using an 8-bit digital color camera controlled by AxioVision 4.5 (Zeiss) or Mercator software (ExploraNova, La Rochelle, France). Exposure times were set so that pixel brightness was never saturated and were held constant during acquisition of all images for each experiment.

Sections processed for double and triple immunofluorescence staining were visualized by confocal laser scanning microscopy (LSM 710 Zen, Carl Zeiss, Jena, Germany) using a 40x (N.A. 1.3) or 63x (N.A. 1.4) objective and sequential acquisition of separate channels. Pinhole was set to 1 Airy unit and the acquisition parameters set to use the full dynamic range of photomultipliers. Stacks of images (1024 x 1024 pixels, pixel size 70 -100 nm) spaced by 0.35 - 0.5 μm were acquired and processed using Imaris software (Bitplane, Zurich, Switzerland). For display, maximal intensity projection images (10-35 layers) were prepared with either merged or color-separated channels.

Quantification and densitometry analysis

The total number of cells immunoreactive for CD3 ($CD3^+$) was determined in the dorsal hippocampus (three sections per mouse) on high magnification images using Mercator software for unbiased quantification. A mask of the cells in the hippocampus was created by outlining the corresponding area. For the analysis, the total number of cells was included; the volume was calculated considering the section sampling fraction (ssf). Data were subjected to statistical analysis (one way ANOVA followed by post hoc multiple comparison test – Bonferroni) and results plotted using Prism (Graph Pad, San Diego, CA, USA).

Densitometry measurements of CD68 immunoreactivity were performed to quantitatively assess the degree of microglia activation using MCID software (Imaging Research, St. Catharines, ON). Digital images were acquired using a 12-bit digital camera. Exposure times were set so that pixel brightness was never saturated and were held constant during acquisition of all images. RODs were calibrated with a grey-value density scale. Staining intensity was measured in defined regions of interest in the ipsilateral and contralateral hippocampus (CA1 pyramidal cell layer, stratum radiatum, stratum oriens, granule cell layer, molecular layer, hilus). Background was measured in the thalamus and subtracted from measurements made in the same section. RODs were averaged per brain region of interest and animal. Two sections per animal were analyzed.
Data were analyzed using two-way ANOVA with the statistical software GraphPad Prism 5 (La Jolla, CA, USA). Post-hoc multiple comparison test-Bonferroni was performed. Genotype and treatment were the main between-subjects factors, while regions of interest were the main within-subjects factors.

Correlation between number of F4/80 positive cells and integrity of the granule cell layer of the dentate gyrus

The analysis was performed in sections of KA-treated hippocampus to evaluate the impact of macrophage depletion on granule cell dispersion in the dentate

gyrus. The width of the granule cell layer was measured on calibrated 12-bit digital images using MCID software (Image Research, St. Catharines, ON). In each section analysed, the granule cell layer was subdivided into 6 segments (3 in the upper blade and 3 in the lower blade). In each segment, the average width of the granule cell layer was measured and the number of $F4/80^+$ cells in the molecular and granule cell layers was counted. The analysis was performed in 4 sections per mouse, yielding 24 pairs of data per mouse. Data were analyzed statistically using linear regression analysis in order to correlate the thickness of the granule cell layer to the number of $F4/80^+$ cells.

Luminex assay

Luminex's xMAP technology allows measuring the concentration of a large number of analytes, for instance cytokines and chemokines, simultaneously in each sample with high sensitivity. The xMAP technology uses 5.6 µm polystyrene microspheres which are internally dyed with red and infrared fluorophores. The xMAp microsphere sets are created using different intensities of the 2 dyes for different batches of microspheres each with a unique spectral signature determined by its red/infrared mixture. Each microsphere carries a unique signature and the xMAP detection system can identify to which set it belongs. Therefore, multiplex up to 100 tests in a single reaction is possible. The surface chemistry on the xMAP microspheres allows simple chemical coupling of capture reagent. The assay is carried out in a 96-well plate format with 17 tests per well. High tech fluidics based on the principles of flow cytometry cause the stream of suspended microspheres to line up in a single raw prior to passing through the detection chamber. A total number of 66 samples were analyzed with Luminex's xMAP technology.

In brief, the ipsilateral and contralateral dorsal hippocampus from C57BL6/J and RAG-1 KO mice 7, 10 and 14 days after KA injection and 10 days after saline injection were collected (see Table 5). Animals were anesthetized with Nembutal (60 mg/kg, i.p.) and perfused with ice-cold artificial cerebrospinal fluid (ACSF) to wash the blood from the brain and cool down the tissue. Cytokines and

chemokines are mainly present in the blood but the aim of our assay was to assess cytokines in the brain parenchyma, specifically in the hippocampus after KA or vehicle injection. Following the perfusion, the brain was rapidly extracted on ice, cut into 400 mm-thick sections with a vibratome and tissue containing the dorsal hippocampus was microdissected out and homogenized by sonication (N. Zivy&Ciesa, Switzerland) in EBC buffer (50 mM Tris, 120 mM NaCl, 0.5% NP-40) containing a cocktail of protease and phosphatase I and II inhibitors (SIGMA P9599). The homogenate was centrifuged at 4°C for 1 hour and protein concentration was determined with the Pierce® BCA Protein Kit Assay.

All specimens were immediately aliquoted, frozen, and stored at −80°C. We assayed cytokines and chemokines using commercially available microspheres (Millipore, Billerica, MA) according to the manufacturer's instructions. Microspheres of defined spectral properties conjugated to antibodies directed against mouse brain proteins were pipetted into a 96-well plate together with our protein extracts. The median fluorescent intensity of microspheres specific for each cytokine was recorded for each well and compared to the known standard values included in the manufacturer's kit. We used an automated immunoassay analyzer (Luminex™ 100 IS System, Luminex, Austin, TX).

Table 5: Samples analyzed by Luminex

Treatment	***Time point***	***C57BL/6J (n)***	***RAG1-KO (n)***	***Ipsi and contra***
No treatment	-	2	2	x
Saline	10 days	3	3	x
KA	2 days	5	5	x
KA	7 days	5	5	x
KA	14 days	5	5	x

Data were normalized per μg protein and average values (± SEM) per time-point calculated. No statistical analysis was performed, as visual inspection of the histograms (vehicle versus KA) revealed no variation across all samples analyzed.

Results

Chapter 1

KA-induced lesion leads to activation of adaptive and innate immunity in the hippocampal formation

Effects of unilateral intrahippocampal kainate injection in C57BL/6J mice

The KA mouse model of TLE was used in these studies because it mimics major pathophysiological features of mTLE (degeneration in CA1 and hilar neurons, extensive astrogliosis, and occurrence of focal SRS after a latent phase of epileptogenesis). To study the potential role of innate and acquired immunity on neurodegeneration and glial cell activation we focused mainly on the chronic phase of the model, starting with the onset of SRS, around 14 days post-KA.

As this model was initially characterized in outbred Swiss mice, whereas most lines of mutant mice used here were maintained on the inbred C57BL/6J background, we determined the pattern and extent of neurodegeneration induced by KA in wild-type B6 mice.

Nissl-stained sections were examined 14 (n=11) and 28 (n=6) days after KA and saline treatment (Fig. 1.1B, C). At 14 days post-KA treatment, the characteristic pattern of neuronal loss in the CA1 and CA3c areas and in the hilus of the dentate gyrus was evident, along with extensive gliosis in the CA1 pyramidal cell layer. The CA3a,b area was partially preserved, as well as the granule cell layer, where neuronal dispersion has started. These effects were restricted to the ipsilateral (ipsi) dorsal hippocampus and no changes in hippocampal cytoarchitecture were apparent contralaterally (contra), as well as in animals treated with vehicle only (0.9% NaCl) (Fig. 1.1A). The dispersion of granule cells resulted in an enlargement of the dentate gyrus. At 4 weeks post-KA treatment, the cytoarchitecture of the injected dorsal hippocampus was changed markedly compared to control. In particular, profound cell death led to atrophy of the entire CA1 area, whereas the dentate gyrus was markedly enlarged, due to granule cell hypertrophy and extensive dispersion. Overall, CA3a,b was still partially preserved, whereas neuronal loss was nearly complete in CA3c and the hilus. These features were seen consistently in all animals successfully injected with KA into the dorsal CA1

area. Therefore, the effects of KA are similar in C57BL/6J mice as in other strains used for this model of TLE.

Invasion of CD3$^+$ T cells into the KA-treated hippocampal formation

Previous immunohistochemical experiments in the laboratory (Zattoni and Frei, personal observations) have revealed the presence of CD3$^+$ T lymphocytes, but not of CD45R/B220$^+$ B-cells, in hippocampal tissue resected from patients with intractable mTLE. The presence of these immune cells in brain parenchyma coincided with a marked increase in pro-inflammatory cytokines and chemokines, detected by gene array and RT-PCR analysis (van Gassen et al., 2008).

Here, to determine whether the KA mouse model of TLE is suitable for investigating the underlying mechanisms and the role of T-cells infiltrating an epileptic focus, we analyzed immunohistochemically the presence of CD3$^+$ T lymphocytes in the brain parenchyma of KA-treated C57BL/6J mice, at day 2, 7, 14 and 28 after injection (Fig. 1.2). Saline-treated mice were used as control; no CD3$^+$ T cells were detected in any of them. In contrast, a small number of CD3$^+$ T lymphocytes were seen mainly associated with brain microvessels and rarely in the brain parenchyma, at day 2 after KA-treatment. Thereafter, a gradual accumulation of CD3$^+$ T cells was observed in the epileptic hippocampus reaching a maximum at 2 weeks post-injection (Fig. 1.2C) and remaining present at 4 weeks

Figure 1.1: Neurodegenerative and morphological changes induced by unilateral kainic acid (KA) injection into the dorsal hippocampus, as visualized by Cresyl Violet staining. (A) Saline-injected control, 14 days after injection. No morphological changes were observed when comparing the injected (ipsi) hippocampus to the contralateral (contra) side. (B) At 14 days post-KA neuronal cell death was clearly visible in CA1, the pyramidal cell layer appeared thinner and mainly containing pyknotic cells. Likewise, profound cell loss was evident in CA3c and the hilus, whereas CA3a,b was partially spared. Granule cell dispersion was pronounced in the dentate gyrus. (C) At 28 days post-KA the entire CA1 area was degenerated, CA3 was much reduced and most of the space was occupied by the dentate gyrus, owing to the dispersion of granule cells. The contralateral hippocampus (contra) remained unaffected in all the time points analyzed. All images are at the same magnification. Scale bar (all panels) = 250μm. Ipsi, ipsilateral; contra, contralateral; CA, Cornu Ammonis; DG, dentate gyrus; HL, hilus.

Figure 1.1

Saline control

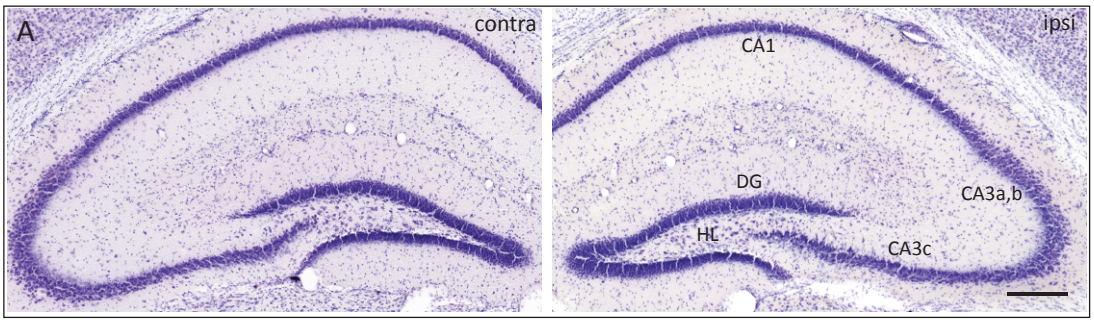

Kainate injection

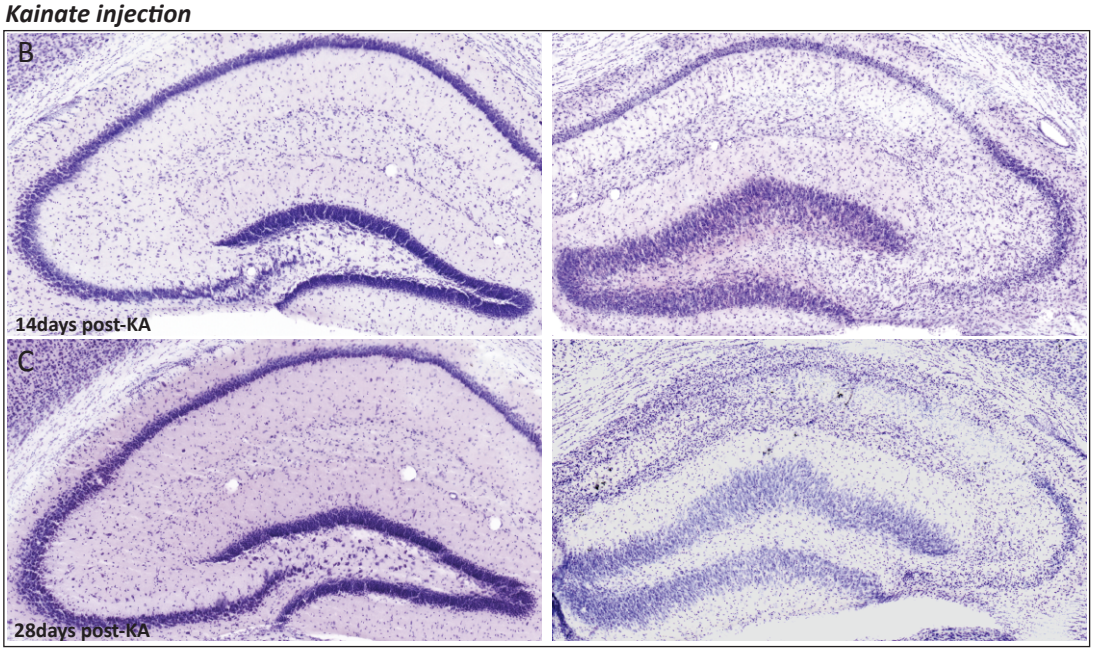

during the chronic phase. In particular, $CD3^+$ T cells were found throughout the CA1 and CA3 areas, most numerous in stratum radiatum and stratum lacunosum molecolare. Very few cells were seen in the dentate gyrus and hilus. Remarkably, no $CD3^+$ T cells were seen contralaterally or in other regions of the brain at all time points analyzed.

We performed an unbiased quantitative evaluation of the number of $CD3^+$ T cells infiltrating the ipsilateral dorsal hippocampus (Fig. 1.2E). Statistical analysis confirmed the accumulation of $CD3^+$ T cells in the KA-lesioned hippocampus 2 and 4 weeks after-KA injection (One way ANOVA, $F_{3,17} = 6.18$, $p<0.0049$). The significant increase of $CD3^+$ T cells at 14 days post-KA in the dorsal hippocampus of epileptic mice (Fig. 1.2E) coincides with the onset of SRS and the beginning of the chronic phase in this mouse model.

Next, to better understand which population of T cells was infiltrating the lesioned hippocampus, we analyzed separately, $CD4^+$ and $CD8^+$ cells, which represent helper T cells and cytotoxic T cells, respectively. Double immunofluorescence staining (CD3/CD4 and CD3/CD8) was performed at 14 days post-KA injection in 4 mice (Fig. 1.2F). It revealed that 60-75% of T cells present in the hippocampus were $CD8^+$, suggesting that a preferential infiltration of cytotoxic T cells might be a key feature of this model of TLE.

Figure 1.2: $CD3^+$ T cell infiltration in the hippocampus of C57BL/6J mice after KA injection. (A) No $CD3^+$ cells were detectable in sections from control mice. (B) At day 2 after KA, a few $CD3^+$ T lymphocytes were seen ipsilaterally mainly associated with brain microvessels and rarely in the brain parenchyma. No $CD3^+$ cells were detected in the contralateral side. (C) At day 14, a marked increase in the number of $CD3^+$ cells was evident, selectively in the epileptic hippocampus. No $CD3^+$ cells were seen contralaterally. Insets are shown in panel D for the different time points and treatment. (E) Unbiased quantification of T cell infiltration at different time points after KA injection, confirming the significant increase in $CD3^+$ T cell number 14 and 28 days post-KA in the ipsilateral hippocampus. The bars graph shows the total number of $CD3^+$ T cells located within in the ipsilateral dorsal hippocampus. Values are given as a mean ± SEM. *$p<0.05$, (n=6), Bonferroni post-test analysis. (F) Example of double immunofluorescence staining for CD3 (green) and CD8 (red) depicting a subset of double-labeled cells in the CA1 region (arrowheads); overall, the majority of cells present in this field were $CD8^+$ T cells. Scale bars: A-C = 250µm; D = 50µm; F = 30µm.

Figure 1.2

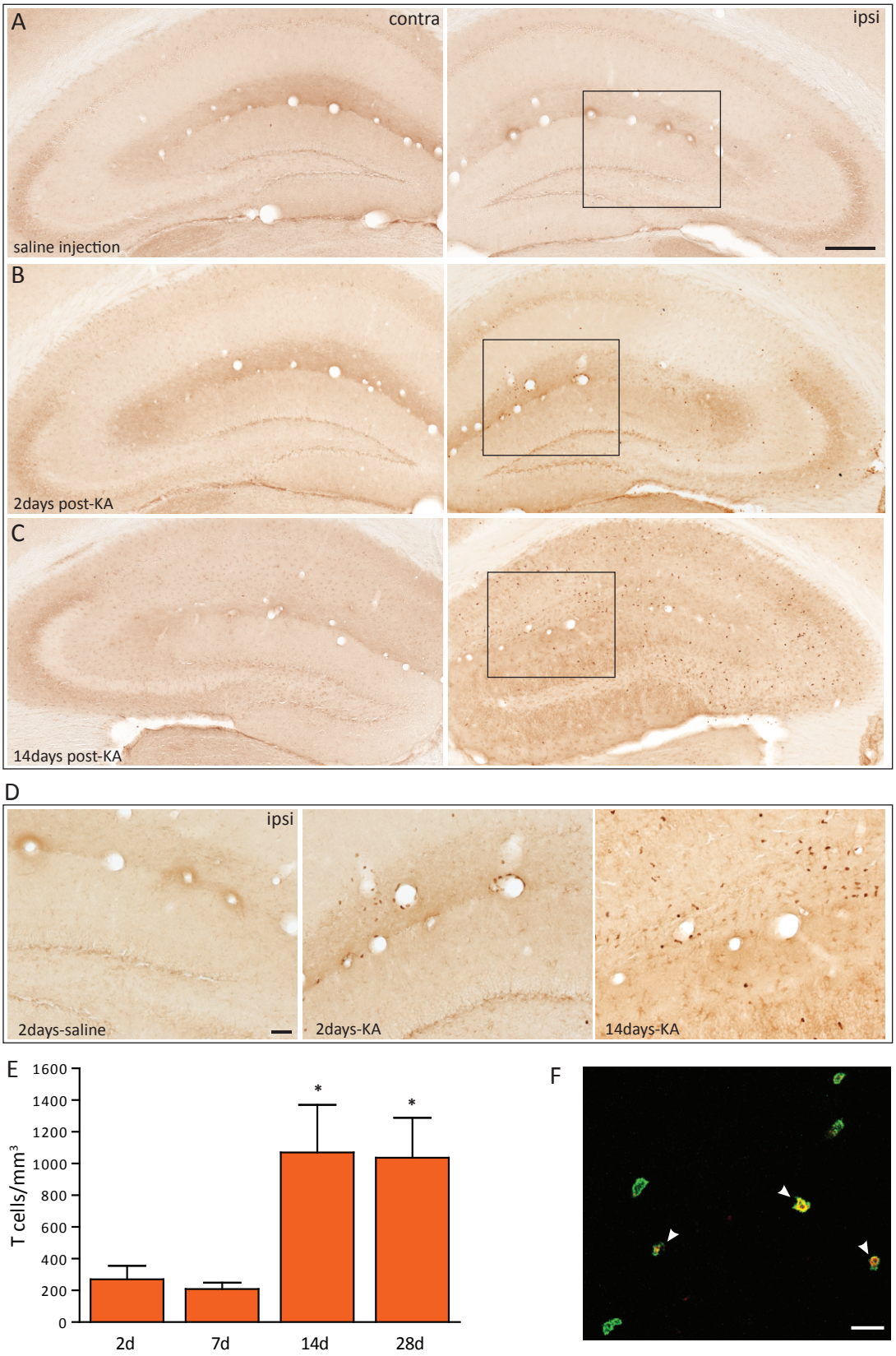
A
contra
ipsi
saline injection
B
2days post-KA
C
14days post-KA
D
ipsi
2days-saline
2days-KA
14days-KA
E
T cells/mm³
1600
1400
1200
1000
800
600
400
200
0
*
*
2d
7d
14d
28d
F

Finally, immunohistochemical analysis for CD45/B220 did not show the presence of B lymphocytes in the KA-injected hippocampus or anywhere else in the brain parenchyma (data not shown), using spleen sections as a positive control.

Microglial cell activation in the KA mouse model of TLE

In this model, the KA-induced neurodegeneration in CA1, CA3c and hilus causes a massive astrogliosis, as described in previous studies (Gouder et al., 2004; Ledergerber et al., 2006). Less attention was given, so far, to microglial cells. Given their role as effectors of innate immunity, we monitored here microglia activation using classical markers of resting (Iba-1, CD11b) and activated (CD68) microglial cells.

With each of these markers, essentially identical results were observed. Iba1 and CD11b, markers recognizing both resting and activated microglial cells, were clearly seen in contralateral (resting) and ispilateral (activated) hippocampus after KA treatment (data not shown).

Since CD68-immunoreactivity (-IR) is very low in resting microglia, it is better suited to investigate microglia activation. Therefore, we analyzed the pattern of

Figure 1.3: Extensive microglial cell activation in KA-treated dorsal hippocampus, as visualized by CD68 staining. (A) Saline control, 14 days after injection. CD68-immunoreactivity (-IR) faintly revealed resting microglia. Note the weak activation of microglial cells close to the injection site (arrow). (B) 14 days post-KA injection. Extensive microglia cell activation was evident at this time point in CA1 and CA3; in the pyramidal cell layer, it precisely reflected the pattern of neuronal cell loss (see Fig. 1.1). In addition, numerous strongly labeled $CD68^+$ cells were evident in the dendritic layers of CA1-CA3. In the dentate gyrus, the increase in staining was less pronounced and only isolated activated microglial cells were present. (C) 28 days post-KA injection. The ongoing CA1 and CA3 pyramidal cell layer degeneration was reflected by prominent $CD68^+$ staining. The contralateral side showed a weak staining for resting microglial cells at all time point analyzed. Scale bar (for all panels) = 250µm. (D) Densitometric analysis of CD68-IR, showing selective increase in areas of neuronal cell loss in comparison to saline-control. The increase was significant in the pyramidal layer of CA1, CA3a,b, and CA3c, in the stratum radiatum and oriens of CA1 and in the hilus. The relative optical density (ROD) are given as mean ± SEM, $^*p<0.05$, $^{**}p<0.01$, $^{***}p<0.001$, Bonferroni post-test, n=11. SP, stratum pyramidale; CA, Cornu Ammonis; GCL, granule cell layer, ML, molecular layer; SO, stratum oriens; SR, stratum radiatum; HL, hilus.

Figure 1.3

Saline injection

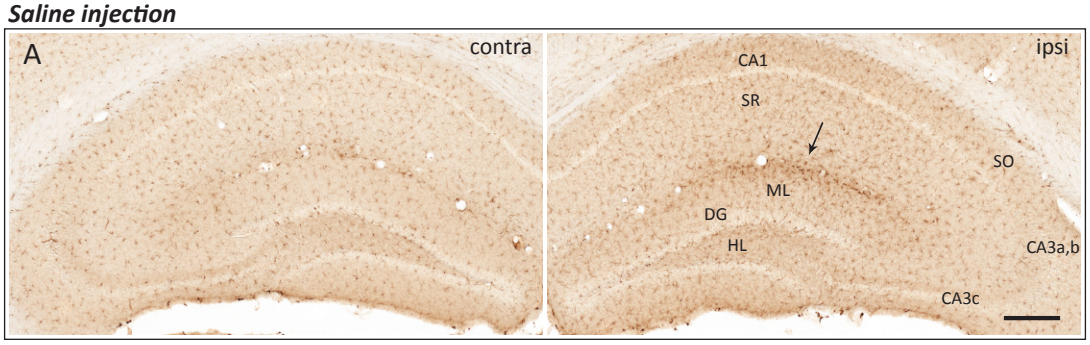

Kainate injection

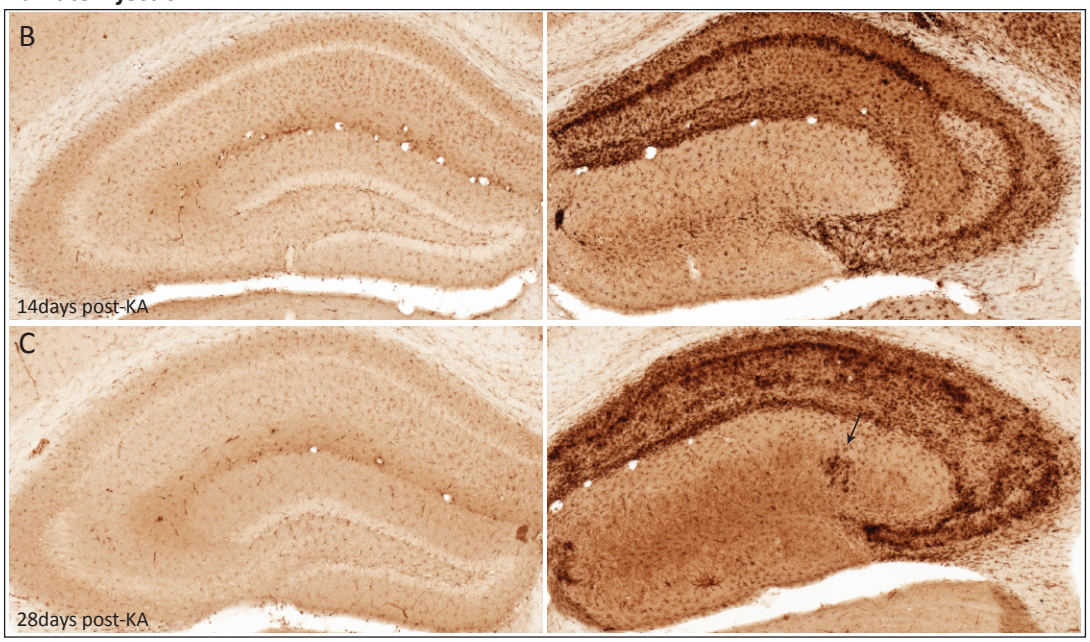

D

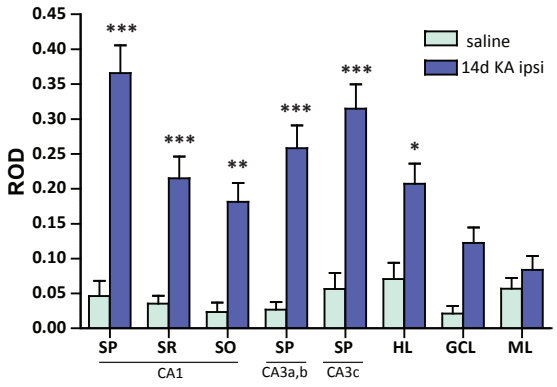

microglial cells activation by CD68 staining in brain sections at 14 and 28 days post-KA and saline injection (Fig. 1.3). Saline-treated animals did not show activation of microglial cells in the injected side except for a weak increase in CD68-IR in the molecular layer due to mechanical lesion by the canula (Fig. 1.3A, arrow). In KA-treated mice, as described above at 2 weeks post-KA (Figure 1.3B), most CA1 pyramidal cells were degenerated and activated microglial cells were most prominent in the CA1 pyramidal cell layer and stratum lacunosum-molecolare. The CA3 area appeared largely normal at this stage and contained much less CD68-IR. Few activated microglial cells were seen in the hilus and no CD68-IR was detected in the granule cell layer. At 4 weeks post-KA injection (Fig. 1.3C), the entire CA1 pyramidal cell layer was labeled by activated microglial cells; in CA3 activation of microglia was also observed, reflecting partial neurodegeneration. In the dentate gyrus, the increase in staining was less pronounced and only isolated microglial cells were present (Fig. 1.3C, arrow). No activated $CD68^+$ microglial cells were seen contralaterally at any time point

Figure 1.4: Appearance of $F4/80^+$ macrophage-like cells in the dentate gyrus of C57BL/6J mice after KA injection. (A) Immunoperoxidase staining for $F4/80^+$ cells 14 days post-KA. F4/80 staining faintly revealed resting microglial cells in the contralateral side (contra), as well as resting and activated microglial cells ipsilaterally (arrow), like CD68 staining (see Fig.1.2B). In addition, macrophage-like cells were detected selectively in the ipsilateral dentate gyrus (arrowheads), mainly in the molecular layer outside of the dispersed granule cells. (B-B'') Insets are shown in B' and B" to better illustrate these strongly immunoreactive macrophage-like cells in the molecular layer; B'' is an enlargement of the frame in B'. (C-D') Representative images of double immunofluorescence staining of the CA1 stratum lacunosum moleculare with Iba-1 antibody (green; labeling resting and activated microglia) and F4/80 (red). Images were acquired by confocal laser scanning microscopy and depicted as maximal intensity projection of 10-15 layers spaced by 0.5 m. $Iba\text{-}1^+$ resting microglial cells recognized by their long and slender processes were seen contralaterally (C). In contrast, activated microglia cells with a "bushy" appearance were visible ipsilaterally (D); in a subset of these cells, F4/80 staining is evident (arrows), as shown in color-separated images (D-D'). (E-E") Representative image from double immunofluorescence staining for Iba-1 and F4/80 in the molecular layer showing "alerted microglia" (green) with an intermediate morphology between resting and activated, along with strongly labeled $F4/80^+$ cells characterized by their larger cell body and short thick processes. These cells, which also were $Iba\text{-}1^+$, represent macrophage-like cells infiltrated in the brain parenchyma. E'-E'' are enlargements of the inset in E. ML, molecular layer; SLM, stratum lacunosum-moleculare. Scale bars: (A) = 250µm; (C-E) = 25µm.

Figure 1.4

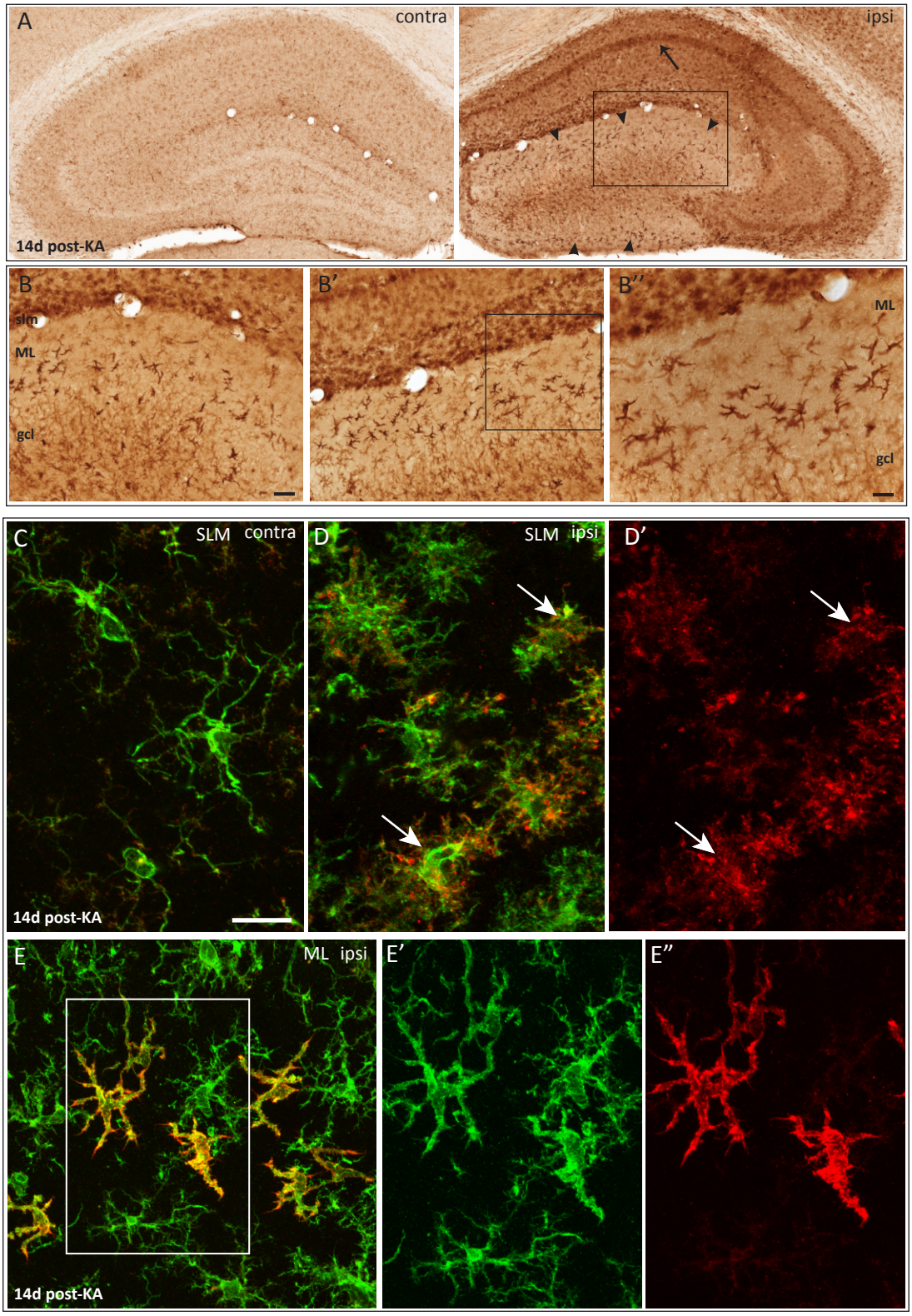
A
contra
ipsi
14d post-KA
B
slm
ML
gcl
B'
B''
ML
gcl
C
SLM contra
14d post-KA
D
SLM ipsi
D'
E
ML ipsi
14d post-KA
E'
E''

analyzed. Altogether, these results demonstrate that microglial cells selectively became activated in hippocampal regions were neuronal death had occurred. Therefore, CD68-IR represents a useful marker to monitor neurodegeneration in this TLE model.

To quantitatively assess the severity and progression of the lesion in the ipsilateral KA-injected hippocampus, we performed a densitometric analysis of CD68-IR compared saline treated controls (Fig. 1.3D). The regions of interest included: CA1pyramidal layer, stratum radiatum, and stratum oriens; CA3a,b and CA3c pyramidal layer; granule cell layer of the dentate gyrus; hilus. Two-way ANOVA revealed a significant difference in CD68-IR between KA- and saline-treated mice ($F_{1,120}$=133.3, p<0.0001), as well as a significant differences among the regions analyzed ($F_{7,120}$ = 5.151, p<0.0001), notably in CA1, CA3, and hilus compared to saline-treated animals.

These results confirm the visual impression that microglia activation is most prominent were neuodegeneration had occurred.

Selective appearance of F4/80$^+$ macrophage-like cells in the ipsilateral dentate gyrus of KA-treated mice

Macrophages, like microglial cells, derive from monocytes. They can be identified immunohistochemically by strong expression of the F4/80 antigen. F4/80 is a member of the epidermal growth factor (EGF)-receptor family and is expressed to various degrees in the entire hematopoietic lineage. To determine whether macrophage-like cells can be detected in the brain following KA-induced degeneration, we examined by immunoperoxidase and immunofluorescence staining the morphology and distribution of cells strongly stained with F4/80 monoclonal antibody in the dorsal hippocampus.

As shown in Figure 1.4, F4/80 antibody labeling of activated microglial cells is similar to that produced with anti-CD68 antibody (described above). In addition, we could observe another population of F4/80$^+$ cells, not detected with anti-CD68, in the molecular layer of the dentate gyrus (Fig. 1.4A). Surprisingly, these F4/80$^+$ macrophages-like cells were seen almost exclusively in the ipsilateral

dentate gyrus. Their distribution in the molecular layer outlined the outer margin of the dispersed granule cells. Some F4/80^{+} cells were also seen within granule cell layer and in the hilus. To distinguish morphologically these F4/80^{+} macrophage-like cells from microglial cells, we performed double immunofluorescence staining with antibodies against F4/80 and Iba-1. In control tissue and in the contralateral hippocampus, resting microglial cells are ramified with long and slender branches in the stratum lacunosum-molecolare, as shown in Figure 1.4C. No F4/80^{+} cells were detected in these areas. Activated microglial cells in KA-treated tissue had a “bushy” appearance with short and thick branches (Fig. 1.4D); some of them were F4/80^{+}, as well (Fig. 1.4D’). Macrophage-like cells in the molecular layer of the dentate gyrus were strongly immunoreactive for F4/80 and Iba-1 and were characterized by a distinctive shape, clearly different from activated microglial cells. The cell body was larger, often elongated and the processes were fewer and thicker (Fig. 4E,E’,E’’).

These results suggest that multiple components of acquired and innate immunity are activated in this model of TLE, with specific spatio-temporal pattern during epileptogenesis. To establish causal relationships between these phenomena, we next investigated the effects of KA injection in immunodeficient mice, lacking B and T cells.

Results

Chapter 2

Aggravation of KA-induced neurodegeneration in RAG1-KO mice

Effects of unilateral kainic acid injection in RAG1-KO mice

RAG-1 and RAG-2 are essential for the generation of mature B and T lymphocytes. RAG1-KO and RAG2-KO mice are viable but lack B and T lymphocytes, because of failure to produce the T cell receptors and immunoglobulins, respectively. They still have monocytes, granulocytes, and natural killer cells.

Since these mice lack adaptive immune cells, we used them to understand the significance of T cell infiltration in the KA mouse model of TLE with regard to activation of innate immunity. RAG1-KO mice treated with KA were analyzed 7 (n=6), 10 (n=4), 14 (n=11) and 28 (n=6) days after treatment and compared to tissue from age-matched C57BL/6J wild-type mice. The neuropathological alterations were analyzed by Cresyl Violet staining. Saline-treated RAG1-KO mice exhibited no abnormality (Fig. 2.1A). At 1 week post-KA injection, a profound loss of hilar neurons, CA3c, and CA1 pyramidal cells was evident unilaterally in Nissl-stained sections in both genotypes (Fig. 2.1B,B'). Most CA3a,b pyramidal cells appeared unaffected in wild-type. In contrast, RAG1-KO mice showed a more severe lesion, with partial loss of neurons in the CA3a,b, as well as pyknotic dentate gyrus granule cells (the latter in a subset of mice). Extensive gliosis was evident throughout the hippocampus in both genotypes. At 10 days post-KA (Fig. 2.1C,C'), the morphology was similar to the 7 days time-point. However, degeneration of CA3 pyramidal cells was more advanced in RAG1-KO mice and of granule cell dispersion was visible in both genotypes, despite the presence of pyknotic cells in the dentate gyrus of RAG1-KO mice. Strikingly, at 14 days post-KA injection, in 7 of 11 RAG1-KO mice neuronal cell loss was markedly aggravated, allowing to distinguish two groups differing in lesion severity (Fig. 2.1D-D'). In the first group, the entire CA1, CA3a,b and CA3c areas were degenerated and all granule cells in the dentate gyrus were pyknotic. This profound cell death led to atrophy of the entire ipsilateral hippocampus, and even more so 28 days after KA injection (Figure 2.1E'). At this point, the cytoarchitecture of the ispilateral

hippocampus was characterized by a strong gliosis and became almost unrecognizable. These changes were restricted to the ipsilateral hippocampus, extending into the ventral part, whereas no changes were apparent contralaterally (contra). In the second group, the lesion seen at 14 days post-KA in the ipsilateral hippocampus was less severe and comparable to the wild-type (Fig. 2.1D). At 28 days post-KA, however, the lesion was markedly aggravated, resembling that seen in the first group (Fig. 2.1E). Typically, the entire pyramidal layer was damaged and most granule cells of the dentate gyrus were destroyed. Thus, KA-induced lesion eventually led to a complete destruction of the ipsilateral hippocampus in RAG1-KO mice, a feature never seen in wild-type mice.

Microglial cell activation in RAG1-KO mice after unilateral KA injection

The profound neuronal cell death occurring in RAG1-KO mice was accompanied by a more severe and widespread activation of microglial cells as seen by CD68 immunostaining, at all time-points analyzed (Fig. 2.2). In saline-injected RAG1-KO mice, as in wild-type, no microglia activation was seen in the contra- and

Figure 2.1: Aggravated neurodegeneration in the hippocampal formation of RAG1-KO mice during the chronic phase of epilepsy, as seen by Nissl staining. (A) Cytoarchitecture of the dorsal hippocampus in saline-treated RAG1-KO mice. No difference was detectable compared to wild-type C57BL/6J mice (see Fig. 1.1); likewise, no morphological changes were found in the ipsilateral saline-treated hippocampus compared to the contralateral (contra) side. At 7 days and 10 days post-KA injection, corresponding to the latent phase of epileptogenesis in this TLE model, the lesion was more severe in RAG1-KO (B', C') compared to wild-type controls (B, C). The entire CA1-CA3 pyramidal cell layer was degenerated and pyknotic cells were visible in the dentate gyrus (arrowheads). Note the profound loss of hilar neurons in both genotypes. At 10 days post-KA (C-C'), granule cell dispersion was evident in both genotypes. At 14 days post-KA (D-D'), RAG1-KO mice could be separated in two groups differing in lesion severity. In 7 out of 11 mice, neuronal cell loss was markedly aggravated, as illustrated in a representative case (D'); the entire CA1 and CA3 areas were degenerated and most granule cells in the dentate gyrus were pyknotic. At 28 days (E'), cell death was so extensive that it led to atrophy of the entire ipsilateral hippocampus. Most of the remaining cells were glial cells. In the second group, the lesion seen at 14 days post-KA (D) was less severe and comparable to wild-type. At 28 days post-KA however, the lesion was markedly aggravated, resembling that seen in the first group, although the overall cytoarchitecture of the hippocampal formation remained recognizable (E). CA, Cornu Ammonis; DG, dentate gyrus; HL, hilus. Scale bar (all panels) = 250µm.

Figure 2.1

Saline injection in RAG1-KO mice

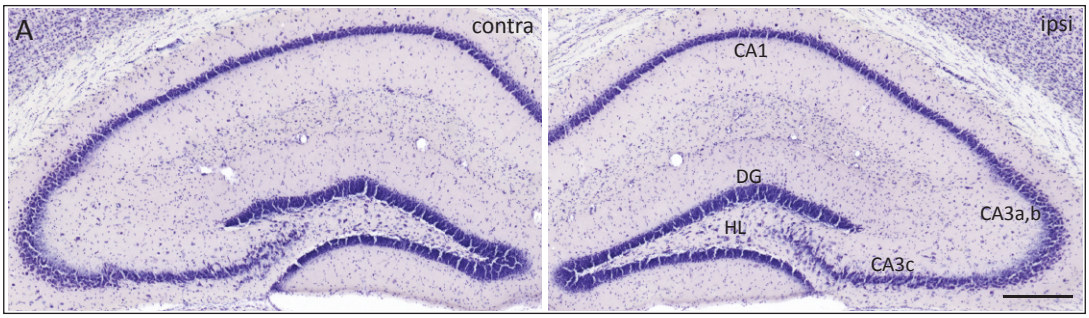

Kainate injection (latent phase)

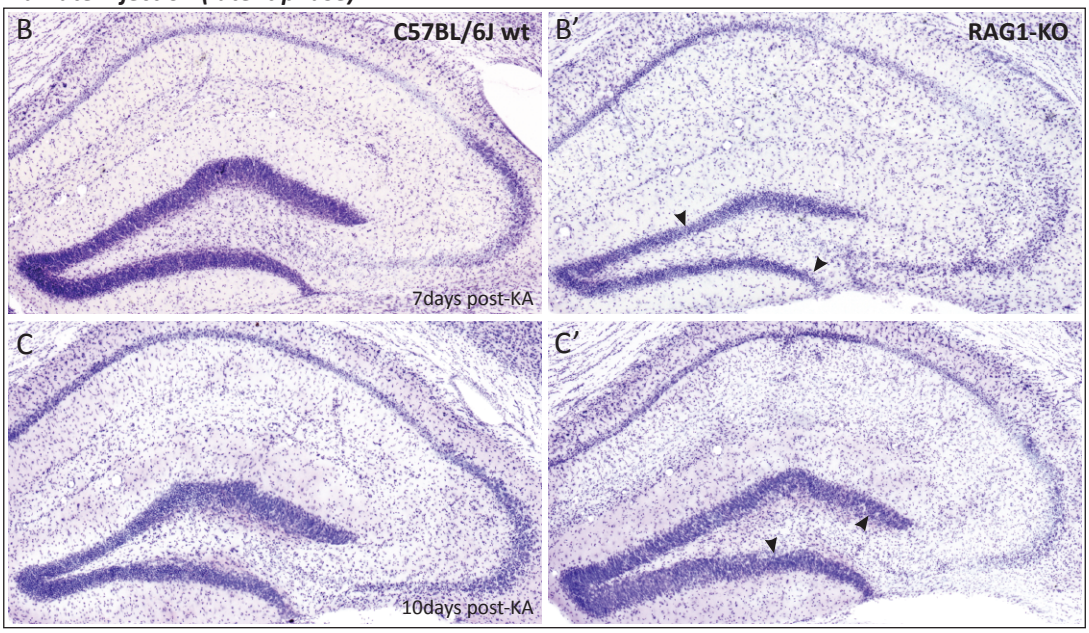

Kainate injection in RAG1-KO mice (chronic phase)

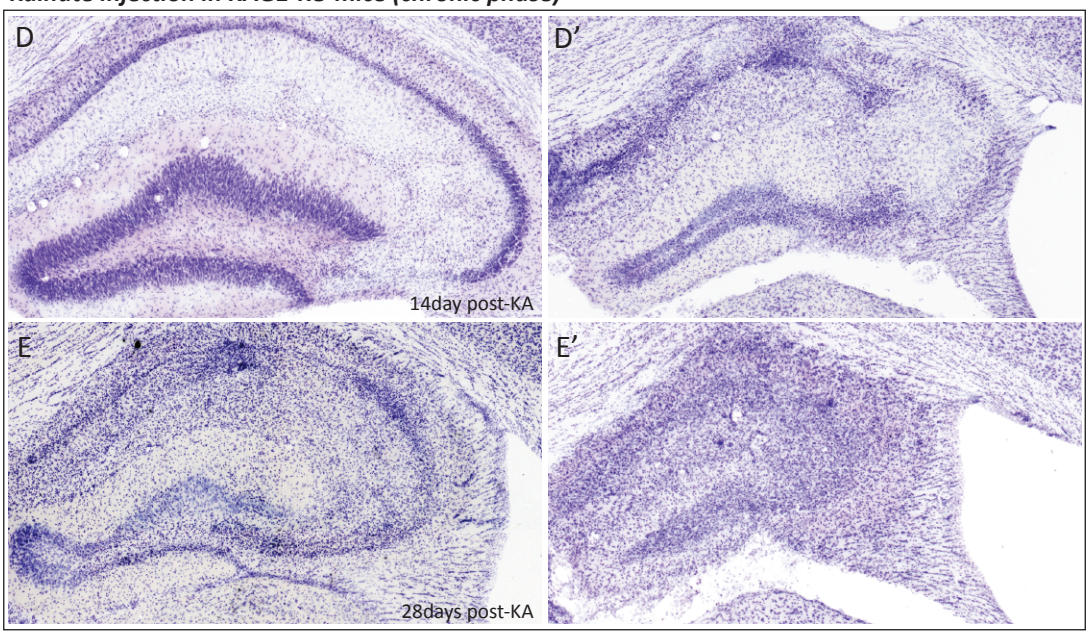

ipsilateral hippocampus, in which resting microglial cells appeared faintly labeled. A weak and transient microglial cell activation was detected only at the injection site (Fig. 2.2A) like in wild-type mice (see chapter 1). At 7 days post-KA injection, the reaction of microglial cells was severely exacerbated in the CA1 and CA3 b,c areas, as well as the granule cell layer of the dentate gyrus, coinciding with the neuronal cell death seen by Nissl staining. Contralaterally, we observed a transient activation of microglia in the stratum radiatum and oriens of CA1-CA3 disappearing at the later time points. At 10 days post-KA (Fig.2.2C), microglia activation was most prominent in areas of extensive cell death; the contralateral side was similar to control. At 14 days post-KA (Fig. 2.2D-D') CD68-IR reflected the severity of the lesion in the 2 groups of mice. In severely affected mice, the entire CA1 and CA3 regions were strongly labeled (Fig. 2.2D'). When the lesion was moderate the pattern of microglial cells activation resembled the wild-type situation (2D), notably in the dentate gyrus, where only isolated activated microglial cells could be detected. At 28 days post-KA (Figure 2.2E'), exacerbated microglial activation was evident throughout the hippocampal formation (Fig. 2.2E). Thus, ongoing CA1 and CA3 pyramidal cell degeneration was reflected by a further increase in CD68 staining.

Figure 2.2: Microglial cell activation mirrors the pattern of neuronal loss in KA-lesioned RAG1-KO mice, as shown by immunoperoxidase staining for CD68. (A) Saline-injected control, 14 days after injection. CD68 staining faintly revealed resting microglia in the ipsilateral as well as in the contralateral side. Note the weak activation of microglial cells close to the site of saline injection (arrow). (B-C) At 7 and 10 days post-KA injection, extensive microglia activation was evident ipsilaterally in CA1 and CA3 pyramidal layer and the hilus, reflected by the strong CD68-IR in these regions (B'-C'). Note the weak microglial cell activation in the contralateral hippocampus at 7 day (B), mainly in CA1-CA3 stratum radiatum and oriens. This activation was transient and not detectable anymore at the following time-point analyzed (C). (D-D') At 14 days post-KA injection, CD68-IR reflected the severity of the lesion in the 2 subsets of mice (see Fig. 2.1D-D'). In severely affected mice, the entire CA1 and CA3 pyramidal cell layers were strongly labeled (D'). (D) The pattern of microglial cell activation was similar to wild-type control when the lesion was moderate. At 28 days post-KA (E-E'), exacerbated microglia activation was evident throughout the hippocampal formation, underlying the extensive neuronal cell death seen in Nissl stained sections. Scale bar (all panels) = 250µm.

Figure 2.2

Saline injection

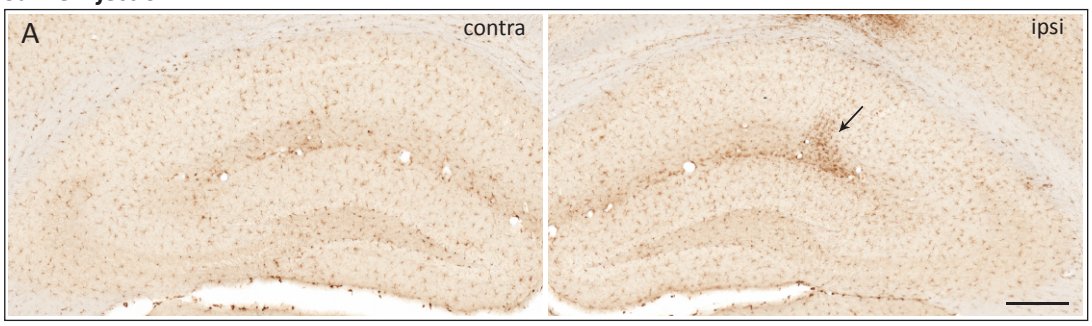

Kainate injection (latent phase)

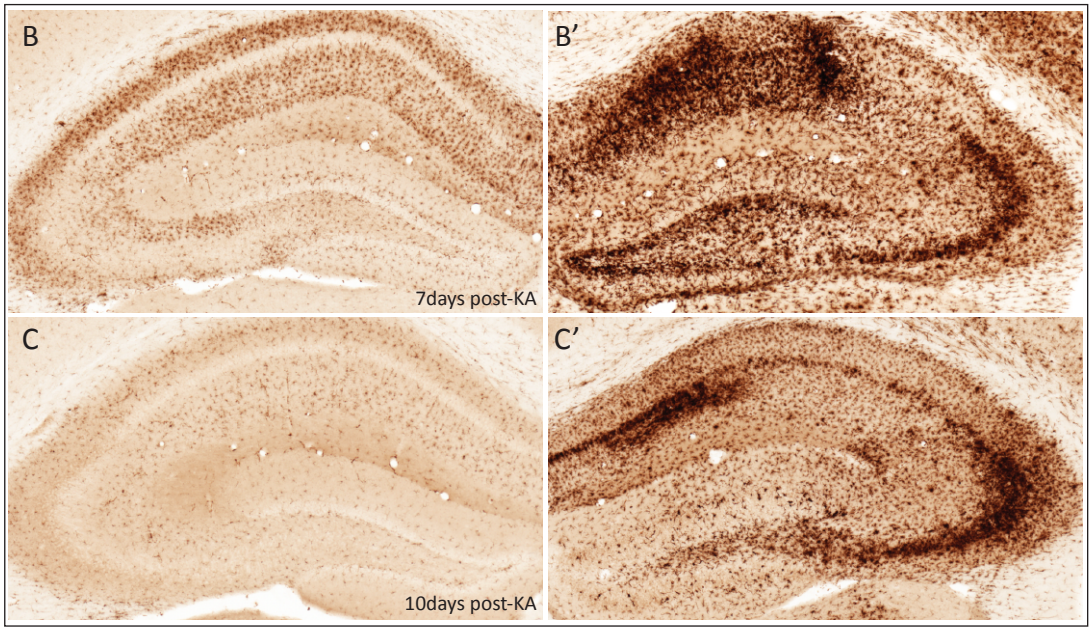

Kainate injection in RAG1-KO mice (chronic phase)

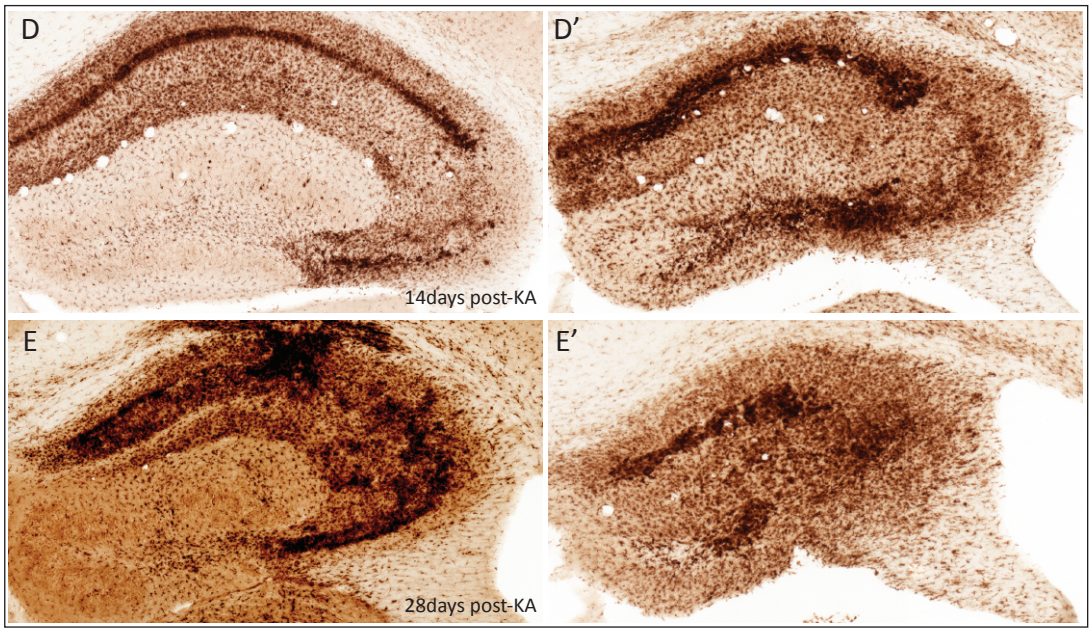

To quantify the extent of neurodegeneration in the ipsilateral KA-injected hippocampus in RAG1-KO mice, we again performed densitometric analysis of CD68-IR. Two-way ANOVA revealed a significant difference in CD68-IR between RAG1-KO and wild-type mice ($F_{1,158}$= 53.3; p<0.0001), as well as significant differences among the regions analyzed ($F_{7,158}$ = 14.57; p<0.0001) (Fig.2.3), notably in the pyramidal layer and stratum radiatum of CA3a,b and CA3c, but not in the granule cell layer and molecular layer of the dentate gyrus compared to wild-type mice.

Altogether, these results suggest that RAG1-KO mice are more sensitive to the acute neurotoxic of KA, notably CA3a,b pyramidal cells. In addition, and most strikingly, the absence of T and B cells leads to a fundamentally different outcome during the chronic phase, with a complete destruction of neurons in the hippocampal formation, accompanied by a pronounced microglial reaction.

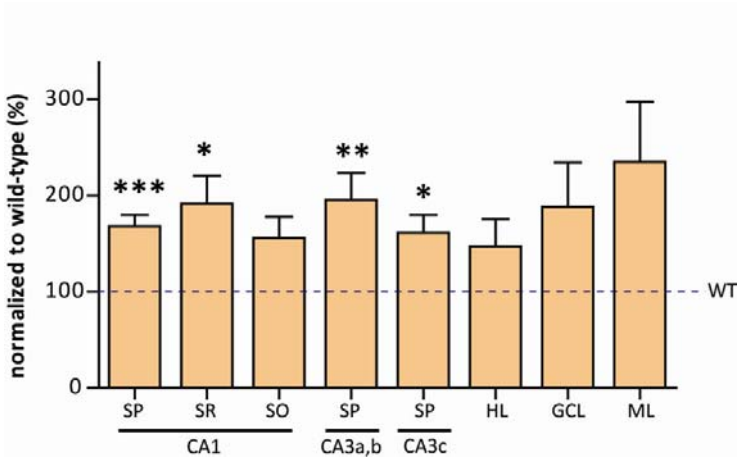

Figure 2.3: Increased CD68-IR in KA-treated RAG1-KO mice compared to wild-type mice. Densitometric analysis of CD68 staining confirmed the enhanced microglial activation occurring in RAG1-KO throughout the ipsilateral dorsal hippocampus 14 days after KA-injection in comparison to C57BL/6J mice (see Fig. 1.3). The difference was significant in the pyramidal layer and stratum radiatum of CA1, pyramidal layer of CA3a,b and CA3c, but not in the granule cell layer and molecular layer of the dentate gyrus. Values are given as percent of wild-type mice (indicated by a dashed line). (Two way ANOVA, $F_{1,158}$= 53.3; p<0.0001; Bonferroni post-test; * p<0.05, ** p<0.01, *** p<0.001). SP, stratum pyramidale; SR, stratum radiatum; SO, stratum oriens; HL, hilus; GCL, granule cell layer; ML, molecular layer; WT, wild-type (C57BL/6J).

To determine whether microglial cells mediate this destruction, or whether other components of innate immunity are involved, we investigated neutrophils in KA-treated wild-type and RAG1-KO mice.

Extensive cell loss in RAG1-KO mice mediated by neutrophils

To explore whether the pronounced degeneration of hippocampal formation in the immunodeficient mice was a phenomenon involving components of innate immunity, we performed Gr-1 immunohistochemistry in RAG1-KO and wild-type mice post-KA and –saline injection. The Gr-1 epitope, as detected by the RB6-8C5 antibody, is present in two molecules, Ly-6Gand Ly-6C, both markers of early myeloid lineage commitment, which are expressed on mature neutrophils.

Gr-1 immunoreactivity was absent in the hippocampus of immunodeficient mice after saline injection (Fig. 2.4A'). Instead, a diffuse staining was evident in wild-type mice (Fig. 2.4A) suggesting the possible expression of this marker by glial cells. Even at high magnification, we were not able to detect the characteristic lobulated nuclei of neutrophils. It was absent from neurons, as seen by the lack of staining in the pyramidal cell layer and granule cell layer (Fig. 2.4A). At 7-10 days post-KA injection, a diffuse staining was detected in wild-type mice reflecting the activation of microglial cells in the CA1 pyramidal cell layer (Fig. 2.4B). On the contrary, Gr-1-IR revealed the presence of a few, isolated Gr-1^+ cells in the hippocampal formation of RAG1-KO mice (Fig. 2.4B'). Surprisingly, the number of Gr-1^+ cells infiltrating the lesioned hippocampus in RAG1-KO mice was increased in CA1 at 10 days after KA, notably around the injection, while remaining rare in the dentate gyrus (Fig.2.4C'). Furthermore, in the group of severely lesioned mice, a massive infiltration of Gr-1^+ neutrophils occurred in dorsal hippocampus 14 days after KA injection in RAG1-KO mice (Fig. 2.4D') and persisted at 28 days post-KA (Fig. 2.4E'), coinciding with neurodegeneration. No Gr-1^+ cells were seen contralaterally in RAG1-KO mice (data not shown). No Gr-1^+ neutrophils were found in the brain parenchyma of the KA-injected hippocampus when the lesion was moderate (Fig. 2.4D) emphasizing their contribution to late neurodegeneration. Likewise, Gr-1^+ neutrophils were not seen in wild-type mice

14 post-KA. However, Gr-1-IR reflected microglial activation, as seen at earlier time points and emphasizing the granule cell dispersion in the dentate gyrus at 14 and 28 days post-KA (data not shown). At 28 days post-KA injection, robust neutrophil infiltration could be observed in five out of six RAG1-KO mice. In one case (Fig. 2.4E), Gr-1$^+$ neutrophils were few and mainly located in the pyramidal layer of the CA1.

The delayed infiltration of Gr-1$^+$ cells in the lesioned hippocampus of RAG1-KO mice and its complete absence in wild-type mice strongly suggests that they are responsible for the extensive neurodegeneration occurring during the chronic phase. In addition, these results suggest that the presence of T cells in wild-type mice prevents infiltration by neutrophils.

As a corollary, it appears unlikely that microglial cell activation is involved in neurodegeneration. Therefore, to uncover why their number increases so much at 14 and 28 days post-KA, we morphologically investigated potential interactions between microglia and neutrophils in RAG1-KO mice. To this end, we performed double immunofluorescence labeling using Gr-1 and Iba-1 as markers for

Figure 2.4: Selective infiltration of Gr-1$^+$ neutrophils in the dorsal hippocampus of KA-treated RAG1-KO mice. The infiltration was evaluated after 7, 10, 14 and 28 days post-KA injection in both genotypes (A-C, wild-type; A'-C' and D-E', RAG1-KO mice). (A) Saline-treated wild-type mice. Gr-1 immunoreactivity revealed a diffuse staining in the hippocampal formation, suggesting expression of this marker by microglial cells. Note the pyramidal cell layer and the granule cell layer of the dentate gyrus lacking Gr-1-IR. The contralateral side was comparable to the ipsilateral one (data not shown). (A') Gr-1-IR was undetectable in the ipsilateral hippocampus of RAG1-KO mice after saline injection. The contralateral hippocampus exhibited the same labeling pattern (not shown). (B) At 7 days post-KA injection, Gr-1 staining in wild-type mice weakly labeled activated microglial cells in CA1 pyramidal cell layer, coinciding with the increased CD68-IR shown in Figure 2.2. (B') In contrast, a few cells strongly positive for Gr-1 were evident in the ipsilateral (but not contralateral) hippocampus of RAG1-KO mice, representing neutrophils based on their morphology (see Fig. 2.5). (C) At 10 days-post-KA injection, Gr-1 staining was further enhanced in activated microglial cells of wild-type mice, whereas in RAG1-KO mice (C'), the number of Gr-1$^+$ neutrophils was massively increased in CA1 and CA3. (D-D') Infiltration of Gr-1$^+$ cells at 14 days post-KA was seen only in mice with severe neurodegeneration (see Fig. 2.1). It persisted at 28 days post-KA, with five out of six RAG1-KO mice showing massive neutrophil infiltration (E'). Only in one case (E), Gr-1$^+$ cells were few and restricted to the pyramidal layer of the CA1. Gr-1$^+$ cells were not detected contralaterally at any time-point analyzed. Scale bar (all panels) = 250µm.

Figure 2.4

Saline injection

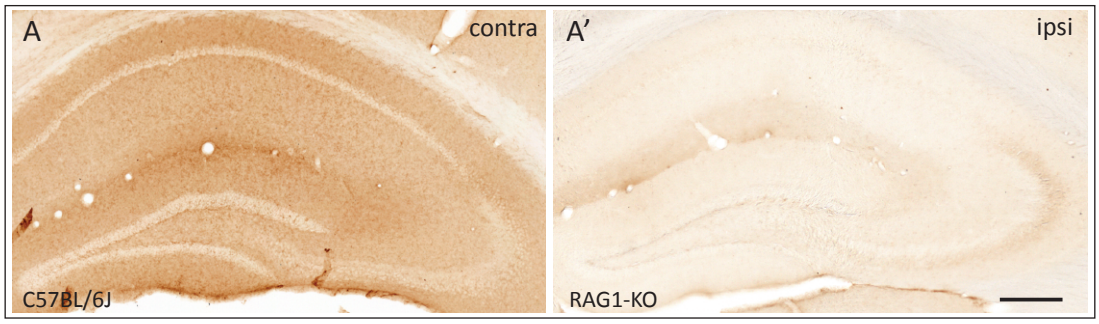

Kainate injection (latent phase)

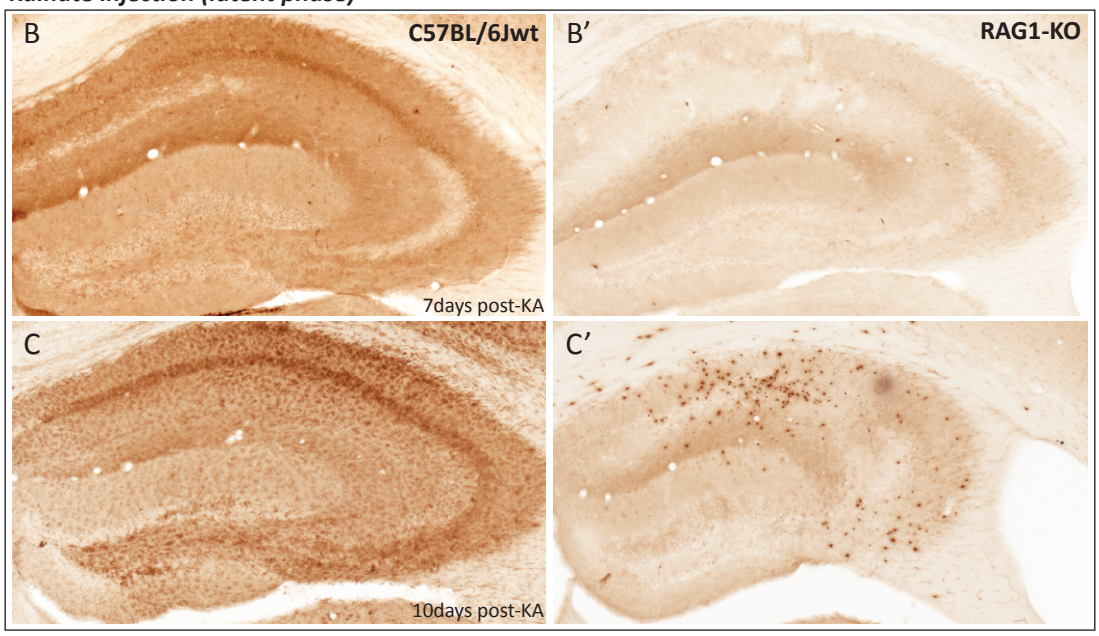

Kainate injection in RAG1-KO mice (chronic phase)

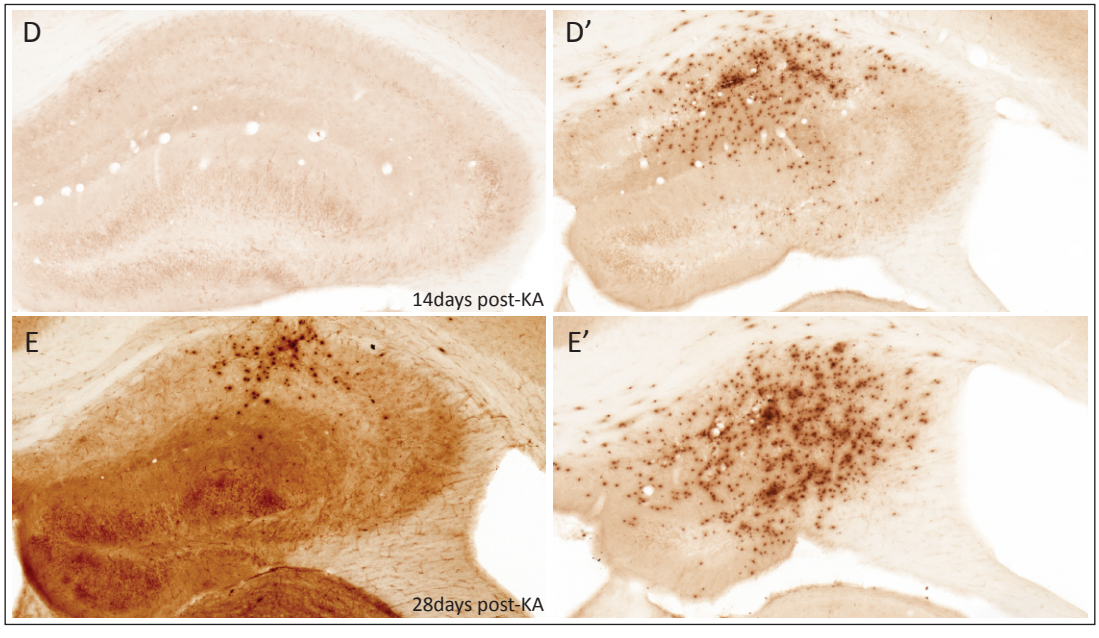

neutrophils and microglia, respectively, in combination with the nuclear dye Sytox green in hippocampal sections of RAG1-KO and wild-type mice. High resolution analysis by 3D-confocal laser scanning microscopy showed the characteristic lobulated nuclei of the neutrophils (Fig. 2.5B'- C'). No difference in morphology of activated microglial cells was detected after KA-injection in wild-type compared to RAG1-KO mice (Fig. 2.5A-B), characterized by their "bushy" appearance in both genotypes. As expected, no Gr-1^+ neutrophils were found in the dorsal hippocampus of wild-type mice at 14 days post-KA (Fig. 2.5A). Interestingly, in RAG1-KO mice, we observed that microglial cells closely surrounded Gr-1^+ neurotrophils with their processes (Fig. 2.5B-C). Indeed, Iba-1^+ microglial cells established direct contacts with most Gr-1^+ neutrophils and even engulfed some of them entirely, suggesting phagocytosis in the inflamed tissue. Therefore, these results suggest a potential protective role of microglial cells for phagocytosis of neutrophils in RAG1-KO mice.

Altogether, these results demonstrate that the absence of T cells aggravates the long-term degeneration of the epileptic hippocampus because it allows invasion of the lesioned hippocampus by neutrophils. Therefore, activation of innate immune responses is exacerbated in the absence of acquired immunity and might contribute to neutrophil-mediated neurodegeneration.

Figure 2.5: Engulfment of Gr-1^+ neutrophils by activated microglial cells in RAG1-KO mice, as visualized by double immunofluorescence staining with antibodies against Gr-1 (red) and Iba-1 (green). Nuclei were counterstained with Sytox™ green (blue). Images were acquired by confocal laser scanning microscopy and depicted as maximal intensity projection of 10-15 layers spaced by 0.5 µm. (A) Representative image from a wild-type mouse, stratum radiatum of CA1, 14 days post-KA injection, depicting the bushy appearance of activated microglial cells. The weak Gr-1 staining, observed in wild-type animals, was not here detected due to the laser setting used for these images (B-C) Images from a RAG1-KO mice 14 days post-KA injection. Gr-1^+ cells (red) were identified as neutrophils based on their lobulated nucleus, as shown in color-separated images (B'-C'); the * in panels B-B' indicates a transversally cut capillary; note that most nuclei belong to microglial cells, emphasizing their predominance in the lesioned tissue. Gr-1^+ neutrophils were surrounded by one or several activated microglial cell, often strongly labeled for Iba-1 (arrows in B), or even engulfed by them (arrowheads in B). These features are illustrated at higher magnification in C, depicting two microglial cells establishing direct contacts with a Gr-1^+ neutrophil, covering more of its plasma membrane. Scale bars: A-B = 20µm; C = 10µm.

Figure 2.5

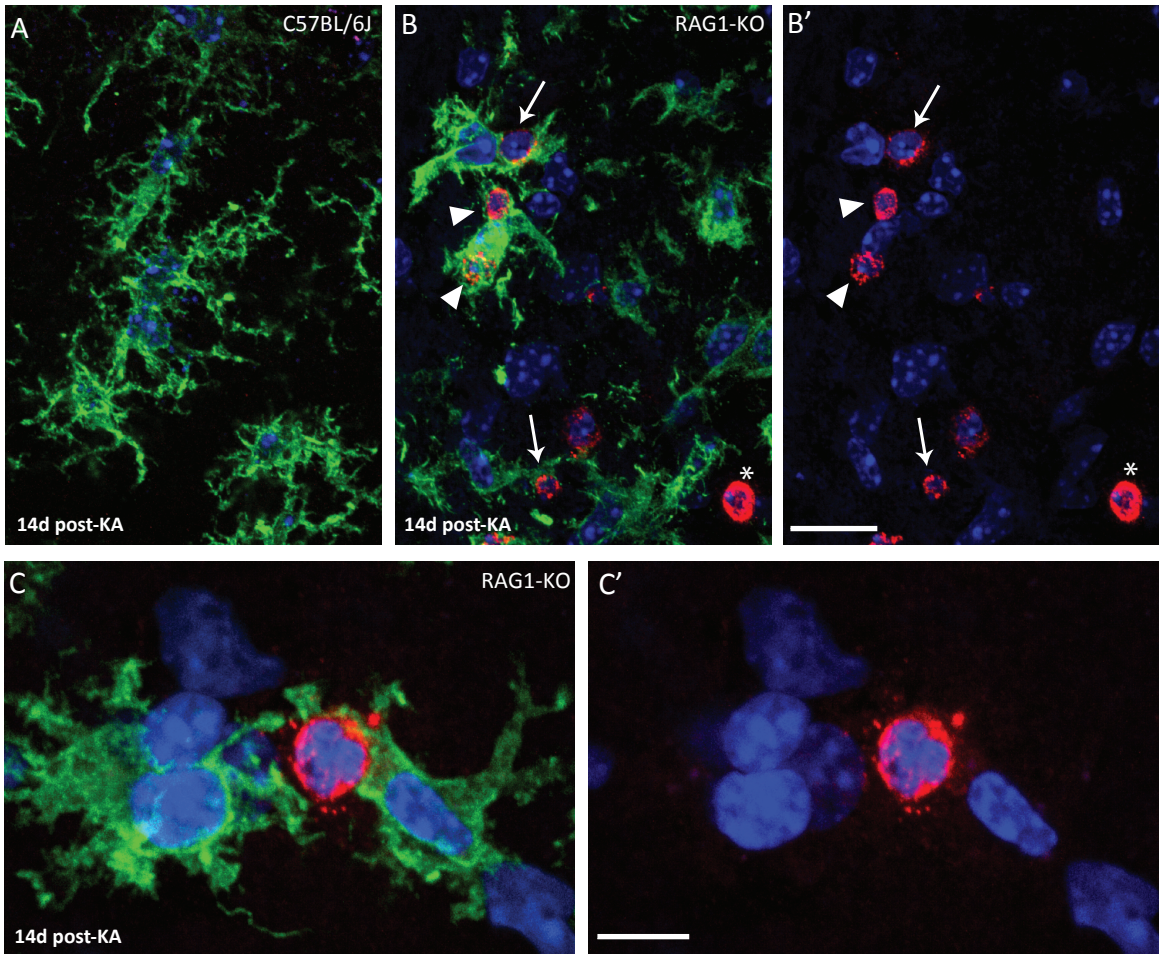
A
C57BL/6J
14d post-KA
B
RAG1-KO
14d post-KA
B'
C
RAG1-KO
14d post-KA
C'

Results

Chapter 3

Modulation of KA-induced neurodegeneration by interfering with intraparenchymal immune cell infiltration

The results in RAG1-KO mice demonstrated that the integrity of the immune system is crucial for controlling neurodegeneration in a KA-induced epileptic focus. The recruitment of specific leukocyte subsets, in particular $CD3^+$ T cells, from the blood stream into the hippocampus of KA-treated mice is not detrimental, unlike in many others neurological diseases. In fact, mice lacking adaptive immunity show a more severe phenotype compared to wild-type mice, due to massive neutrophil infiltration.

Furthermore, we have observed that microglial cell activation precisely mirrors the pattern of neurodegeneration, becoming more severe in RAG1-KO mice. However, in these mutants microglial cells appear to interact with neutrophils and possibly phagocytose them, presumably representing a line of defense rather than being detrimental for neuron survival. Besides microglia, we have uncovered the presence of macrophage-like cells in the dentate gyrus, raising the question of their origin (from resident microglia or peripheral monocytes) and role in this model of TLE. To address all these issues, we have performed three pharmacological interventions in wild-type and in RAG1-KO mice aiming at (1) neutralizing neutrophils, (2) preventing leukocyte diapedesis into the brain parenchyma, and (3) depleting mononuclear phagocytes in the blood and lymphoid organs. The results of these three experiments are presented sequentially in this chapter.

Neutrophil depletion by anti-Gr-1 treatment

Effects in wild-type mice

To determine whether neutrophil trafficking into the KA-treated hippocampus influences the acute phase of neurodegeneration, we treated C57BL/6J mice with a neutrophil-inactivating antibody, Ly6G/Gr-1. This antibody was selected because

it is a good tool to deplete neutrophils in blood and lymphoid system for up to 2-3 days after i.v. or i.p. administration (Stirling et al., 2009). Treatment was started one day before KA injection and repeated every 3-4 days until day 10 (total of 4 injections, see Materials and Methods). Neuropathological changes were evaluated in hippocampal sections by Cresyl violet staining. At 10 days post-KA treatment, the characteristic pattern of loss of neurons in the CA1 and CA3c area and in the hilus of the dentate gyrus was evident (Fig. 3.1A), along with microglial cell activation (Fig.3.1B) visualized by anti-CD68 immunohistochemistry. The CA3a,b area was partially preserved and the dispersion of dentate granule cells had started. These cytoarchitectural changes were essentially similar to those seen in wild-type animals at 10 days-post KA without anti-Gr-1 treatment. Examination of the spleen revealed a profound depletion of Gr-1$^+$ cells (data not shown). However, anti-Gr-1-treatment did not change the typical diffuse Gr-1 labeling seen in the hippocampus of mice injected with KA alone, confirming the expression of this marker by microglial cells.

Since microglial cell activation mirrors the pattern of the neuronal loss, we quantified CD68-IR in different regions of the hippocampal formation after repeated systemic Gr-1 treatment (Fig. 3.1D). Two-way ANOVA analysis showed no effect of treatment ($F_{1,112}$= 1.24; p= 0.2672) but significant difference amongthe regions analyzed ($F_{7,112}$= 17.59, p<0.0001); however, no single region

Figure 3.1: Anti-Ly6G/Gr-1 treatment in C57BL/6J mice has no significant effect on the morphological changes induced by unilateral intrahippocampal injection of KA. (A) Representative image of a Nissl-stained section showing the neuropathological alterations induced by KA in a mouse treated with anti-Gr-1 IgGs. The antibody treatment did not change the extent of the lesion, as seen 10 days post-KA injection. Neurodegeneration was evident in the CA1 and CA3c areas together with the loss of hilar neurons. The dispersion of granule cells had started in the dentate gyrus. (B) Corresponding pattern of CD68-IR, showing that anti-Gr-1 treatment did not modify the extent and pattern of microglia activation induced by KA. (C) Likewise, immunoperoxidase staining for Gr-1 showed that antibody treatment prior to sacrifice did not prevent the increased Gr-1-IR in activated microglial cells (arrowheads). (D) Densitometric analysis of CD68-IR in KA-mice treated with anti-Gr-1, compared to mice injected with KA-only. No single region of interest had significantly different intensity of CD68-IR in treated versus control mice (dotted line). CA1-3, Cornu Ammonis; SR, stratum radiatum; SO, stratum oriens; SP, stratum pyramidale; ML, molecular layer; GCL, granule cell layer; HL, hilus. Scale bar (A-C) = 250 μm.

Figure 3.1

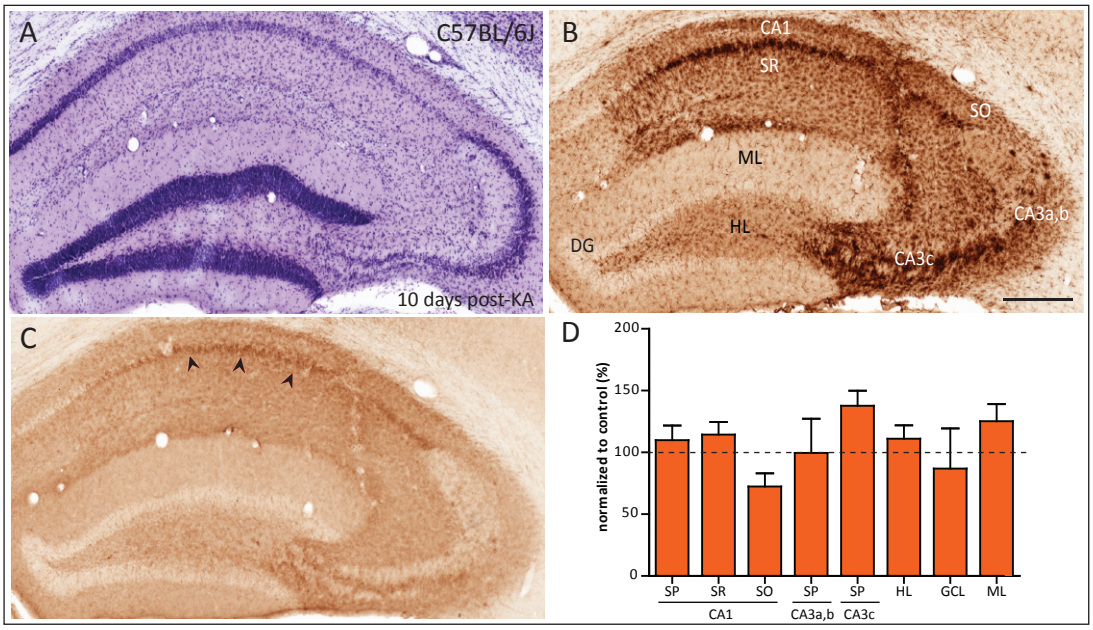
A
C57BL/6J
10 days post-KA
B
CA1
SR
SO
ML
HL
CA3a,b
DG
CA3c
C
D
normalized to control (%)
200
150
100
50
0
SP
SR
SO
SP
SP
HL
GCL
ML
CA1
CA3a,b
CA3c

showed a significantly different intensity of CD68-IR in Gr-1-treated versus control mice, as revealed by post-hoc analysis.

Altogether, these observations suggest that neutrophil depletion does not influence the pattern of KA-induced neurodegeneration and the activation of microglial cells in wild-type mice during the early phase of epileptogenesis. Therefore, the lesion caused by KA does not depend on neutrophils in this model of TLE.

Effects in RAG1-KO mice

Since KA injection in the dorsal hippocampus of RAG1-KO mice induces a robust neutrophil response around day 10 post-KA injection (see chapter 2), leading to a complete destruction of the hippocampal formation after 4 weeks, we asked whether neutralizing neutrophils with Gr-1 antibodies would prevent this exacerbated neuronal cell loss. For this purpose, we treated KA-injected RAG1-KO mice with anti-Gr-1 antibody, starting at day 6 post-KA and repeatedly every 3

Figure 3.2: Anti-Gr-1 treatment prevents the aggravated neuronal cell loss observed in RAG1-KO mice 14 days post-KA. (A, C) Cresyl violet staining of two different RAG1-KO mice treated with anti-Gr-1 illustrating the variability of the lesion induced by KA injection in the ipsilateral (ipsi) hippocampus. Both cases exhibited the typical cell loss in CA1, CA3c and hilus, as well as dispersion of granule cells. However, as shown in A, some mice exhibited extensive preservation of the CA3a,b area, as in wild-type, whereas others (C) were more affected. Nevertheless, the granule cell layer was well preserved in both cases. No morphological changes were seen in the contralateral hippocampus (data no shown). (B, D) Corresponding CD68 immunoperoxidase staining, confirming the neuroprotective effect of anti-Gr-1 treatment, notably in CA3a,b. (E-E') Densitometric analysis of CD68-IR; (E) A significant decrease of CD68-IR in the lesioned hippocampus, reaching almost 50% in the CA1-CA3pyramidal cell layer, CA1 stratum radiatum, and molecular layer, was observed in RAG1-KO mice treated with anti-Gr-1 IgGs compared to control (dashed line) (*<0.05, **<0.01; Bonferroni post-hoc tests), confirming reduced neurodegeneration (compare to Fig. 2.2D). (E') No significant difference was observed at 14 days post-KA when comparing antibody-treated RAG1-KO mice with wild-type mice (dashed line; Fig. 1.3B). (F-G) Gr-1 staining in two representative cases confirming that neutrophils were either much reduced (arrowheads in F) or absent (G) in RAG1-KO mice treated with anti-Gr-1 IgGs; in G, the arrows point to weakly stained activated microglial cells. CA1-3, Cornu Ammonis; SR, stratum radiatum; SO, stratum oriens; SP, stratum pyramidale; ML, molecular layer; GCL, granule cell layer; HL, hilus. Scale bars (A-D, F-G) = 250 µm.

Figure 3.2

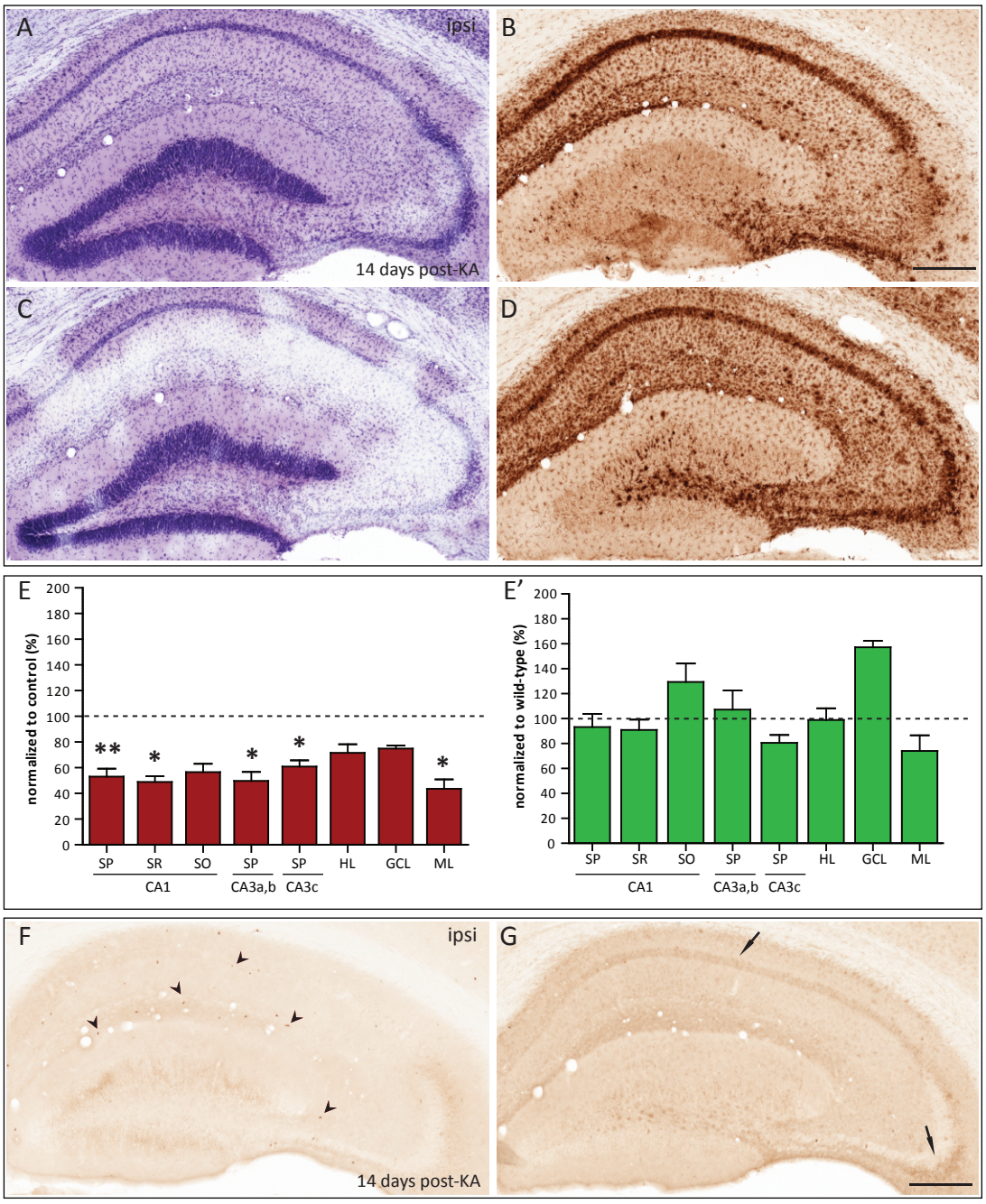
A
ipsi
14 days post-KA
B
C
D
E
normalized to control (%)
200
180
160
140
120
100
80
60
40
20
0
**
*
*
*
*
SP
SR
SO
SP
SP
HL
GCL
ML
CA1
CA3a,b
CA3c
E'
normalized to wild-type (%)
F
ipsi
14 days post-KA
G

days until day 14 (total 4 injections, see Materials and Methods) to deplete the pool of circulating neutrophils during the transition between the latent and chronic phase of epileptogenesis.

Neuropathological alterations and microglial cell activation were evaluated by Cresyl Violet and CD68 staining, respectively. The massive neuronal cell loss observed in RAG1-KO mice 14 days post-KA was diminished by anti-Gr-1 treatment, in particular in the dentate gyrus, where a prominent granule cell hypertrophy and dispersion became evident. Figure 3.2 illustrates 2 different RAG1-KO mice to illustrate the range of effects achieved with anti-Gr-1 treatment. In total 6 mice were analyzed. A profound loss of CA1 and CA3c pyramidal cells along with hilar neurons was evident unilaterally in Nissl-stained sections (Fig. 3.1A, C). The granule cell layer of the dentate gyrus was dispersed and in most cases devoid of pyknotic cells (Fig.3.2A). The extent of damage in CA3a,b was more variable, ranging from minimal (Fig. 3.2A) to severe (Fig. 3.2C). However, while loss of CA3a,b neurons was observed only in some cases, the CA1 area was always destroyed, as seen in wild-type mice. The pattern of microglial cell activation, as always, mirrored neuronal cell loss in the lesioned hippocampus, confirming the observations derived from Nissl-stained sections (Fig. 3.2B, D).

Densitometric analysis of CD68-IR in RAG1-KO mice to assess the pattern of degeneration after Gr-1 treatment (Fig. 3.2E, left) revealed a significant decrease in staining intensity (about 50%) in most regions of interest analyzed compared to RAG1-KO mice injected only with KA. Two-way ANOVA analysis confirmed this finding by revealing a significant effect of Gr-1 treatment ($F_{1,102}$ = 42.44; $p<0.0001$); as well as significant difference among the regions analyzed ($F_{7,102}$= 7.323; $p<0.0001$), notably in the CA1 pyramidal cell layer and stratum radiatum, and CA3a,b and CA3c pyramidal cell layer compared to untreated animals. In addition, when KA-injected RAG1-KO mice treated with anti-Gr-1 antibody were compared to KA-injected wild-type mice, two-way ANOVA analysis revealed no significant differences ($F_{1,64}$= 2.72; p= 0.1041) (Fig. 3.2E, right), confirming that the neutralization of neutrophils was sufficient to reverse the extensive neurodegeneration and microglial cell activation observed in RAG1-KO mice.

In conclusion, these results demonstrate that neutrophil depletion by anti-Gr-1 treatment is an effective step to prevent the severe neuronal cell loss observed in the lesioned hippocampus of RAG1-KO mice.

To confirm this conclusion we assessed immunohistochemically the degree of neutrophil infiltration within the KA-lesioned hippocampus after Gr-1 treatment in RAG1-KO mice. Intraparenchymal neutrophils were found only in one out of six mice treated with Gr-1 antibody (Fig. 3.2F, arrowheads), corresponding to the mouse exhibiting severe damage in CA3a,b (Fig. 3.2C). Instead, a diffuse staining was evident in the hippocampal formation of the other RAG1-KO mice (Fig. 3.2G), resembling the pattern seen in wild-type mice. Gr-1 labeling was sparse in the hippocampus, suggesting expression by activated microglial cells. Effective neutrophil depletion was confirmed in all animals by the analysis of Gr-1^+ cells in the spleen (data not shown).

Altogether, these results show that depleting neutrophils during the second week after KA treatment is sufficient to prevent the delayed neuronal cell loss observed in RAG1-KO mice. This finding confirms that neutrophil invasion in RAG1-KO mice is responsible for the extensive destruction of hippocampal neurons after KA injection.

The success of this anti-Gr-1 strategy to deplete neutrophils prompted us to investigate further the role of lymphocyte and monocyte trafficking across the endothelium in KA-treated mice. Therefore, we decided to perform experiments aiming to block diapedesis across the endothelium into the brain parenchyma.

Functional neutralization of the cell surface receptor α_4 integrin

Leukocyte infiltration from the periphery into the CNS is mediated by sequential interaction of different adhesion and signaling molecules on leukocytes and endothelial cells lining the vessel wall. It is well established that lymphocyte migration across this wall requires α_4 integrins to mediate initial contact with, as well as firm adhesion to, the endothelium. Therefore, we treated wild-type and RAG1-KO mice with α_4 integrin-specific mAb, starting 1 day before KA injection

and continuing every 3-4 days until day 14 (total 4 injections; see Materials and Methods). The effect of blockade of leukocyte adhesion mechanisms on KA-induced neuropathological alterations was evaluated by Cresyl Violet staining (Fig. 3.3). The left column (Fig. 3.3A, C, E) and right column (Fig. 3.3B, D, F) depict images from three wild-type and three RAG1-KO mice, respectively, to illustrate the range of effects observed in both genotypes. The total number of animals used for the experiment was 12 (6 mice per genotype).

In wild-type mice, blocking α_4 integrin caused a worsening of neuronal cell loss 14 days post-KA injection, with CA3b pyramidal cells being degenerated to various degrees (arrows in fig. 3.3A, C, E), in addition to the characteristic loss of hilar neurons, CA3c, and CA1 pyramidal cells. Only CA3a appeared unaffected in all the animals analyzed. The dispersion of granule cells in the dentate gyrus was more pronounced, albeit variable; sometimes, pyknotic cells were visible in the upper (Fig. 3.3A, arrowheads) or lower (Fig. 3.3C, arrowheads) blade of the dentate gyrus, suggesting partial neuronal cell loss in the granule cell layer. The contralateral hippocampus remained unaffected (data not shown).

By contrast, neurodegeneration was reduced in RAG1-KO mice treated with anti-α_4 integrin antibody, resembling the effect of anti-Gr-1 treatment. Thus, the KA-lesioned hippocampus was characterized by neuronal cell loss in CA1 and CA3c

Figure 3.3: Differential effects of α_4-integrin neutralization on the cytoarchitecture of KA-lesioned hippocampus in wild-type and RAG1-KO mice. Nissl-stained sections from three representative wild-type (A,C,E) and RAG1-KO mice (B,D,F) are shown14 days after KA injection to illustrate the variability of the outcome. While all mice exhibit the typical loss of CA1, CA3c, and hilar neurons, differences are evident in the dentate gyrus and in CA3a,b area. (A) Normal lesion in CA1-CA3, but partial destruction of granule cells with the upper blade of the dentate gyrus containing pyknotic cells (arrowheads). (C) In this mouse, the lesion was more extensive in CA3b (arrow); however, granule cell dispersion was more pronounced, except in the lower blade of the dentate gyrus, which contained some pyknotic cells (arrowheads). (E) Profound loss of neurons in the CA3a,b area (arrows), accompanied by marked but irregular granule cell dispersion. By contrast, anti-α_4-integrin treatment in RAG1-KO mice diminished the severe neuronal cells loss observed after KA injection alone. (B) Example of a mouse showing widespread protection in CA3 and in the dentate gyrus, resulting in strong granule cell dispersion. (D) Partial preservation of CA3a,b neurons, along with irregular granule cell dispersion. (F) Opposite case, with a severe lesion in CA1-CA3, but good preservation of the granule cell layer. Scale bar (all panels) = 250 μm.

Figure 3.3

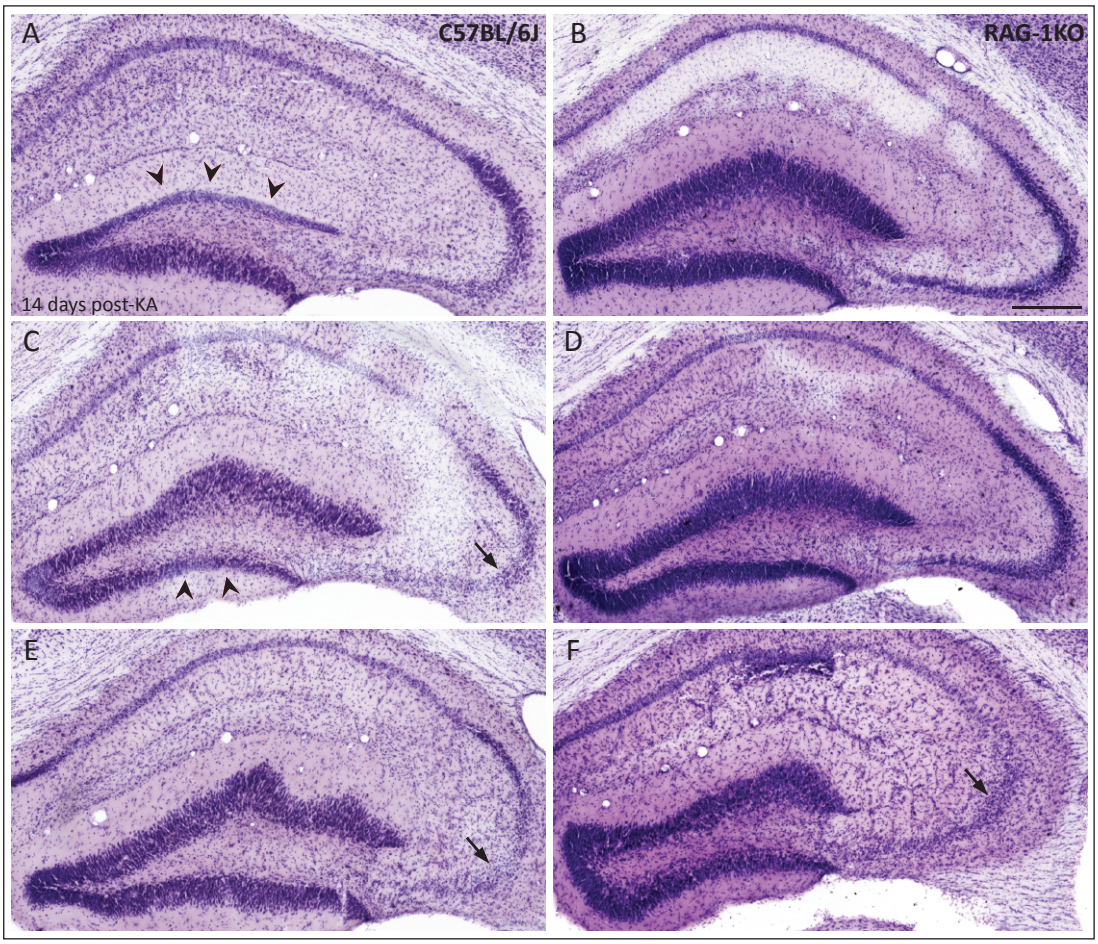

(Fig. 3.3B, D,F), whereas CA3a,b was well preserved in most mice. The dispersion of the granule cell layer was pronounced (Fig. 3.3B), resembling that seen in anti-Gr-1-treated mice (see Fig. 3.2). Only one RAG1-KO mouse treated with anti-α_4 integrin mAb showed a severe lesion (Fig.3.3F) with extensive degeneration of CA3a,b pyramidal cells and the presence of pyknotic granule cells in the dentate gyrus. However, this cell death did not cause any atrophy of the ipsilateral hippocampus and the cytoarchitecture of the entire hippocampus was still recognizable. These effects were restricted to the dorsal ipsilateral hippocampus and no changes in hippocampal cytoarchitecture were apparent contralaterally (data not shown).

As in the previous experiments, microglial cell activation, as monitored by CD68 staining, was intense in regions of neurodegeneration. Thus, in wild-type mice, more severe neuronal cell loss occurring in CA3 and dentate gyrus was mirrored by a corresponding increase in CD68-IR in these regions (Fig. 3.4A,C,E). Conversely, RAG1-KO mice (Fig. 3.4B, D, F) showed less CD-68-IR after anti-α_4 integrin treatment, to become similar to wild-type mice.

Densitometric analysis of CD68-IR partially confirmed these observations. However, two-way ANOVA analysis in wild-type mice showed no significant treatment effect, due to high variability between animals ($F_{1,120}$= 1.037; p=0.3105), but significant differences among the regions analyzed ($F_{7,120}$= 12.41; p<0.0001). By contrast, the activation of microglial cells was diminished by ~40%

Figure 3.4: Region-specific microglial cell activation in KA-treated C57BL/6J and RAG1-KO mice injected with anti-α_4-integrin antibody. The same mice as in Figure 3.3 are depicted, illustrating the presence of numerous $CD68^+$ cells in the dentate gyrus when the granule cell layer was affected. Extensive microglial activation occurred in CA1 and CA3c, but was variable in CA3a,b (arrowheads), mirroring neurodegeneration. Scale bar (A-F) = 250 µm. (G-G') Densitometric analysis of CD68 staining; (G) In wild-type mice, a significant effect of anti-α_4-integrin treatment was observed compared to non-treated mice, but post-hoc tests revealed no significant difference within any region of interest. (G') By contrast, intensity of CD68-IR was diminished by ~40% in CA1-CA3 area of RAG1-KO mice; however, post-hoc tests did not reach the significance level of 0.05, due to high inter-individual variability. Dashed lines refer to untreated mice injected only with KA. CA1-3: Cornu Ammonis, SR: stratum radiatum, SO: stratum oriens; SP: stratum pyramidale; ML: molecular layer; GCL: granule cell layer; HL: hilus.

Figure 3.4

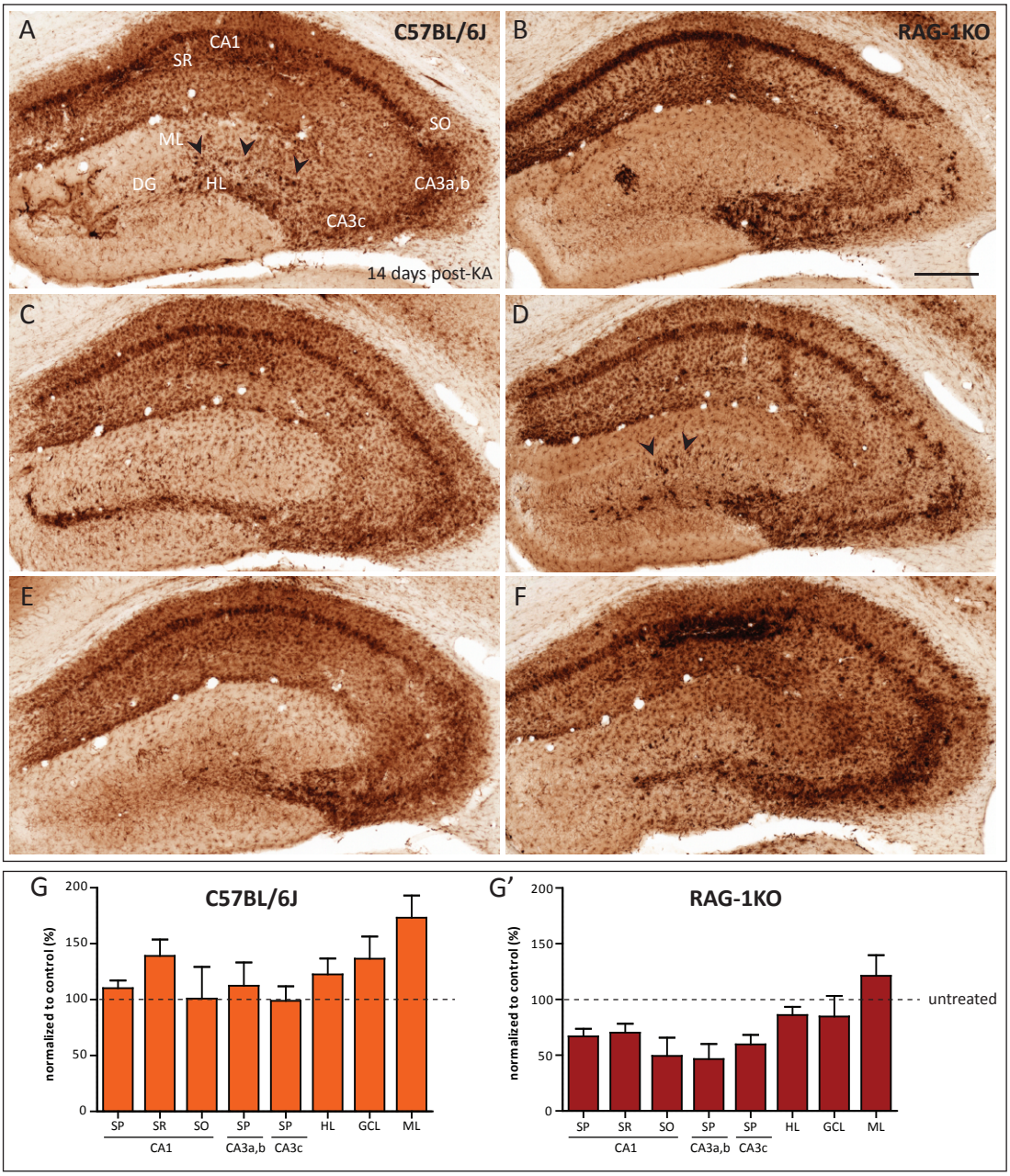
A
C57BL/6J
CA1
SR
SO
ML
DG
HL
CA3a,b
CA3c
14 days post-KA
B
RAG-1KO
C
D
E
F
G
C57BL/6J
normalized to control (%)
200
150
100
50
0
SP
SR
SO
SP
SP
HL
GCL
ML
CA1
CA3a,b
CA3c
G'
RAG-1KO
normalized to control (%)
untreated

in CA1-CA3 area of RAG1-KO mice treated with anti-α_4-integrin, resembling the effect of anti-Gr-1 treatment (see Fig. 3.2G). Two-way ANOVA analysis showed a significant effect of treatment ($F_{1,104}$=12.63; p=0.0006) and significant differences among the regions analyzed ($F_{7,104}$= 5.55; p<0.0001); however, post-hoc analysis indicated that no single region had significant difference in CD68-IR in anti-α_4-integrin-treated versus control mice.

Altogether, these results indicate that preventing immune cell infiltration into the brain by blocking interactions with the vascular endothelium has moderate detrimental effects in wild-type mice and moderate protective effects in RAG1-KO mice, suggesting differential roles of various types of immune cells (including $CD3^+$ T cells, neutrophils, and possibly macrophages). Therefore, we verified to which extent the antibody treatment affected brain penetration of these three cell types.

Reduced T cell and neutrophil infiltration

α_4 integrin is a molecule implicated in the recruitment of monocytes, lymphocytes and eosinophils to the site of inflammation. Recent experimental findings have shown that anti-α_4 integrin treatment main affects T cells, therefore interfering with their extravasation in the brain parenchyma. Here, we analyzed T cell infiltration in KA-treated wild-type mice treated with anti-α_4 integrin antibody.

Figure 3.5: Anti-α_4-integrin treatment reduces infiltration of $CD3^+$ T cells and Gr-1^+ neutrophils into the lesioned hippocampus 14 days after KA-injection. (A-A') Anti-CD3 staining showing diminished number of T cells in the KA-lesioned hippocampus compared to control wild-type mice (see Fig. 1.2). $CD3^+$ cells were mainly present in CA1 and CA3; inset in A is enlarged in A'. (B-E) Effect of anti-α_4-integrin treatment on Gr-1^+ neutrophil invasion. (B,D) Anti-α_4-integrin treatment did not change the typical Gr-1 immunoreactivity of activated microglial cells seen in wild-type mice 14 days post-KA injection. The images correspond to panels C and E of Figure 3.4. (C,E) Anti-α_4-integrin treatment effectively prevented infiltration of Gr-1^+ neutrophils into the hippocampal formation of RAG1-KO mice. Gr-1-IR revealed a diffuse staining similar to the one observed in wild-type mice, suggesting staining of activated microglial cells. The images correspond to panels D and F of Figure 3.4. Scale bars: (A-E) = 250 µm; A' = 50 µm.

Figure 3.5

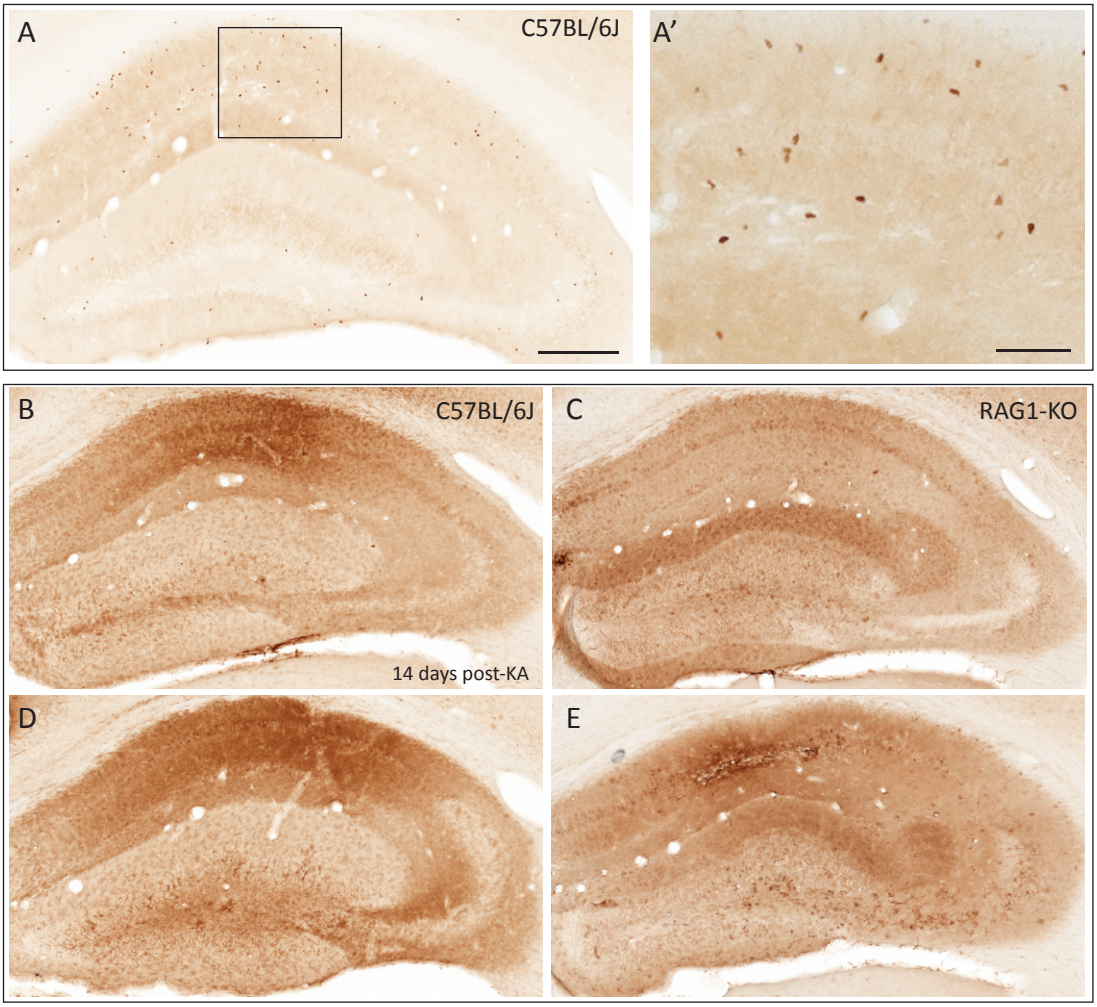

The number of $CD3^+$ cells infiltrating the brain parenchyma at 2 weeks post-KA injection (see Fig. 1.2) was markedly reduced, confirming the effectiveness of the treatment (Fig. 3.5A).

Earlier studies suggested that neutrophils do not express α_4 integrin; however, in recent years, consistent data from several laboratories have shown that this view might be erroneous (Johnston and Kubes, 1999; Ibbotson et al., 2001) and, although the level of expression is lower than in lymphocytes, it can be sufficient for neutrophil adhesion and migration. To test whether the partial protection seen in RAG1-KO mice was due to reduced neutrophil infiltration after administration of anti-α_4 integrin mAb, we used Gr-1 immunostaining at 2 weeks post-KA injection (Fig. 3.5B-E). In wild-type mice treated with anti-α_4 integrin no difference in Gr-1-IR was evident compared to animals treated with KA alone (see chapter 2); in particular, anti-α_4 integrin treatment did not change the typical diffuse staining seen in the hippocampus, suggesting expression of this marker by microglial cells. In RAG1-KO mice, $Gr\text{-}1^+$ neutrophils were not detected in the brain parenchyma (Fig. 3.5C, E). Like in wild-type mice, only a diffuse staining was detected in the hippocampal formation outlining the neuronal cell loss in CA1 region (Fig. 3.5C,E), notably around the injection site. In addition, some microglial cells distinctly positive for Gr-1 were visible in the CA3c area.

Figure 3.6: Anti-α_4-integrin treatment reduces $F4/80^+$ macrophage infiltration in KA-lesioned hippocampal formation, affecting the integrity of the granule cell layer. (A,C) Representative images of KA-lesioned hippocampus after 14 days in wild-type mice pre-treated with anti α_4-integrin. Sections from the same mice are shown in Figure 3.3A and C. The presence of large, strongly stained $F4/80^+$ macrophage-like cells in the molecular layer was evident in the vicinity of granule cells (arrows). Where the granule cell layer was degenerated and contained pyknotic cells (arrowheads), the macrophages were not visible; the insets are enlarged in A'-A'''. (B,D) Representative images of KA-lesioned RAG1-KO mice treated with anti-α_4-integrin, corresponding to the mice shown in Figure 3.3D and F. (B) Note the strong dispersion of the granule cell layer and the presence of macrophages in the molecular layer surrounding the dentate gyrus (arrows). (D) Representative image showing the presence of $F4/80^+$ cells where the granule cells of the dentate gyrus was dispersed (arrows), and their absence in a zone pyknotic cells (arrowheads). Insets are enlarged in B' and D'- D", in which the granule cell layer is outlined. In all cases, the number of $F4/80^+$ cells correlated with the thickness of the granule cell layer; they were absent where the granule cell layer was degenerated (A', D"). GCL, granule cell layer; HL, hilus; ML, molecular layer. Scale bar: (A-D) = 250 µm.

Figure 3.6

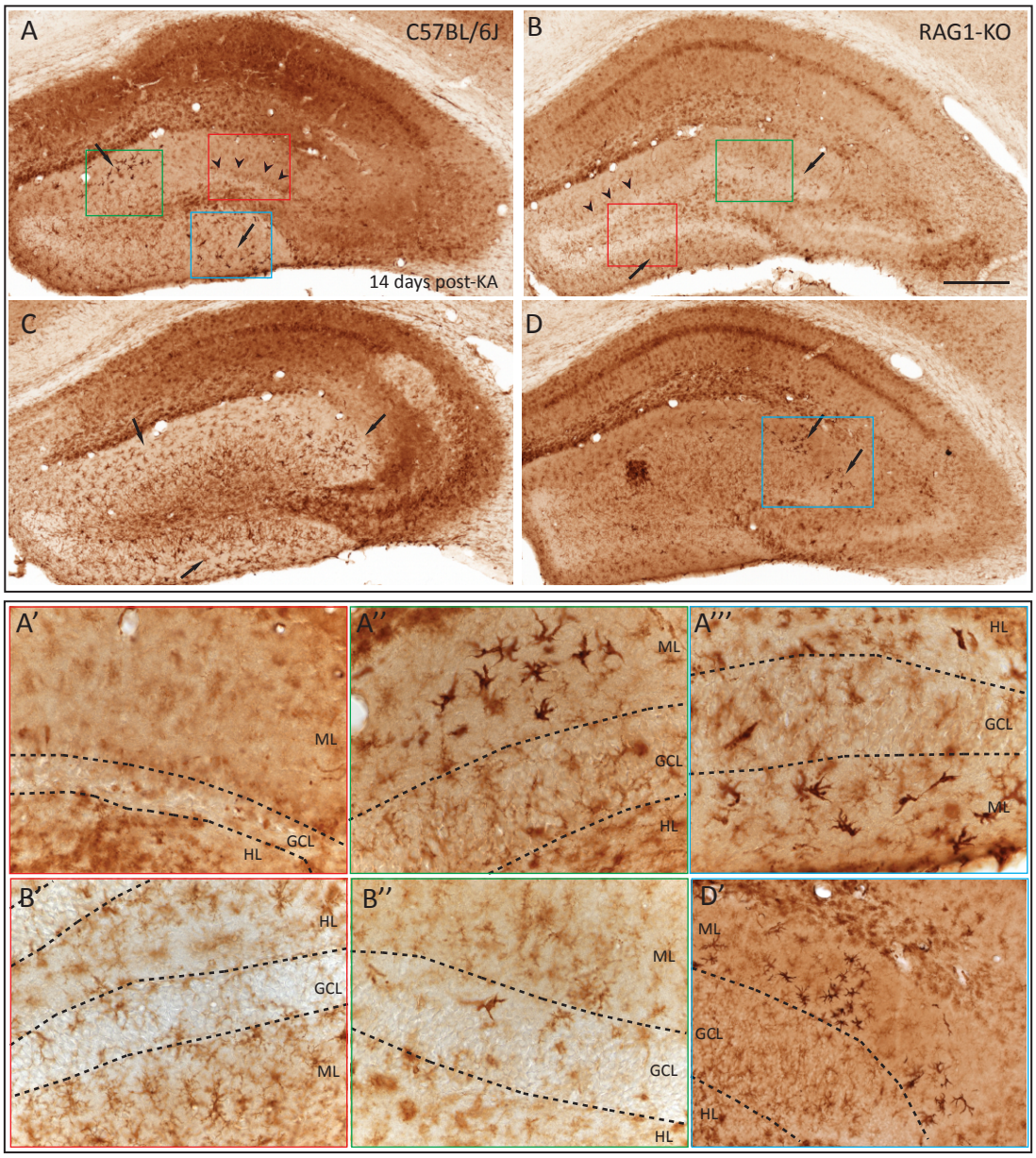
A
C57BL/6J
B
RAG1-KO
14 days post-KA
C
D
A'
ML
GCL
HL
A''
ML
GCL
HL
A'''
HL
GCL
ML
B'
HL
GCL
ML
B''
ML
GCL
HL
D'
ML
GCL
HL

The absence of neutrophils in the lesioned hippocampus of RAG1-KO mice correlates perfectly with the fact that neuronal cell loss in these animals was diminished; corroborating our hypothesis that neutrophil invasion seen in RAG1-KO mice in the absence of the adaptive immunity contributes to extensive neurodegeneration.

Reduced F4/80$^+$ macrophage infiltration

As described in chapter 1, we detected the selective presence of F4/80$^+$ macrophage-like cells in the molecular layer of the dentate gyrus following KA-induced degeneration. When KA-treated wild-type mice received anti-α_4 integrin IgGs, neurodegeneration was more severe, notably in the dentate gyrus. Therefore, we asked whether this unexpected result could be due to absence of macrophages. The presence of F4/80$^+$ cells after neutralization of α_4 integrin was evaluated by immunoperoxidase staining. Overall, a decreased number of these cells was detected in antibody-treated mice compared to mice injected with KA-only. Thus, in a very consistent manner, we observed F4/80$^+$ cells in the molecular layer of the dentate gyrus only where the granule cell layer was clearly dispersed (arrows in Fig. 3.6A, C). On the contrary, these large, strongly positive F4/80$^+$ cells were missing in zones where granule cells were pyknotic (arrowheads in Fig. 3.6A). In such cases, they were replaced by activated microglia, moderately stained for F4/80. Importantly, no F4/80$^+$ cells were visible in the hippocampus (CA1-CA3 areas).

Figure 3.7: Regression analysis of the correlation between granule cell dispersion and density of F4/80$^+$ macrophages. The granule cell layer was subdivided in 6 equal segments and the thickness of each segment, as well as the number of F4/80$^+$ cells found in the granule cell layer and molecular layer of each segment was calculated (see Materials and Methods). Scatter plots depict data from KA-injected mice treated with anti-α4 integrin compared to untreated mice. Regression analysis in each genotype showed a significant correlation in both groups of mice. In addition, effect of anti- 4-integrin treatment was reflected by significantly reduced thickness of the granule cell layer and significantly reduced number of F4/80$^+$ macrophages, occurring in both genotypes. GCL, granule cell layer.

Figure 3.7

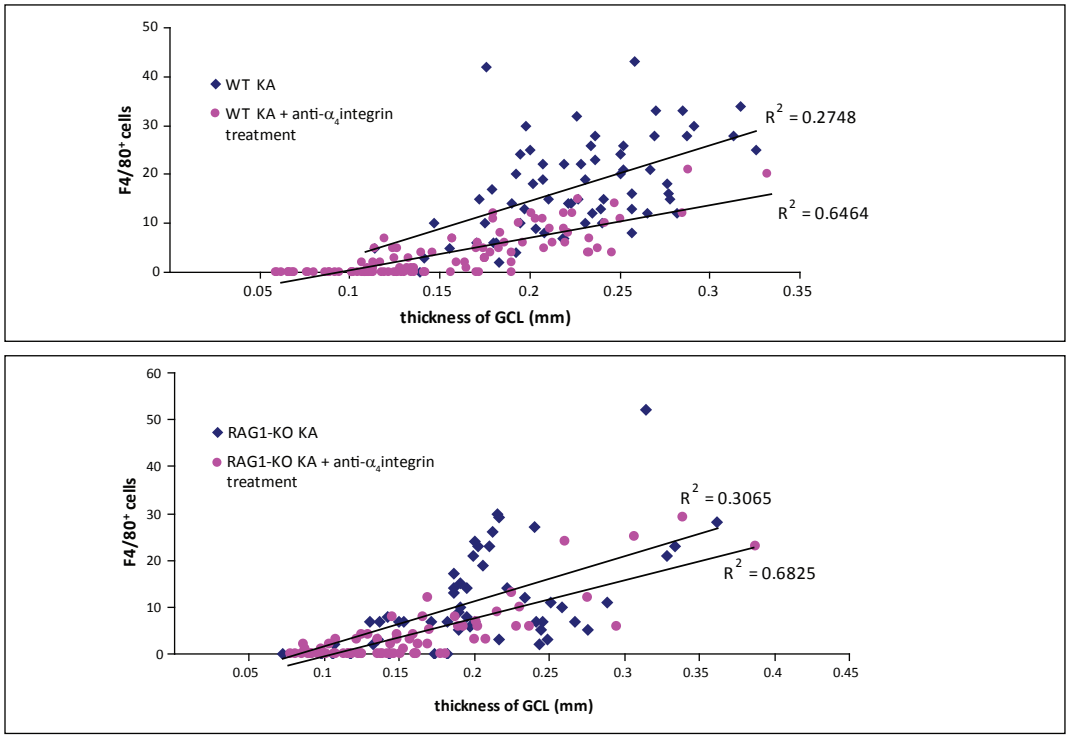
WT KA
WT KA + anti-α4 integrin treatment
R2 = 0.2748
R2 = 0.6464
F4/80+ cells
thickness of GCL (mm)
RAG1-KO KA
RAG1-KO KA + anti-α4 integrin treatment
R2 = 0.3065
R2 = 0.6825
F4/80+ cells
thickness of GCL (mm)

Likewise, F4/80 staining in KA-treated RAG1-KO mice that received anti-α_4 integrin IgGs showed a marked accumulation of macrophages in the molecular layer of the dentate gyrus when the granule cell layer was strongly dispersed (Fig. 3.6B). The only case in which we did not detect them, were when no or very little granule cell dispersion had occurred in the lesioned hippocampus (Fig. 3.6D). The precise correspondence between the presence of macrophage-like cells and the enlargement of the granule cell layer of the dentate gyrus is illustrated at high magnification in the bottom of Figure 3.6.

We next performed a quantitative analysis to correlate the dispersion of the granule cell layer and the presence of macrophages. For this purpose, we subdivided the granule cell layer into 6 equal segments (3 in the upper blade and 3 in the lower blade), measured the thickness of the granule cell layer in each segment, and counted the number of F4/80$^+$ cells in the granule cell layer and molecular layer in each segment (Fig. 3.7F). The analysis was performed in 4 sections per mouse (KA-treated, with or without anti-α_4 integrin administration), yielding 24 pairs of data per mouse. Three main different conditions could be identified: 1) pronounced dispersion of the granule cell layer (thickness > 200 μm) and high number of F4/80$^+$ macrophage-like cells (>15 cells per segment); 2) moderate dispersion of the granule cell layer (thickness ≈ 150 μm) and few macrophages (5-10 per segment); 3) no dispersion, sometimes presence of pyknotic cells in the granule cell layer, and absence of F4/80$^+$ cells. All these conditions could be found in a given section analyzed, as shown in Figure 3.6A. Regression analysis (thickness of granule cell layer versus number of F4/80$^+$ cells) revealed a significant correlation in both genotypes.

Based on these findings, we can say that macrophage infiltration in the dentate gyrus is beneficial for the survival of granule cells and might even promote their dispersion. We hypothesize that these macrophages release some trophic factors allowing granule cell survival and dispersion after KA injection.

Altogether, these results show that anti-α_4 integrin treatment produces mixed effects in wild-type and RAG1-KO mice by preventing entry of beneficial cells (i.e., macrophages) and detrimental cells (i.e., neutrophils in RAG1-KO mice) into the brain parenchyma. Moreover, these results suggest a possible link between

granule cell dispersion and macrophages infiltration. To establish a causal relationship between these phenomena and demonstrate that these macrophages originate from the periphery rather than from resident microglial cells, we next investigated the effect of macrophage depletion in wild-type and RAG1-KO mice.

Macrophage depletion by clodronate liposome

Differential effects on KA-induced neurodegeneration of wild-type and RAG1-KO mice

To further our knowledge of the origin and role of macrophages in the KA mouse model, we depleted peripheral monocytes and macrophages using clodronate liposomes, first administered two days before KA injection and continuing every 3 days until day 10 post-KA (total 4 injections, see Materials and Methods for details). The analysis was then performed similarly to that described for mice treated with anti-α_4 integrin antibodies, using Cresyl violet staining and immunohistochemistry for CD-68, Gr-1, and F4/80 (see previous section).

Liposomes are artificially prepared lipid vesicles, consisting of concentric phospholipid bilayers entrapping aqueous compartments. They can be used to encapsulate strongly hydrophilic molecules dissolved in aqueous solutions, such as clodronate, a toxic bisphosphonate. After systemic injection, liposomes are ingested and digested by mononuclear phagocytes causing intracellular release and accumulation of clodronate, leading to apoptosis. Despite these effects, liposomes combined with the KA injection were relatively well tolerated by the mice in this study; however, the dose had to be reduced in RAG1-KO mice (0.5 mg/20 g instead of 1.5 mg/20 g) to limit mortality. Effectiveness of the treatment was verified by F4/80 immunostaining in the spleen (not shown).

The neuropathological alterations in hippocampal sections were analyzed by Cresyl Violet staining at 10 days after KA injection. Figure 3.8 demonstrates the effect of repeated liposome administration in wild-type (left column) and RAG1-KO mice (right column). For each genotype, 4 different animals are shown,

illustrating the range of effects obtained upon macrophage depletion. 8 animals for wild-type and 10 for RAG1-KO were treated with clodronate liposome; in each group 6 mice survived and were used for analysis. In wild-type mice, a general worsening of the KA-lesion was evident in the CA3a,b area and in the dentate gyrus, with the granule cell layer being affected to variable degrees: 1) Pronounced and irregular dispersion of the granule cell layer, without evidence for loss of granule cells (Fig. 3.8A). 2) Moderate dispersion of the granule cell layer, with few pyknotic granule cells being present (Fig. 3.8B). 3) Mixture of granule cell dispersion and degeneration, evidenced by pyknotic cells in entire portions of the granule cell layer (Fig. 3.8C). 4) Lack of granule cell dispersion and presence of pyknotic granule cells (Fig. 3.8D). These results confirm that macrophages have a protective effect against KA lesion in the dentate gyrus and possibly on the CA3a,b area.

In contrast, in RAG1-KO mice, clodronate liposome treatment markedly reduced neurodegeneration in CA3 and in the dentate gyrus, but again with variable effects on pyramidal cells and dentate gyrus granule cells. Four different situations are illustrated in Figure 3.8: 1) Lesion resembling a wild-type mouse (Fig. 3.8E). 2) and 3) Preservation of the CA3a,b area, but variable dispersion of the granule cell layer (Fig. 3.8F,G). 4) Severe lesion, resembling case 3 in the wild-type mice (Fig. 3.8H). These results apparently replicate those seen in mice treated with anti-α4 integrin antibodies, suggesting that depletion of macrophages might interfere with neutrophil infiltration in RAG1-KO mice.

Figure 3.8: Effects of clodronate liposome treatment on neurodegenerative changes induced by KA injection in the dorsal hippocampus of wild-type and RAG1-KO mice. Nissl-stained sections at 10 days post-KA injection from four different wild-type (A, C, E, G) and RAG1-KO (B, D, F, H) mice are depicted, illustrating variable damage in the granule cell layer and CA3a,b area. Sections are sorted by increasing severity of alterations in the granule cell layer; arrowheads point to the presence of pyknotic cells. Secondarily, damage in the CA3a,b areas is indicated by arrows. In panels B, D and F, G dispersion is reduced in parts of the GCL that are devoid of pyknotic cells. Note that lesion severity in CA3a,b was overall less marked in RAG1-KO compared to wild-type mice. The contralateral hippocampus remained unaffected in both genotypes (data not shown). Scale bar (all panels) = 250 µm.

Figure 3.8

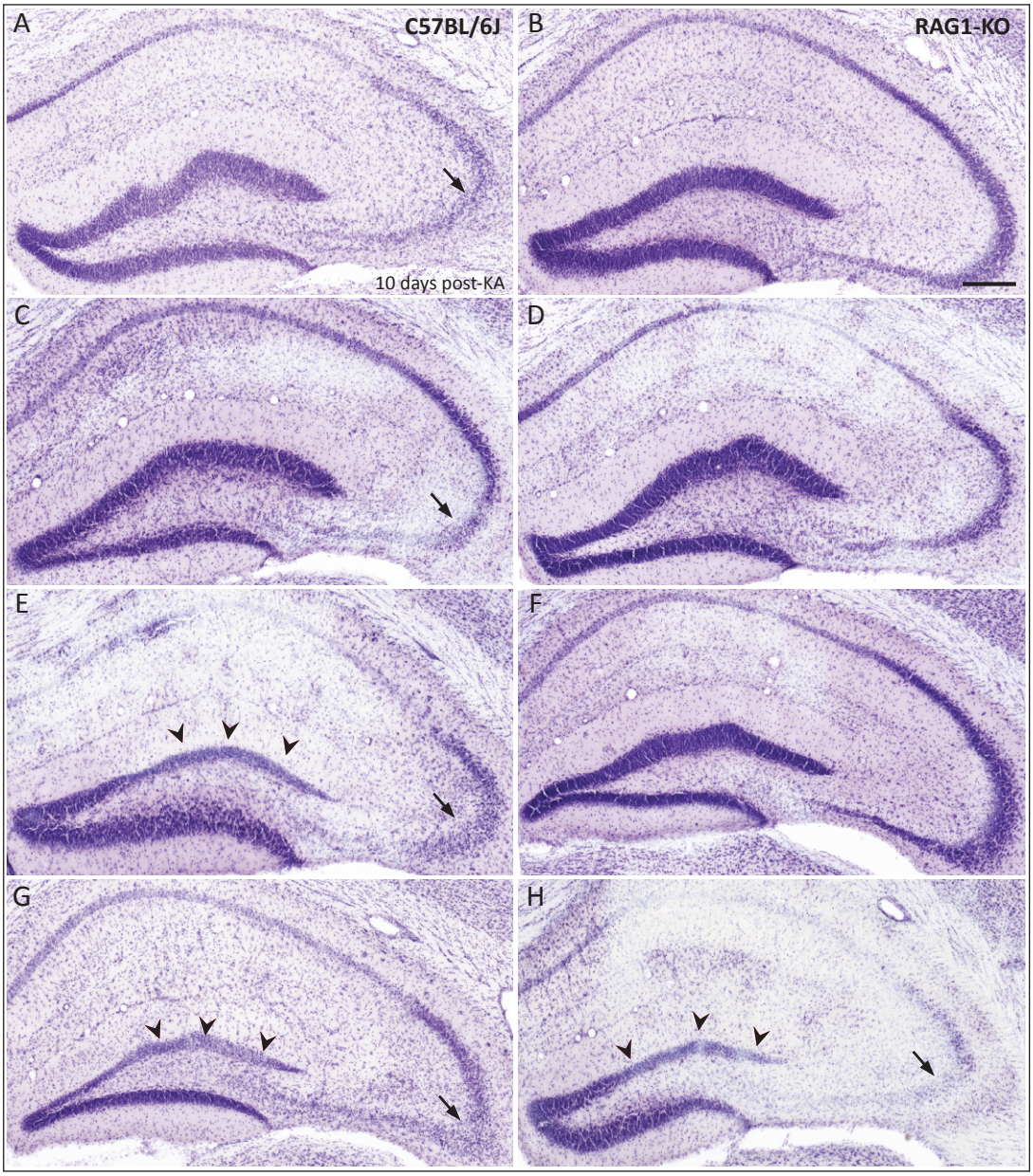

Microglial cell activation after macrophage depletion

To confirm these findings, analysis of microglial cell activation was done with CD68 staining. In wild-type mice treated with clodronate liposomes, at 10 days-post KA, increased neuronal cell loss occurring in CA3a,b and the dentate gyrus was mirrored by a corresponding increase in CD68-IR in these regions (Fig. 3.9A,B,C,D). By contrast, clodronate liposome treatment in RAG1-KO mice resulted in reduced activation of microglial cells, as shown in Figure 3.9 (E,F,G,H). In particular, CD68-IR was much reduced in the CA1-CA3c area and in the hilus compared to either RAG1-KO mice injected with KA only, or to wild-type mice treated with clodronate liposomes.

Densitometric analysis of CD68-IR in wild-type and RAG1-KO mice confirmed our visual impression (Fig. 3.9I). In wild-type mice, two-way ANOVA analysis showed a significant effect of the treatment ($F_{1,134}$=37.15; p<0.0001), as well as significant differences among the regions analyzed ($F_{7,134}$= 19.48; p<0.0001), notably in the stratum radiatum of CA1 and in the pyramidal layer of CA3a,b compared to control mice. By contrast, in RAG1-KO mice, two-way ANOVA analysis revealed a significant decrease in CD68-IR in liposome-treated mice ($F_{1,128}$=48.74;

Figure 3.9: Effect of clodronate liposome treatment on microglial cell activation in KA-treated dorsal hippocampus of wild-type and RAG1-KO mice, as visualized by CD68 immunoperoxidase staining. The same wild-type (A, C, E, G) and RAG1-KO (B, D, F, H) mice as in Figure 3.8 are depicted, illustrating that activation of microglial cells in both genotypes precisely reflected the extent of neurodegeneration, notably in the granule cell layer (arrowheads) and in CA3a,b (arrows). Side-by-side comparison of the two genotypes showed that microglial cell activation was more severe in wild-type than in RAG1-KO mice, underscoring the widespread protection induced by macrophage depletion in mutants and the more severe degeneration in wild-type. The contralateral side showed only a faint CD68-IR in resting microglial cells (data not shown). Scale bar (A-H) = 250 µm. (I-I') Densitometric analysis of CD68-IR. (I) Post-hoc analysis showed that macrophage depletion in wild-type mice induced a significantly more pronounced activation of microglial cells in CA1 stratum radiatum and CA3a,b pyramidal cell layer compared to mice treated with KA-only (*<0.05). (I') By contrast, in RAG1-KO mice, a significant decrease of CD68-IR was seen in all hippocampal regions of interest analyzed (*P<0.05; **P<0.01). CA1-3, Cornu Ammonis; SR, stratum radiatum; SO, stratum oriens; SP, stratum pyramidale; ML, molecular layer; GCL, granule cell layer; HL, hilus.

Figure 3.9

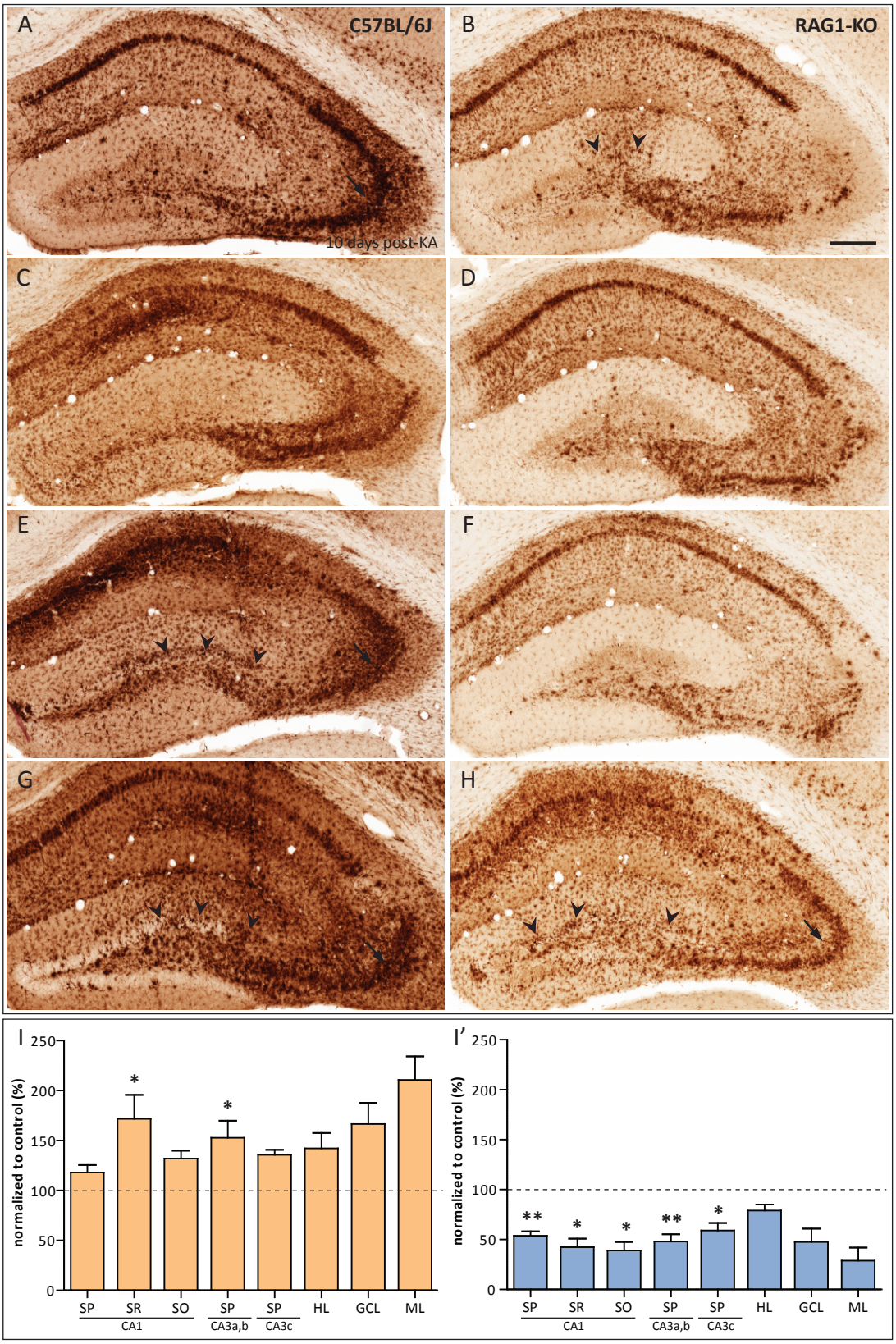
A
C57BL/6J
10 days post-KA
B
RAG1-KO
C
D
E
F
G
H
I
normalized to control (%)
250
200
150
100
50
0
SP
SR
SO
SP
SP
HL
GCL
ML
CA1
CA3a,b
CA3c
I'
normalized to control (%)
250
200
150
100
50
0
SP
SR
SO
SP
SP
HL
GCL
ML
CA1
CA3a,b
CA3c

$p<0.0001$) as well as significant differences among the regions analyzed ($F_{7,128}= 11.5$; $p<0.0001$), notably in the pyramidal layer and stratum radiatum of CA1 and in the pyramidal cell layer of CA3a,b and CA3c compared to untreated animals.

Interference with neutrophil infiltration in RAG1-KO mice

To explain the reduced neurodegeneration seen in RAG1-KO mice treated with clodronate liposomes, we investigated the effect of macrophage depletion on the recruitment of Gr-1^+ neutrophils. At 10 days post-KA, Gr-1^+ cells were absent in wild-type mice; a diffuse staining was evident in the hippocampal formation reflecting again the expression of this marker by microglial cells (Fig. 3.10A and B). These changes were observed in all the animals analyzed, indicating that clodronate liposome treatment had no effect on cells expressing Gr-1 in wild-type mice. Macrophage depletion in RAG1-KO mice led to blockade of neutrophil infiltration into the KA-lesioned hippocampus; diffuse and sparse Gr-1 staining was visible in the hippocampal formation, in particular in the stratum lacunosum moleculare and in CA3a,b area (Fig. 3.10C), as seen in mice treated with antibodies against α_4-integrin (Fig. 3.5). No Gr-1^+ neutrophils were found in the brain parenchyma, except in one mouse, which showed a few isolated Gr-1^+ neutrophils mainly localized in the CA1 pyramidal layer and stratum oriens (Fig. 3.10D). These results indicate that macrophage depletion by clodronate liposome treatment interferes with neutrophil infiltration, leading to a less severe lesion induced by KA in RAG1-KO mice.

Figure 3.10: Clodronate liposome-treatment prevented Gr-1^+ neutrophil infiltration in the dorsal hippocampus of RAG1-KO mice, as seen at 10 days post-KA injection. Gr-1 staining in wild-type (A, C) and in RAG1-KO (B-D) mice after clodronate liposome treatment revealed a diffuse staining in the hippocampal formation, with notably increased intensity in the CA1 area, suggesting the expression of this marker by microglial cells similar to that observed in animals treated with KA only. No Gr-1^+ neutrophils were detected in the brain parenchyma, except in one case (D), which showed a few Gr-1^+ cells in CA1 close to the injection site. Scale bar (all panels) = 250 µm.

Figure 3.10

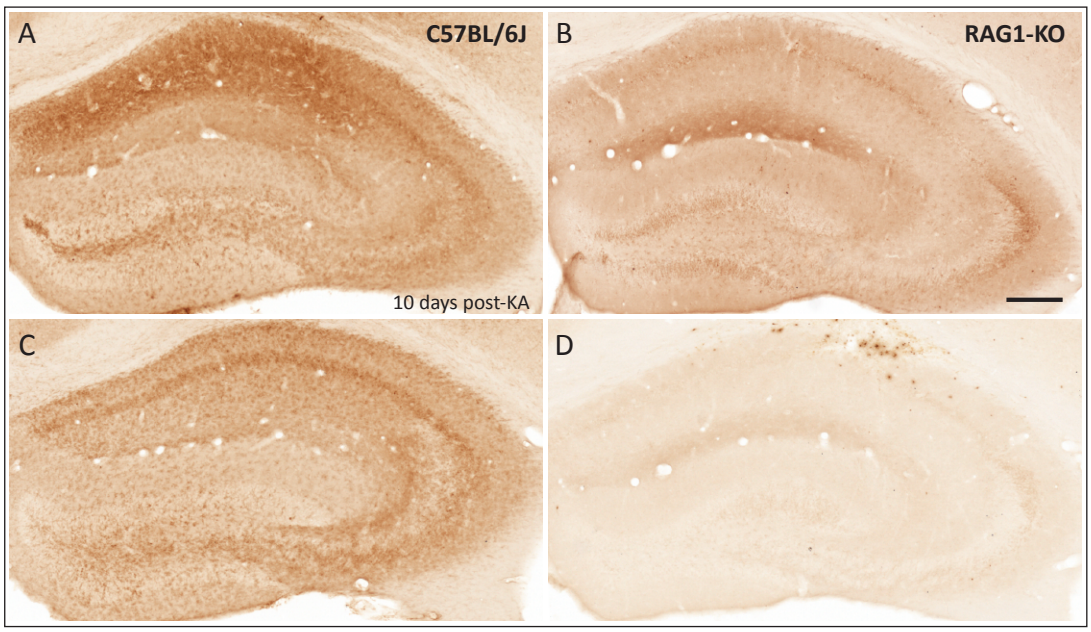

Reduced macrophage infiltration in the dentate gyrus of KA-treated mice

Clodronate liposome treatment had a deleterious effect on the integrity of the granule cell layer, in particular in wild-type mice. Therefore, we wondered whether this effect was due to the absence of macrophages, as seen after blockade of α_4 integrin (Fig. 3.6). Therefore, we examined the presence of macrophages in treated mice using F4/80 immunohistochemistry. At 10 days post-KA, a clear reduction of macrophages was observed in the KA-lesioned hippocampus in both genotypes (Fig. 3.11A-H), compared to KA-injected mice not treated with clodronate liposomes. Furthermore, the variable degree of granule cell dispersion and degeneration corresponded precisely to the local reduction of F4/80$^+$ macrophages in the dentate gyrus. This is best seen in the high magnification images at the bottom of Figure 3.11. In particular, absence of F4/80$^+$ cells strictly correlated with the presence of pyknotic cells in the granule cell layer, whereas the variable granule cell dispersion reflected incomplete depletion of macrophages. Furthermore, since F4/80 is also expressed by activated microglial cells, we could observe their presence in zones of the granule cell layer containing degenerating cells (Fig. 3.11B, C, H). These results replicate the findings obtained in mice treated with anti-α_4-integrin, suggesting a local protective effect on granule cells provided by macrophages penetrating into the dentate gyrus.

Figure 3.11: Clodronate liposome treatment reduces the density of macrophages in the dentate gyrus of wild-type and RAG1-KO mice after KA-injection, as visualized by F4/80 immunoperoxidase staining. Sections from the same wild-type (A, C, E, G) and RAG1-KO mice (B, D, F, H) as in Figures 3.8 and 3.9 are depicted. Since F4/80-IR also labels activated microglial cells, the same overall differences between genotypes were evident as seen with CD68-IR (see Fig. 3.9). In addition, in both genotypes, clodronate liposome treatment induced a strong decrease in the number of F4/80$^+$ cells in the molecular layer of the dentate gyrus. Close examination of the sections, best seen in the enlarged insets (D', E', E'', F', G', H'), revealed isolated F4/80$^+$ cells in sectors where granule cell dispersion had occurred (F', G'); F4/80$^+$ cells were undetectable where the granule cell layer contained pyknotic cells, but were replaced by activated microglial cells, moderately stained for F4/80 (E', E'', G', H'). Dashed lines outline the boundaries of the granule cell layer. GCL, granule cell layer; HL, hilus; ML, molecular layer. Scale bar = 250µm.

Figure 3.11

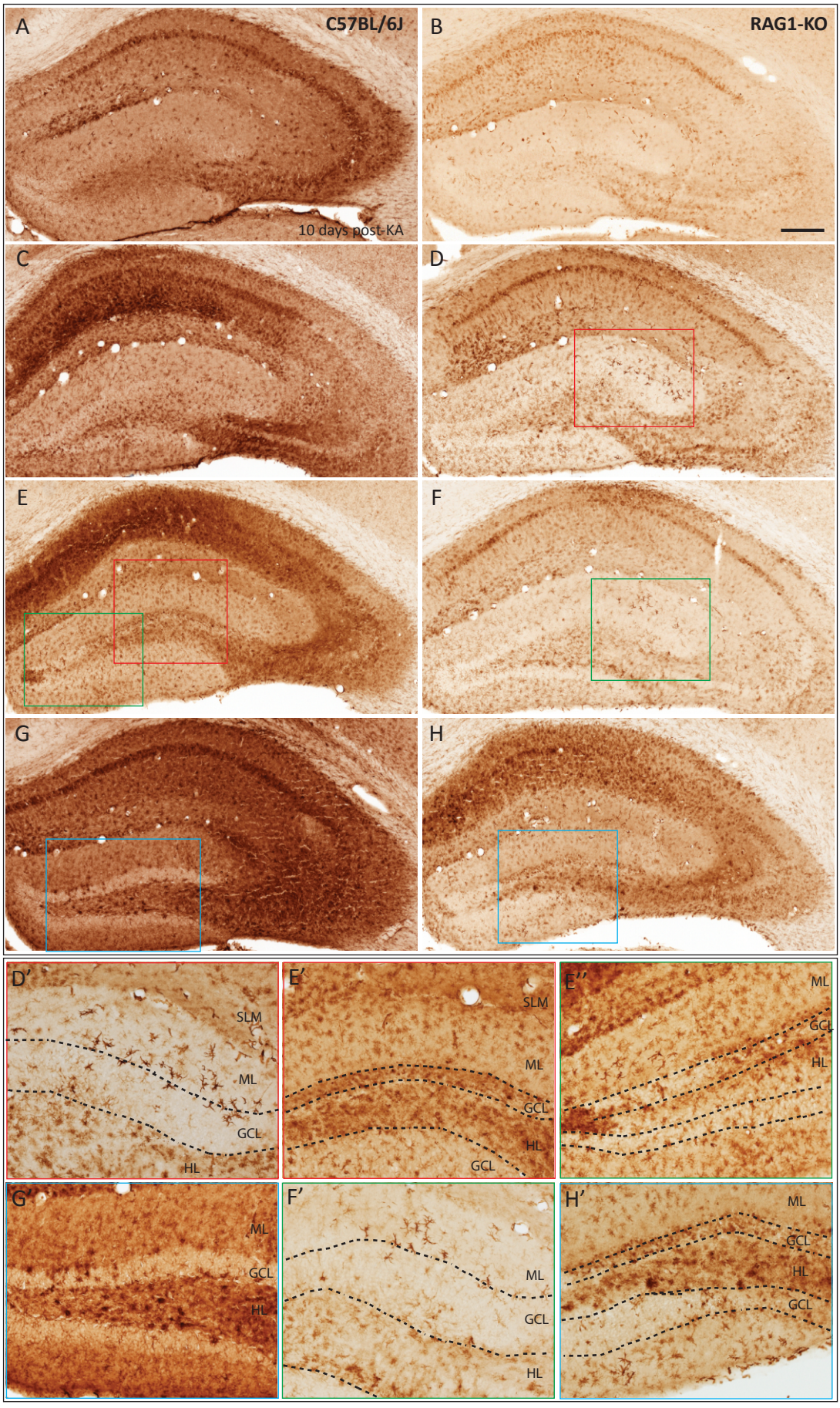
A
C57BL/6J
10 days post-KA
B
RAG1-KO
C
D
E
F
G
H
D'
SLM
ML
GCL
HL
E'
SLM
ML
GCL
HL
GCL
E''
ML
GCL
HL
G'
ML
GCL
HL
F'
ML
GCL
HL
H'
ML
GCL
HL
GCL

To better see the spatial relationship between macrophages and granule cells and to make a clear distinction between the population of F4/80$^+$ macrophages and activated microglial cells, we performed double immunofluorescence staining, using antibodies to F4/80 and Iba-1 in combination with the nuclear dye DAPI on hippocampal sections of wild-type and RAG1-KO mice (Fig. 3.12). In control tissue (contralateral dentate gyrus of KA-treated mice), Iba-1$^+$ resting microglial cells, recognized by their long and slender processes were readily seen in wild-type (Fig. 3.12A) and in RAG1-KO mice (data not shown); in contrast, in the ipsilateral dentate gyrus, where granule cell dispersion was evident, "alerted" microglia with an intermediate morphology between resting and activated, could be detected, along with strongly labeled F4/80$^+$ cells characterized by their large cell body and short thick processes (Fig. 3.12B). The latter cells, which also express Iba-1, likely represent blood-born macrophage cells infiltrating in the brain parenchyma, because their number was much reduced in tissue from mice treated with clodronate liposomes (Fig. 3.12C-E). Instead, in both genotypes, we observed in the absence of F4/80$^+$ macrophages that Iba-1-labeled cells exclusively were activated microglia located within the degenerating granule cell layer, as illustrated for two cases in a wild-type (Fig. 3.12C,D) and a RAG1-KO mouse (Fig.

Figure 3.12: Representative images of double immunofluorescence staining in the granule cell layer and molecular layer of the dentate gyrus with Iba-1 antibody (green; labeling resting and activated microglia) and F4/80 (red; microglia and macrophages) in KA-treated wild-type (A-D) and RAG1-KO mice (E); cell nuclei were counterstained with DAPI (blue). Images were acquired by confocal laser scanning microscopy and depicted as maximal intensity projection of 10-15 layers spaced by 0.5 µm. (A-B) Representative images from a wild-type mouse treated with KA-only. (A) Contralaterally, Iba-1$^+$ resting microglial cells were recognized by their long and slender processes and faint F4/80-IR. (B) In contrast, ipsilaterally, "alerted" microglial cells were seen along with strongly labeled F4/80$^+$ macrophage-like cells characterized by their larger cell body and short and thick processes. Note the preservation of granule cells, which were enlarged and dispersed. (C-E) Representative images from KA-injected wild-type and RAG1-KO mice treated with clodronate liposomes. Numerous granule cell nuclei were pyknotic; in the molecular layer, activated microglial cells, with a "bushy" appearance, were present, whereas strongly labeled F4/80$^+$ macrophages were conspicuously absent. In these images, F4/80-IR was scanned with the same acquisition parameters as in panel B to underscore the difference in expression between macrophage-like cells and activated microglia. Scale bars: A-B and C-E = 20 µm.

Figure 3.12

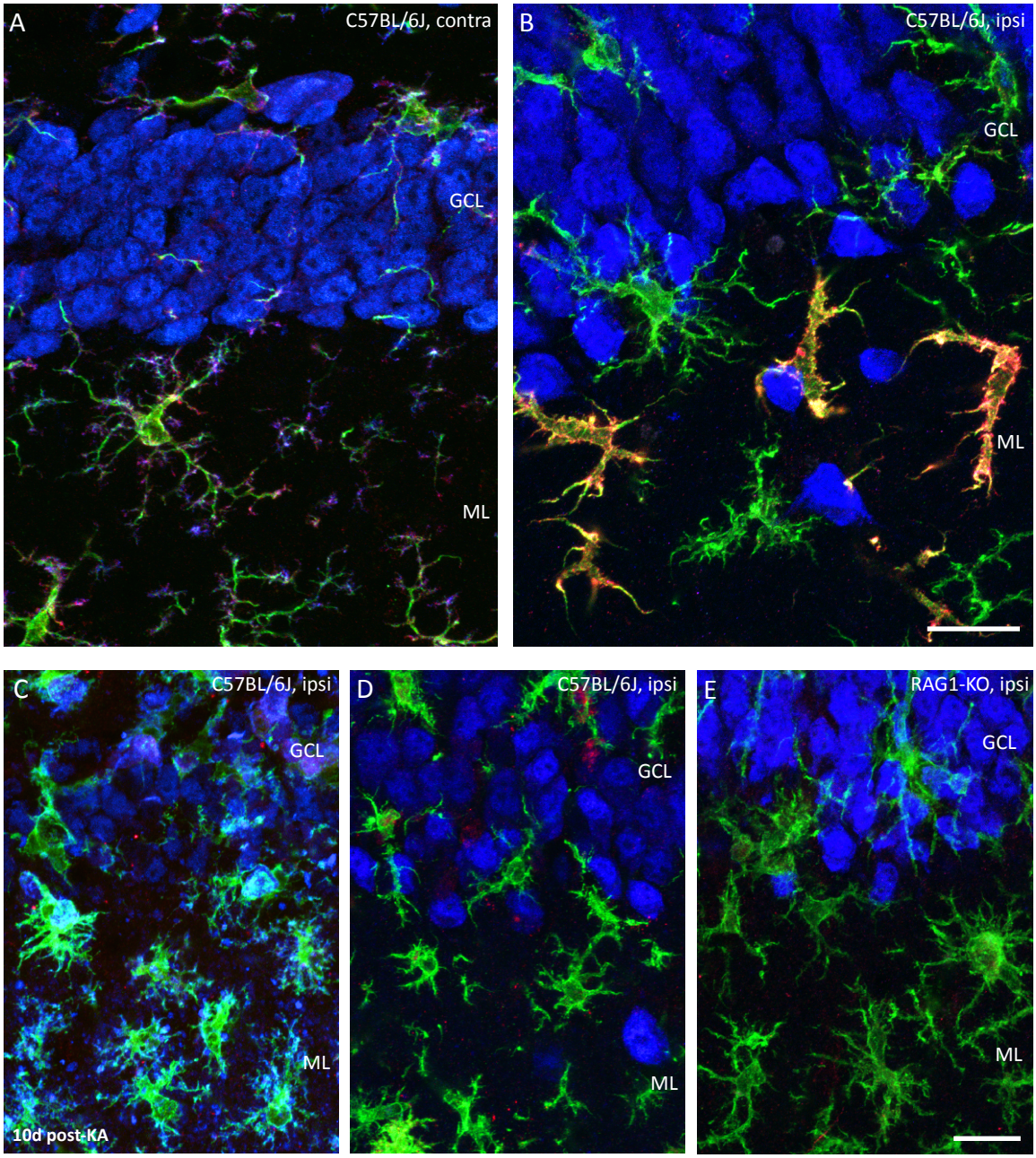
A
C57BL/6J, contra
GCL
ML
B
C57BL/6J, ipsi
GCL
ML
C
C57BL/6J, ipsi
GCL
ML
10d post-KA
D
C57BL/6J, ipsi
GCL
ML
E
RAG1-KO, ipsi
GCL
ML

3.12E). F4/80-IR in these images appears very weak, because it was acquired with the same settings as in panel B to emphasize that its expression level is lower in microglial cells than in macrophages. Finally, we performed the same quantitative analysis as in mice treated with anti-α_4 integrin IgGs to correlate the degeneration of granule cells with the depletion of macrophages. The analysis (thickness of the granule cell layer versus number of F4/80$^+$ cells) again revealed a significant correlation in both genotypes (Fig. 3.13), confirming that macrophages are required for survival and dispersion of granule cells in this model of TLE.

Altogether these findings indicate that circulating macrophages penetrate into the brain parenchyma following KA-induced lesion; they selectively localize in the dentate gyrus where they exert a protective role on granule cells and facilitate their dispersion. Furthermore, these macrophages are involved, along with CD3$^+$ T cells, in the recruitment of neutrophils into the hippocampus of KA-treated RAG1-KO mice.

To complement our morphological data and provide insight into their functional significance, our next question was to understand whether activation of the adaptive and innate immunity contributes to epileptogenesis and onset of recurrent seizures in this mouse model of TLE.

Figure 3.13: Regression analysis of the correlation between granule cell dispersion and density of F4/80$^+$ macrophages. See Materials and Methods and legend of Figure 3.7 for details. The granule cell layer was subdivided in 6 segments and the thickness of each segment as well as the number of F4/80$^+$ cells in the granule cell layer and molecular layer was calculated. Data are depicted as scatter plots to compare KA-injected mice treated with clodronate liposomes and untreated control mice. Regression analysis (thickness of granule cell layer versus number of F4/80$^+$ cells) revealed in each genotype a significant correlation in both groups of mice. In addition, effect of clodronate liposome treatment was reflected by significantly reduced thickness of the granule cell layer and significantly reduced number of F4/80$^+$ macrophages, occurring in both genotypes.

Figure 3.13

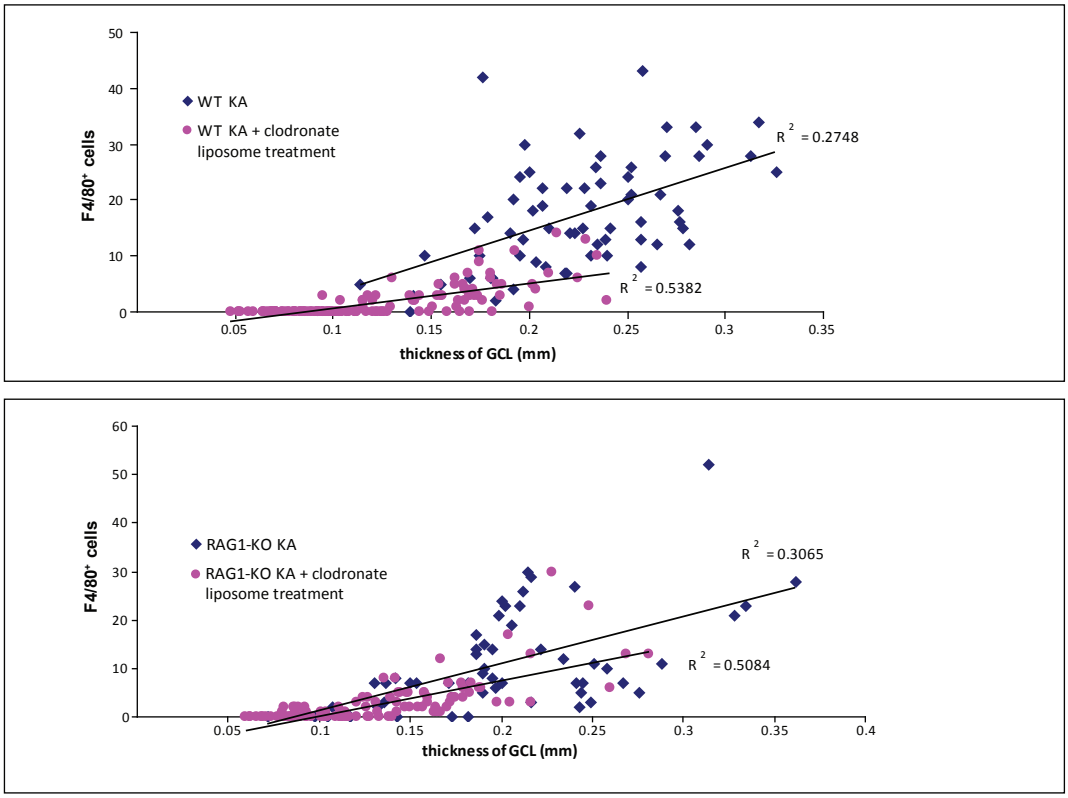
F4/80+ cells
WT KA
WT KA + clodronate liposome treatment
R2 = 0.2748
R2 = 0.5382
thickness of GCL (mm)
F4/80+ cells
RAG1-KO KA
RAG1-KO KA + clodronate liposome treatment
R2 = 0.3065
R2 = 0.5084
thickness of GCL (mm)

Results

Chapter 4

Intrahippocampal EEG recordings

To determine the functional relevance of the leukocyte infiltration into the KA-treated hippocampus in wild-type mice and the specific role of $CD4^+$ and $CD8^+$ T cells, we used EEG analysis during the latent and chronic phase in this model. In total, mice from six different genotypes were analyzed (C57BL/6J, RAG1-KO, B6-RAG2-KO, Cg-RAG2-KO, β2-microglobulin-KO, MHC II-KO; see Materials and Methods, Tables 1-2). No EEG were recorded from mice treated with antibodies or with clodronate liposomes, because the treatment already was a considerable burden for these animals and they would not have tolerated well the additional manipulations related to electrode implantation and repeated EEG recording sessions.

Intrahippocampal EEG recordings were performed with bipolar electrodes implanted into the ipsilateral dorsal hippocampus immediately after KA injection. Their position was confirmed at the end of the experiment in Nissl-stained sections. Due to the dispersion of granule cells, the tip of the electrode typically was located within the granule cell layer.

Wild-type mice (C57BL/6J)

As described earlier (Riban et al., 2002; Arabadzisz et al., 2005), intrahippocampal EEG recordings reveal three distinct phases of paroxysmal activity following unilateral KA injection in adult wild-type mice: (i) a non-convulsive SE, (ii) a latent phase lasting approximately 2 weeks, during which theta oscillations are disrupted and replaced by irregular spikes and waves, and (iii) a phase of chronic seizure activity with spontaneous, non-convulsive recurrent hippocampal paroxysmal discharges of focal origin, characterized by high amplitude sharp waves at the onset and a duration of 20-150 s.

To confirm these findings made in Swiss and NMRI mice, we have recorded here intrahippocampal EEG in six C57BL/6J mice between day 2 and 21 post-KA to determine whether a similar pattern was evident in this strain. Each mouse was recorded every second day during 3-4 hours following 30 min habituation in the

recording chamber. No hippocampal paroxysmal discharges were detectable before day 12 post-KA in any of the six mice recorded (Figs. 4.1A-B, 4.2A). The hippocampal paroxysmal discharges were limited to the dorsal hippocampal formation and lasted between 20 and 100 s (Table 4.1). Their rate of occurrence was variable between animals with a maximum of about 10 seizures per hour (Table 4.1). Their frequency was also variable within any given animal, and sometimes no hippocampal paroxysmal discharges could be recorded up to 1 hour. Typically, behavioral arrest with head nodding could be observed concomitantly with hippocampal paroxysmal discharges.

Histological controls performed at the end of the experiments (about 21 days after KA injection) revealed the typical pattern of hippocampal damage on the injected side described in chapter 1 (see Fig. 1.1).

Therefore, the latent phase of about two weeks is also present in C57BL/6J mice. It appears as a critical period of reorganization of hippocampal circuits leading to the onset of recurrent seizures.

RAG1-KO and RAG2-KO mice

Next, we investigated whether the lack of the adaptive immune system was affecting the process of epileptogenesis. Intrahippocampal EEG recordings in RAG1-KO mice were performed every second day starting at days 6-7 post-KA injection in one group of mice and at days 2-3 post-KA in a second group of mice.

Figure 4.1: Representative hippocampal EEG recordings during the latent and chronic phases of TLE. (A-B) C57BL/6J mice during the latent phase (2 days) and at the onset of the chronic phase (14 days) post-KA injection; only isolated spikes were detected during the latent phase. (C-D) KA-treated RAG1-KO mice at 2 and 14 days post-KA; in both cases, paroxysmal events with similar discharge frequency and duration were detected. The boxed areas in the upper trace (10 s duration) are depicted with better time resolution. (E-F) Recordings in KA-treated RAG2-KO bred on the C57BL/6 and BALB/c background during the latent phase, showing prolonged seizures. Hippocampal paroxysmal discharges during the latent phase in RAG1- and RAG2-KO mice and in the chronic phase (all four genotypes) typically started with large amplitude sharp waves followed by a train of spikes of increasing frequency. Scale: 5 s (horizontal) and 20 mV (vertical).

Figure 4.1

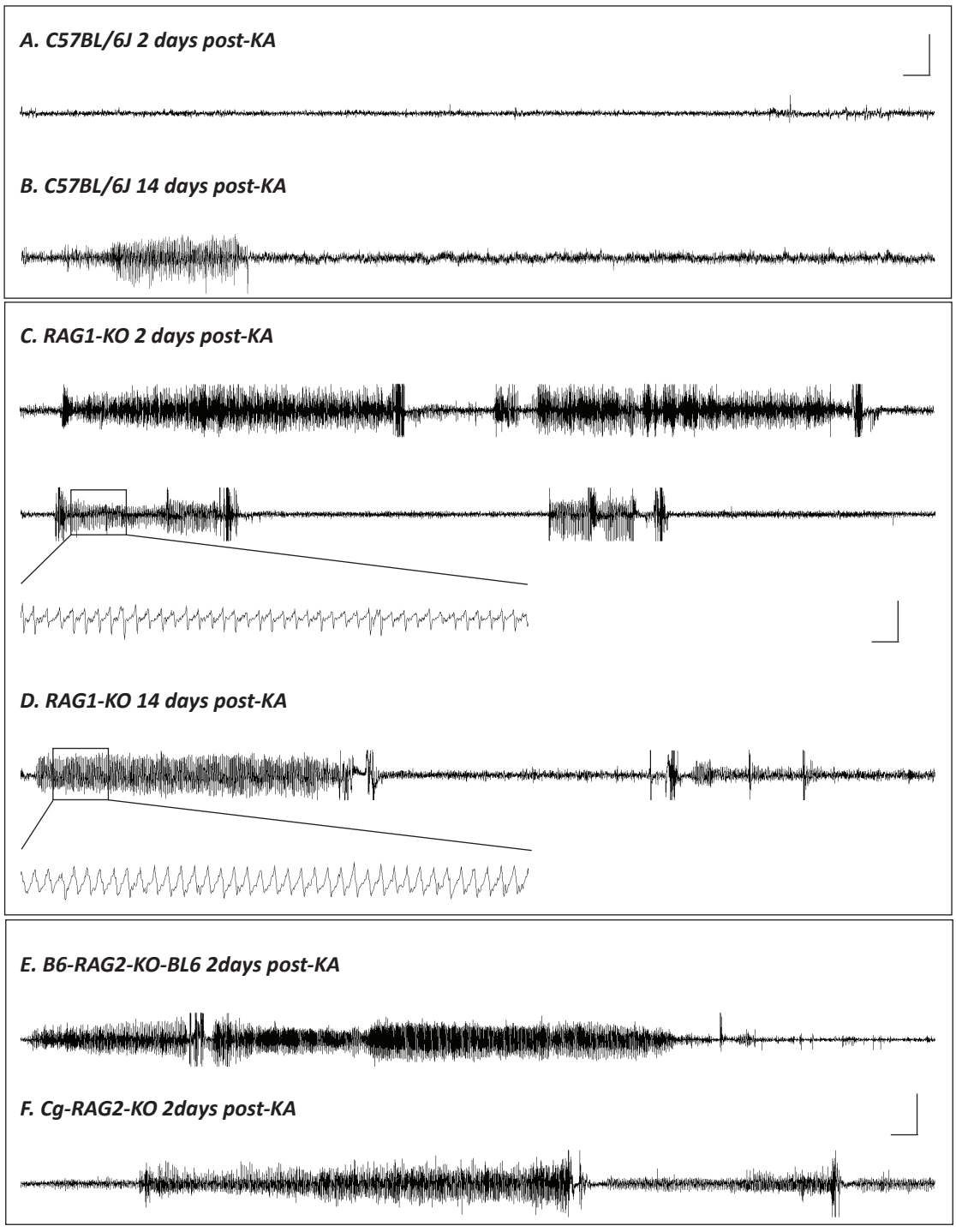
A. C57BL/6J 2 days post-KA
B. C57BL/6J 14 days post-KA
C. RAG1-KO 2 days post-KA
D. RAG1-KO 14 days post-KA
E. B6-RAG2-KO-BL6 2days post-KA
F. Cg-RAG2-KO 2days post-KA

Both groups were recorded until days 16-17 post-KA. Strikingly, characteristic hippocampal paroxysmal discharges were recorded already during the first session in all the animals analyzed, indicating a dramatic shortening of the latent phase (Figs. 4.1C and 4.2B), or even its abolition in mice recorded at day 2 post-KA. These hippocampal paroxysmal discharges lasted between 20 and 300 s (Table 1) and their frequency was variable between and within animals with a maximum of 12 seizures per hour. The seizures observed at 2-3 days post-KA in RAG1- KO mice were indistinguishable from the ones observed during the chronic phase in wild-type animals (Fig. 4.1B-C).

These results were unexpected and we wondered whether the early occurrence of SRS in the latent phase of RAG1-KO mice was correlated to the severity of the KA lesion usually observed in this mutant (see Fig. 2.1). Therefore, the histological changes present in the KA-injected hippocampus were analyzed by Nissl staining at the end of the experiments. These observations revealed that 3 of the 10

Figure 4.2: Scatter plot graphs showing the frequency of intrahippocampal paroxysmal discharges in C57BL/6J (A), RAG1-KO (B), β2-microglobulin-KO (C), and MHC II-KO (D) mice over time. Each mouse is represented by a given symbol. The color denotes the severity of the lesion, as depicted with a representative image in panels E (yellow, mild lesion; blue, moderate lesion; red, severe lesion). At each time-point on the X-axis, the median seizure frequency over two recording sessions given for every mouse. (A) Note the absence of spontaneous recurrent seizures up to 12-14 days post-KA in wild-type mice. The rate of occurrence was variable with a maximum of 11 discharges per hour. (B) Spontaneous recurrent seizures were detected already at day 2 or 3 post-KA injection in all RAG1-KO mice. No latent phase could be detected. The frequency was variable between animals with a maximum of 12 discharges per hour. The decline in frequency at 14-17 days post-KA might be due to the extensive lesion in the epileptic focus. (C) With one exception, β2-microglobulin-KO mice showed seizure activity during the first recording session; thereafter, seizure frequency declined and several mice stopped having seizures, irrespective of the severity of the lesion. Only 4/10 mice had seizures around 14 days post-KA injection. (D) In MHC II-KO mice, only a subset of animals showed paroxysmal discharges within 2 days after SE; seizure frequency declined thereafter, with only 1 of four mice having paroxysmal discharges after day 14. The median is represented. (E) Cresyl violet staining of the ipsilateral KA-injected hippocampus showing the severity of the KA-lesion. (F) Overview of seizure frequency and duration in KA-treated mice during the latent and the chronic phase. The median frequency (given in seizures per hour) and the duration of paroxysmal events (given in seconds) were determined from at least 4 hours of recordings. No significant difference in seizure duration was observed inn mutant mice during the latent phase, or in all four genotypes during the chronic phase.

Figure 4.2

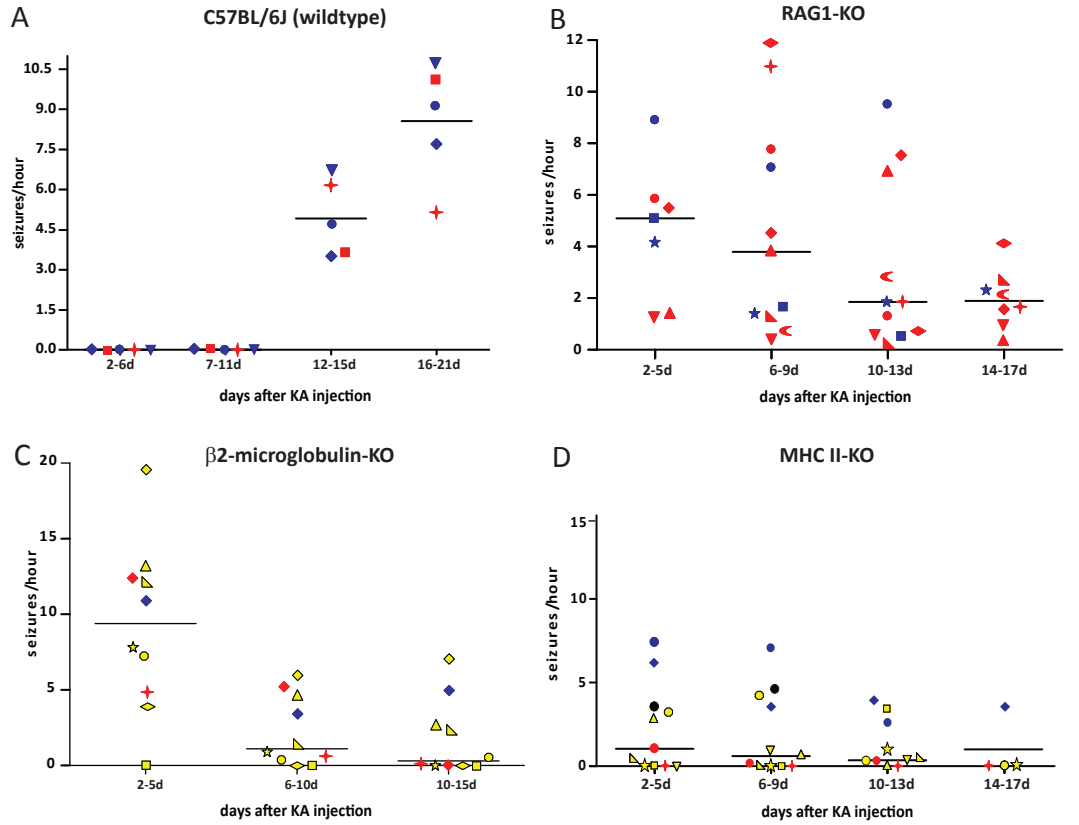

F

	frequency		*duration (sec)*	
	latent phase	*chronic phase*	*latent phase*	*chronic phase*
C57BL/6J	0	4.7	0	31.8
RAG1-KO	5.1	2	42.6	43.3
MHC II-KO	1.1	0.4	78	46.3
β2-microgl-KO	9.4	0.8	57	33.6

recorded mice had a rather mild lesion, with substantial preservation of the CA3a,b area and moderate granule cell dispersion, whereas the other 7 mice had a severe lesion, affecting most of the CA1-CA3 pyramidal layer and leading to prominent dispersion of the granule cell layer (Fig. 4.2E). No mice showed the complete destruction of the hippocampal formation observed in our initial histological assessment (see Fig. 2). Nevertheless, we did not observe a correlation between the severity of the lesion and the frequency of SRS (Fig. 4.2B, E).

Altogether, these results suggest that the occurrence of a latent phase of epileptogenesis in this TLE model is related to the integrity of the adaptive immune system. Deletion of the RAG1 gene is sufficient for abolishing the latent phase, even in mice with a mild lesion, although the mutation selectively affects maturation of lymphocytes. Furthermore, our results suggest that synaptic reorganization in the lesioned hippocampus, notably mossy fiber sprouting, long thought to occur during the latent phase (Bouilleret et al., 1999), is not necessary for the emergence and expression of hippocampal paroxysmal discharges.

However, a potential pitfall in RAG1-KO mice is that this gene is not only expressed in primary lymphocyte differentiation organs (e.g., the thymus) and in B and T cell precursors, but has also been reported in the hippocampus and cerebellum (Mombaerts et al., 1992). To exclude the possibility that the effect observed on epileptogenesis was due to the absence of this specific gene in the hippocampus, we performed the same experiment in mice lacking RAG2. This gene is functionally homologous to RAG1, but is not expressed in the CNS, thereby excluding any confounding effects potentially present in RAG1-KO mice.

RAG2-KO mice were available in two different strains (C57BL6 and Balb/C), allowing us to exclude any strain-related effects. KA-treated B6-RAG2-KO and Cg-RAG2-KO mice were recorded every second day, starting at days 2-3 post-KA injection and continuing until day 16. As seen in RAG1-KO mice, hippocampal paroxysmal discharges occurred already at day 2-3 post-KA injection in all animals analyzed (Fig. 4.1E, F), irrespective of background strain (n=10; data not shown), reproducing the dramatic shortening of the latent phase seen in RAG1-KO mice.

Likewise, the pattern of hippocampal damage caused by the KA injection was comparable in extent and variability in RAG2-KO mice to that shown in Figure 4.2E for RAG1-KO mice. These results demonstrate that the lack of RAG1 gene in the hippocampus was not responsible for the occurrence of hippocampal paroxysmal discharges already at day 2 post-KA and that the mouse strain had no effect on the onset and frequency of seizures.

β2-microglobulin-KO and MHC II-KO mice

As already mentioned previously, RAG1-KO mice lack both $CD4^+$ and $CD8^+$ T cells. Therefore, to determine whether one of these two cell populations selectively is implicated in the abolition of the latent phase observed in KA-treated RAG1-KO mice, we performed intrahippocampal EEG recordings in β2microglobulin-KO and MHC II-KO mice, lacking $CD8^+$ and $CD4^+$ T cells, respectively (Fig. 4.2C, D). The recordings were started at days 2-3 post-KA and were taken every second day until days 14-15 in β2-microglobulin-KO and days 16-17 in MHC II-KO mice. As seen in RAG1/2-KO mice, hippocampal paroxysmal discharges were detected already during the first recording session in β2-microglobulin-KO mice. Their frequency was variable between and within animals with a maximum of 20 seizures per hour. Thereafter, however, we observed a marked reduction of seizure frequency already evident at days 6-10 post-KA, with 60% of the mice having fewer than 2 seizures per hour, and even further at days 10-15, with six mice being nearly seizure-free during three consecutive recording sessions (Fig. 4.2C). Histological analysis revealed that the severity of the lesion in β2-microglobulin-KO mice was generally reduced compared to C57BL/6J mice (Fig. 4.2E). In particular, the dispersion of dentate gyrus granule cells was much less prominent and the CA3a,b region was well preserved. However, one mouse had a moderate lesion and two mice a severe lesion, which did not correlate with frequency, time of onset, and time of disappearance of hippocampal paroxysmal discharges (Fig. 4.2C; Table 4.1).

The analysis of intrahippocampal EEG recording in MHC II-KO mice revealed the presence of two subgroups of animals: i) one cohort (n=5) showing hippocampal paroxysmal discharges already at days 2-3 post-KA, reproducing the dramatic shortening of the latent phase observed in RAG1-KO mice and ii) one cohort (n=4) showing no hippocampal paroxysmal discharges over the entire period analyzed, even past the normal duration of the latent phase. In addition, 2 mice had a few seizures at days 2-5, but not anymore thereafter. Overall, seizure frequency was low (2-5 per hour), revealing a striking difference to wild-type and RAG1-KO mice. Like in β2-microglobulin-KO mice, lesion severity was less than in wild-type mice, although half of the mice had either a "typical" or a "severe" lesion (Fig. 4.2E). Furthermore, absence of seizures was again not related to lesion severity.

Our data demonstrate that spontaneous recurrent paroxysmal discharges in the hippocampal formation following local injections of KA can appear before the latent period of 2 weeks observed in wild-type mice. During this period, major morphological and functional modifications occur. In the dentate gyrus, granule cells become enlarged and undergo dispersion; extensive sprouting of mossy fiber terminals takes place; neuronal cell loss is extensive in CA1 and CA3c. Our present EEG recordings in the various lines of immunodeficient mice show the occurrence of hippocampal paroxysmal discharges already at day 2 post-KA injection. It is known that immune responses in the CNS are critical to first line defense against injury but how this could be correlated with the onset of hippocampal paroxysmal discharges is not clear. We observed leukocyte migration into the KA-injected hippocampus, most likely orchestrated by cytokines (important to carry signals between cells) and/or chemokines (chemotactic cytokines), key mediators of microglial cell response. To better understand which soluble factor might be responsible for the infiltration of lymphocytes into the KA injected hippocampus, as well as neutrophils in RAG1-KO mice, we employed the Luminex 100 platform to determine the cytokine/chemokine protein content in the ipsilateral and contralateral dorsal hippocampus of wild-type and RAG1-KO mice.

Results

Chapter 5

Determination of major cytokines in KA-lesioned hippocampal tissue

Several inflammatory mediators, such as proinflammatory cytokines/chemokines, are expressed in activated glial cells as a hallmark of brain inflammation in various experimental models of seizures and in human epilepsies (see Introduction). Recent experimental studies in rodents with perturbed cytokine systems indicate that these inflammatory mediators can affect neuronal survival by activating transcriptional and posttranslational intracellular pathways (Vezzani et al., 2008). All these data raised the key question of whether this inflammatory process is a mere epiphenomenon of neuronal injury or may contribute to epileptogenesis, and if so, through which mechanisms.

Our experimental data demonstrated strong microglial cell activation in the lesioned hippocampus injected with KA reflecting the neurodegeneration in the TLE model and recruitment of cells of the immune system into the brain parenchyma. Therefore, we aimed to investigate the pattern of cytokines present in the lesioned hippocampus after KA injection. The goal of this study was to identify cytokines or chemokines potentially implicated in leukocyte recruitment to the hippocampus and microglial cell activation. To this end, we used Luminex xMap technology which is combining flow cytometry and bead-based antibody capture for detecting multiple analytes from a single sample with high sensitivity (see Materials and Methods). In the present study, we employed the Luminex 100 platform to determine the cytokines/chemokines content in the lesioned hippocampus of C57BL/6J and RAG1-KO mice at different time-points after saline and KA injection. In the first experiment (Fig. 5.1), we analyzed the ipsilateral dorsal hippocampus isolated from wild-type and RAG-1 KO mice 7 and 14 days after KA injection and 10 days after saline. With this experiment, we expected to determine whether the expression profile of the 17 cytokines/chemokines measured differs between the two genotypes at baseline and during epileptogenesis, and to establish their temporal profile of expression during the latent phase and at the onset of seizures (see Chapter 4). Mice were perfused with ACSF in order to exclude cytokines/chemokines presence in the blood and

focus on the brain parenchyma. We detected IL-1α, IL-1β, MIP-1α, IL-10, IL-17, MCP-1, IL-6, KC and VEGF in hippocampal tissue homogenates but overall there was no significant difference between the different time-points and genotypes (Fig. 5.1A). The concentrations of G-CSF, GM-CSF, INFγ, IL-12(p70), LIF, MIP-1β, MIP-2 and TNFα were below the detection level of the assay. Thus, KA injection caused only minor variation in the concentration of these cytokines and chemokines in the two genotypes at the two time-points analyzed. Unexpectedly, differences in basal cytokines expression level between genotypes, notably IL-1β, MIP-1α, IL-17, IL-6, and KC, were abolished at the two time-points examined in the ipsilateral, KA-injected hippocampus (Fig. 5.1B). Concomitantly, however, none of the cytokines/chemokines analyzed showed a significant alteration in expression at 14 days post-KA compared to baseline, suggesting that a possible change might have occurred earlier or might have been missed in our samples for technical reasons.

Considering the abolition of the latent phase of epileptogenesis in RAG1-KO mice (see Chapter 4), we aimed to determine whether specific cytokines/chemokines show altered expression patterns at an early time-point after KA injection, or whether differences are evident between wild-type and RAG1-KO mice at the time of early seizure onset in the latter animals.

Therefore, for five selected cytokines, we performed a second experiment to determine whether there is significant a difference in the dorsal hippocampus of control naive animals (wild-type and RAG1-KO not injected with KA or saline) compared to the KA-injected hippocampus at 2 days (Fig. 5.2). In this experiment,

Figure 5.1: Expression profile of nine cytokines/chemokines in hippocampal tissue of wild-type and RAG1-KO mice at baseline (10 days after saline injection) and after KA-induced lesion (7 and 14 days post- injection). (A) Histograms depicting the data (pg/mg protein) as mean ± SEM (n=3 saline-treated mice and 5 KA-treated mice); note the different scales of the Y-axis. Statistical analysis revealed no significant difference between the different time-points and genotypes. (B) Basal concentration of cytokines/chemokines in the hippocampus of wild-type and RAG1-KO mice. The differences observed in the basal expression level between genotypes were abolished at the two time-points examined in the ipsilateral, KA-injected hippocampus. Mean is given (n=5). Values in brackets are the percentage of change compared to wild-type mice.

Figure 5.1

A.

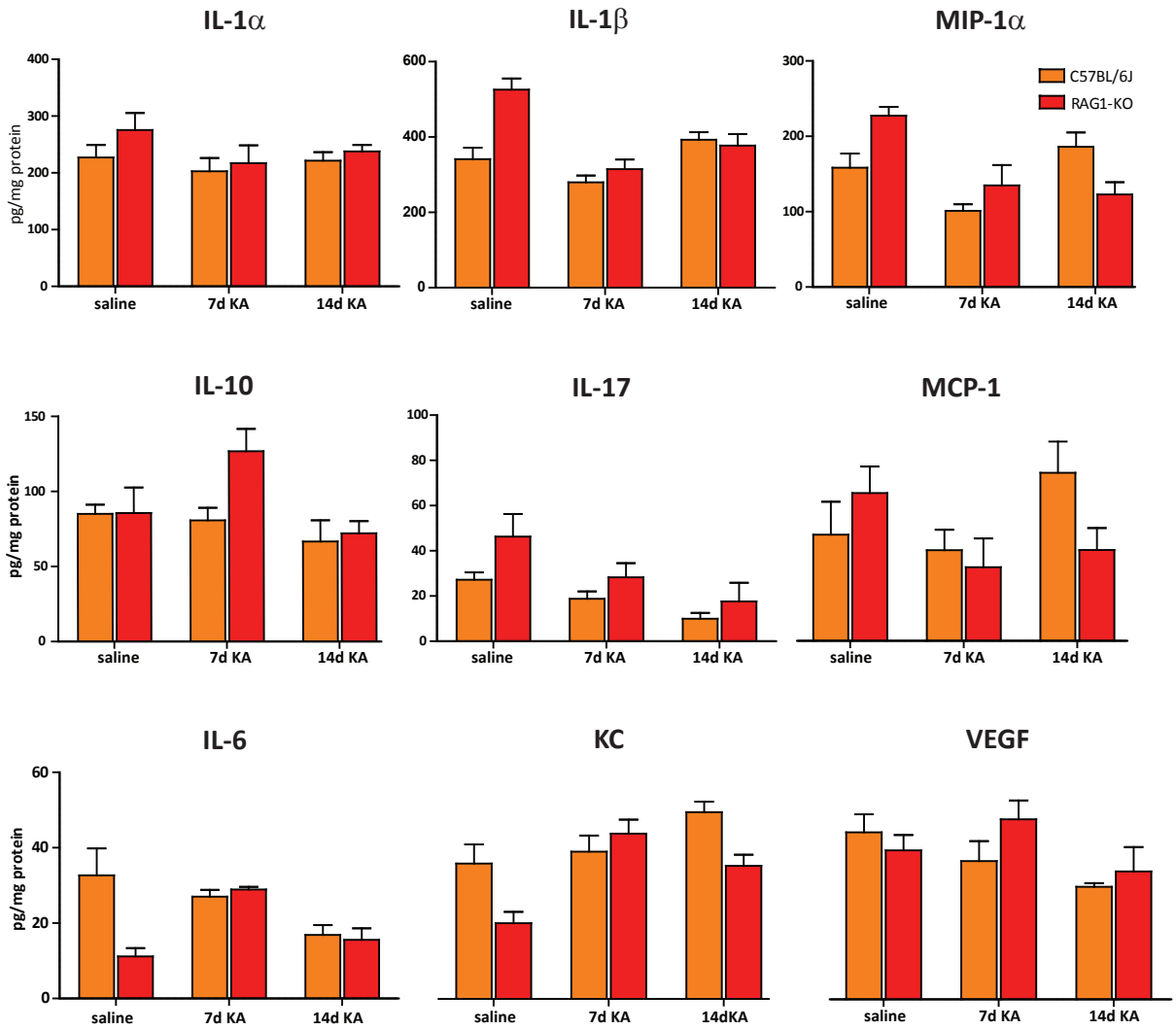

B.

Basal cytokines expression	*C57BL/6J (pg/mg protein)*	*RAG1-KO (pg/mg protein)*	*Detection level (pg/mg protein)*
IL-1α	225	275 (+22%)	27.1
IL-β	340	525 (+54%)	17.7
IL-6	32.5	11 (-66%)	16
IL-10	85	85.5 (--)	21.6
IL-17	27	46 (+71%)	15.8
KC	35	20 (-43%)	16
MCP-1	57	79 (+39%)	37.3
MIP1-α	158	227 (+54%)	14.3
VEGF	43.5	38.5 (-11%)	71.7

KC, MCP-1, and IL-10 were detected at levels that were different from experiment 1 in both control and KA-treated tissue, precluding any comparison between experiments. However, there was no significant change in concentration of these cytokines among the groups and genotypes, suggesting no major role in this model of TLE.

The pro-inflammatory cytokines IL1-β and IL-6 also were not statistically significant between control and KA-treated mice, possibly due to the small sample of animals in each group. However, they were detected at levels similar to those seen in experiment 1. Therefore, we compared these two cytokines between the five conditions analyzed (naive mice, saline-treated mice, KA-treated mice at 2, 7, and 14 days post-injection). Thus, in wild-type mice, IL1-β levels remained unchanged by saline and KA treatment; IL-6 levels, although statistically non-significant in either separate experiment, were lowest in the chronic phase (14 days post-KA). In RAG1-KO mice, the overall comparison suggested enduring decrease of IL1-β levels (by about 40%) in epileptic tissue compared to baseline or saline, and increased expression of IL-6 (by about 100%) in epileptic tissue (Figs. 5.1A and 5.2). As a consequence, the ratio of IL-1β/IL-6 expression was different between the two genotypes at baseline/saline (wild-type = 11-16; RAG1-KO = 27-52) but not in KA-treated hippocampus (2 days post-KA: wild-type = 6.6; RAG1-KO = 7.2; 7 days post-KA: wild-type = 8; RAG1-KO = 11; 14 days post-KA: wild-type = 20; RAG1-KO = 26). These observations argue against a major role of these pro-inflammatory cytokines for neutrophil recruitment in RAG1-KO mice. However, the selective increase in IL-6 in RAG1-KO mice during the early latent phase of epileptogenesis (2-7 days post-KA) might contribute to seizure onset.

Figure 5.2: Expression profile of five selected cytokines (pg/mg protein) in hippocampal tissue of control naïve animals (wild-type and RAG1-KO not injected with KA or saline) and after KA-induced lesion (2 days post-injection). The data (pg/mg protein) are expressed as mean for control mice (n = 2) and mean ± SEM for KA-treated mice (n = 5); note the different scales of the Y-axis. No significant changes were detected between the genotypes and the treatment. Mean values are given (n=5).

Figure 5.2

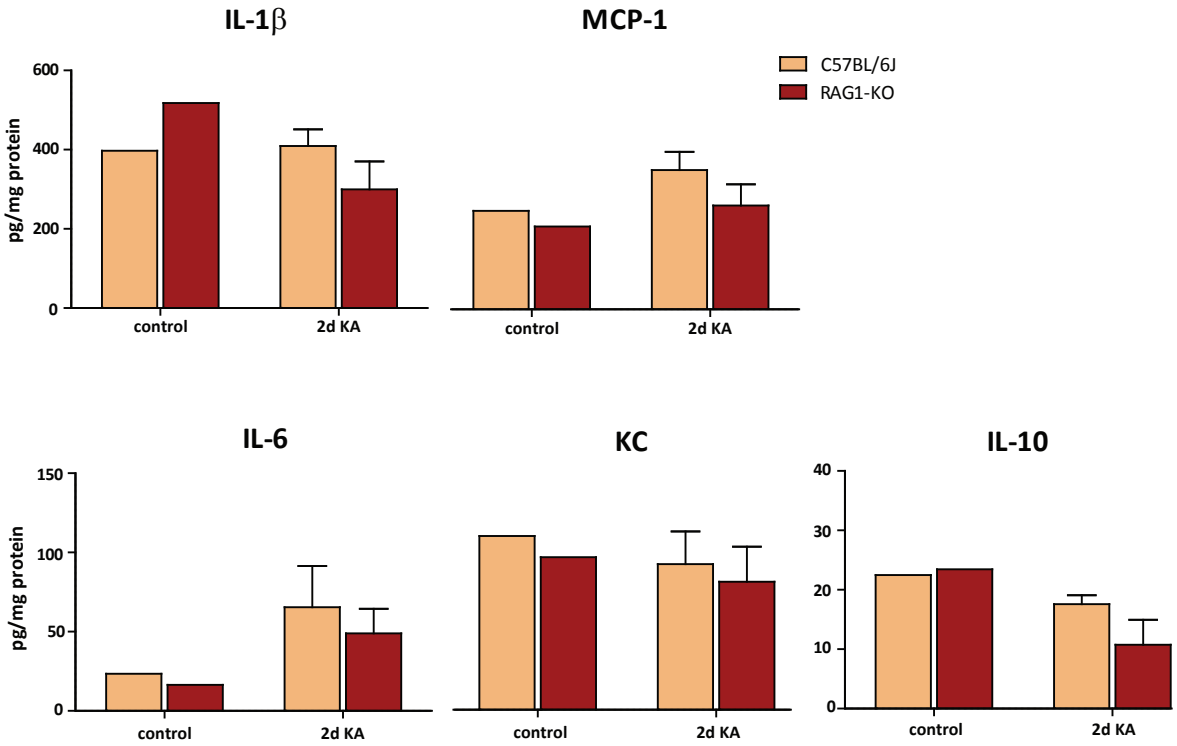
IL-1β
MCP-1
C57BL/6J
RAG1-KO
pg/mg protein
600
400
200
0
control
2d KA
IL-6
KC
IL-10
150
100
50
40
30
20
10

Altogether, despite the fact that the Luminex xMap technology is very powerful to detect multiple analytes in a single sample, this biochemical approach was limited in our experiments to determine the role of cytokines in the differential pathological changes observed in this TLE model between wild-type and RAG1-KO mice. Larger samples would be necessary to achieve statistical power. Furthermore, considering the transient nature of cytokine production and release, the Luminex technology might lack the required temporal resolution.

Discussion

The significance of inflammatory mechanisms for the pathogenesis of epilepsy has long been underestimated and is not well understood. However, there is now compelling evidence that systemic inflammation may have significant effects on normal brain function and may, in particular, lead to SE and epileptic seizures (Fabene et al., 2008). Using the KA mouse model of TLE, we show here that multiple components of acquired and innate immunity are activated in this model leading to strong local inflammation and cellular infiltration. Therefore, not only systemic but also local inflammatory reactions triggered by neurotoxins can contribute to epileptogenesis and chronic recurrent seizures.

In KA-treated C57BL/6J mice, we observed $CD3^+$ T cell infiltration in the lesioned hippocampus during the phase of epileptogenesis, reaching a plateau at 14 days post-KA, thereby replicating a key histopathological feature reported in tissue resected from patients with intractable MTLE. The neuronal cell loss observed in specific regions of the hippocampal formation after KA injection was mirrored by strong microglial cell activation. The level of microglia activation was a reliable correlate of the neuronal loss that occurs over time. Moreover, we observed macrophage infiltration in the molecular layer of the dentate gyrus, surrounding the dispersed granule cell layer. Unexpectedly, genetic and pharmacological interventions to prevent immune cell infiltration and to deplete peripheral macrophages resulted in a marked worsening of the lesion. Thus, in mice constitutively lacking T and B cells, a dramatic shortening of the latent phase prior to recurrent seizure onset was evident, whereas in mice depleted of macrophages, granule cell degeneration occurred in the dentate gyrus. Therefore, the immune responses triggered by KA-induced lesion of the hippocampal formation appeared to contribute to seizure-suppressant and neuroprotective factors in this experimental model, shedding new light on the role of neuro-immune interactions in TLE.

In immunodeficient mice (RAG1-KO) used to unravel the significance of immune cells in the epileptic hippocampus, we observed that the absence of T cells aggravates the long-term degeneration of the epileptic hippocampus because it allows invasion of the lesioned hippocampus by neutrophils, a feature never seen in wild-type mice. Therefore, adaptive immunity in this model of TLE apparently

reduces innate immune responses that trigger neutrophil activation and diapedesis. RAG1-KO mice also exhibit reduced number of F4/80^{+} macrophages in the dentate gyrus along with exacerbated granule cell degeneration (see Figs. 3.7 and 3.13), notably in the group of severely affected mice. Since neutrophils were only few in the dentate gyrus at days 10-14 post-KA, activation of adaptive immunity might also provide chemoattractant signals for peripheral macrophages to enter the brain.

Using neutralizing antibodies against Gr-1, we could demonstrate that neutrophil depletion does not influence the pattern of KA-induced neurodegeneration in wild-type mice, but is an effective step to prevent the severe neuronal cell loss observed in the lesioned hippocampus of RAG1-KO mice. In addition, neutralizing antibodies against α4-integrin markedly reduced the pattern of neurodegeneration in RAG1-KO mice by interfering with neutrophil infiltration. In wild-type mice, the antibody treatment induced a more severe lesion due to concomitant interference with macrophage infiltration.

Depletion of peripheral macrophages with systemic administration of clodronate liposomes revealed that infiltration of blood-born macrophages is essential for granule cell survival after KA injection in wild-type and mutant mice. Unexpectedly, in RAG1-KO mice, the depletion of macrophages blocked the entrance of neutrophils into the lesioned hippocampus, thus leading to a less severe lesion. Therefore, peripheral monocytes/macrophages or infiltrating macrophages might be involved in the recruitment of neutrophils into the hippocampus of KA-treated RAG1-KO mice.

Altogether, the neuroprotective and neurotrophic effects of immune cells in this model of TLE are based on multiple interactions likely involving a vast array of signaling molecules both in the periphery and in the brain. Therefore, therapeutic strategies targeting the immune systems will have to be highly elaborated to avoid unwanted blockade of neuroprotective action of specific immune modulators in the epileptic focus.

Validation of the KA mouse model

Several animal models of chronic limbic epilepsy have been developed in rodents to reproduce specific clinico-pathological features of MTLE. Importantly, the focal nature of the mouse KA epilepsy model corresponds to a strict unilaterality and absence of epileptic discharges in neighboring structures, including the overlaying neocortex (Riban et al., 2002). The ventral hippocampus and the contralateral side remain morphologically unaffected, providing an internal control, particularly useful for quantification of immunohistochemistry. Likewise, in patients with MTLE, pathological alterations are usually limited to the epileptic focus, allowing its surgical resection without loss of cognitive or mnemonic functions. Moreover, the KA mouse model is more similar to human MTLE than other lesional models used in rodents for at least two reasons. First, in animals treated systemically with KA or pilocarpine, pyramidal neurons are preferentially damaged in the CA3 subfields, whereas this region (CA3a,b) is largely protected in human epileptic temporal lobes. In human MTLE, the major regions of neuronal cell death are the same in KA-treated mice, including the hilus of the dentate gyrus and the entire CA1 area, whereas CA3a,b are relatively well preserved. Second, SRS are of focal nature, rarely leading to secondary generalization.

A key feature of the KA mouse model is the clear segregation between the acute, latent, and chronic phases of epilepsy, allowing to separate the effects of excitotoxic action of KA from the delayed neurodegeneration and granule cell dispersion, which are two hallmarks of this model. The present results call for a re-interpretation of the mechanisms of epileptogenesis during the latent phase, since it is curtailed in mutant mice lacking specific subsets of T cells or the MHC II complex.

A major potential limitation of the KA mouse model is the mechanical and chemical lesion caused by the KA injection into the dorsal hippocampus, which induces a local disruption of the BBB and could be a contributory factor to the inflammatory response observed. However, this mechanical lesion is not sufficient, because control mice injected with the same volume of saline did not present with any sign of inflammation, except for a minor activation of microglial

cells at the site of injection. Rather, our results indicate that KA injection into the dorsal hippocampus causes a local neuroinflammation, which explains the facts that the activation of the innate immune cells of the brain, like microglia/macrophages, and that infiltration of lymphocytes and neutrophils was observed only within the lesioned hippocampal formation. Therefore, interactions between activated immune cells and the endothelial cell wall were restricted to the inflamed tissue, whereas the BBB leakage caused by mechanical tissue disruption played no significant role in the disease process.

Despite the accuracy of stereotaxic surgery, a major constraint is represented by the inter-individual variability of the KA-induced lesion. KA exerts potent excitotoxic and pro-convulsant action related to its selective action on kainate receptors. The concentration of KA injected in the dorsal hippocampus is critical for the outcome of the lesion. Overall, wild-type mice responded consistently to the dose of KA used, showing a stereotyped pattern of neuronal loss in CA1, CA3c and the hilus, whereas RAG1-KO mice showed more variability. They appeared to be more sensitive to KA and exhibited a steep dose-response curve, with a severe aggravation of neurodegeneration above a certain threshold.

However, the KA mouse model of TLE does not exhibit the striking differences in sensitivity reported for inbred strains of mice after systemic treatment, and which are due to genetic polymorphisms (Schauwecker and Steward, 1997; Schauwecker, 2000, 2003). In our studies, we used C57BL/6J wild-type mice because the immunodeficient mice were obtained from this strain; however, in earlier experiments performed in NMRI mice a similar pattern of neuronal cell death was observed compared to C57BL/6J mice, allowing to exclude an effect of genetic background on the alterations observed. Therefore, the effects of various targeted mutations can be analysed in this model without strain-related confounding factors.

In conclusion, the KA mouse model appears to be very well suited for investigating disease-relevant neuro-immune interactions underlying morphological and functional reorganization of the hippocampal formation in TLE.

Benefits of the immune responses in the CNS

The limitation of immune responsiveness in the mammalian CNS has been attributed to the intricate nature of neuronal networks, which would appear to be more susceptible than other tissues to the threat of permanent disorganization when exposed to massive inflammation (Schwartz et al., 1999). This line of logic led to the conclusion that all forms of CNS inflammation would do more harm than good and, hence, the less immune intervention the better. However, our results are in line with mounting evidence indicating that some forms of immune system intervention can help to protect or restore CNS integrity. Indeed they found that autoimmune T cells that are specific for a component of myelin confer neuroprotection and, in some context, repair. Autoreactive T cells protect local axons and neurons from degenerating after a traumatic injury to the spinal cord through a process referred to as “protective autoimmunity” (Schwartz et al., 1999). Moreover, in normal hippocampal neurogenesis, immune activity is required since neurogenesis is impaired in T cell-deficient mice; the restoration of T cell activity improved the number of adult neurons and spatial learning (Ziv et al., 2006). The mechanism by which immune cell subsets confer neuroprotection or recovery remains speculative, but leukocytes are known to express a range of neurotrophic factors, including the neurotrophin class of survival and regenerative factors for neural cells during development and in adulthood (Yong and Rivest, 2009). It is conceivable that even in classic inflammatory disease of the CNS, like multiple sclerosis, where extensive and dysfunctional immune reactivity contribute to the pathology, many of the immune cells that accumulate in the CNS express neurotrophic factors. Other beneficial mechanisms of immune cells for the CNS include their clearance of toxic molecules and the removal of cellular debris.

In our experiments, we observed a relatively small number of $CD3^+$ T cells infiltrating the KA-treated hippocampal formation, and even fewer macrophages within the dentate gyrus. The magnitude of the deleterious effects observed in their absence in RAG1-KO and in clodronate liposome-treated mice suggests that their action is strongly amplified by powerful signalling cascades preventing the

production of chemoattractant factors for neutrophils or mediating neuroprotective effects onto dentate gyrus granule cells.

In the following paragraphs, we discuss the possible role of each of the mediators of adaptive and innate immunity activated upon intrahippocampal KA injection and their contribution for or against neurodegeneration and epileptogenesis.

$CD3^+$ T cells in the KA-injected hippocampus: good or bad?

The effect of T cells in the CNS is context-dependent, as their presence has been shown to promote neuronal survival following certain types of injuries, or conversely, contribute to CNS pathology, such as in experimental autoimmune encephalomyelitis (EAE) and models of bacterial or viral brain infection (Martino and Hartung, 1999; Serpe et al., 1999; Schwartz, 2001; Nau and Bruck, 2002; Byram et al., 2004). Particularly striking are recent findings that activation of $CD8^+$ T cells infiltrated in the brain parenchyma can lead to BBB disruption upon neuronally-mediated enhancement of VEGF expression (Suidan et al., 2010).

Facial nerve axotomy, leading to massive retrograde degeneration and inflammatory reactions in the facial motor nucleus despite preservation of BBB integrity and absence of mechanical lesion in the CNS, is a well established model system for studying neuro-immune interactions. Although trafficking of T cells into the injured facial motor nucleus has been assumed to depend on injury severity, findings from Ha et al., revealed no correlation between T cell trafficking exacerbates neuronal cell death (Ha et al., 2006; Ha et al., 2008).

Schaftel and collaborators (Shaftel et al., 2007) demonstrated that chronic IL-1β expression in a transgenic mouse model IL-β^{XAT} leads to massive leukocyte infiltration, BBB leakage (induction of monocyte chemoattractant protein 1 and intercellular adhesion molecule 1) without evidence of neuronal degeneration.

In our KA mouse model, we found $CD3^+$ T cells exclusively in the KA injected hippocampus; all the other regions of the brain as well as the contralateral hippocampus did not show lymphocyte infiltration. Since their number peaked at the time of seizure onset, about 14 days post-KA, this finding raised the question whether $CD3^+$ T cells contribute to the etiopathogenesis of the seizures in our

model, prompting us to study immunodeficient mice (RAG1-KO). However, our results unambiguously demonstrate that absence of T cells not only aggravates the long-term degeneration of the epileptic hippocampus but also curtails the latent phase of epileptogenesis; pointing out the relevance of the integrity of the immune system for protection against pathological conditions involving changes in neuronal excitability.

However, it is not fully understood what is the driving force behind leukocyte recruitment in the KA-lesioned hippocampus. There are numerous possibilities but an interesting one is represented by IL-1β. It is known that IL-1β is a powerful stimulus for leukocyte recruitment to the CNS (Gibson et al., 2004). In addition, IL-1β induces MCP-1 (monocyte chemoattractant protein 1), primarily credited for recruitment of macrophages but also acting as T-cell chemoattractant, and ICAM-1 (intercellular adhesion molecule 1), essential for binding leukocyte-expressed integrins and, therefore, involved in the migration of leukocytes into brain parenchyma. Finally, recent studies have reported increases in inflammatory cytokines in the CNS and plasma in experimental models of seizures and in clinical cases of epilepsy (Vezzani, 2005; Vezzani and Granata, 2005). However, while these studies concluded that blockade of IL-1β might be beneficial to prevent development of epilepsy after SE, our findings indicate that blockade of $CD3^+$ T cell infiltration into an established epileptic focus could be detrimental and lead to further neurodegeneration.

Neuroprotective effect of microglial cells

Microglial cells are main innate immune cells of the brain; they respond quickly to pathogens and injury, accumulate in regions of neurodegeneration, produce a variety of pro-inflammatory molecules and eliminate cellular debris via phagocytosis.

It is well established that following changes in the CNS parenchyma, like chronic and acute neurodegeneration, microglial cells are activated and respond by undergoing morphological changes, migrating, proliferating and modifying their patterns of gene expression to reinforce the expression of inflammatory factors

such as cytokines, chemokines and their receptors. In particular, direct evidence that microglial activation is important for development of inflammatory CNS diseases was provided in CD11b-HSVTK transgenic mice, in which administration of ganciclovir prevents microglial response and effectively protects CNS tissue from injury (Heppner et al., 2005).

However, it is important to remember that the microglia response is among others dependent on the CNS region, the degree of the tissue damage, the presence of neuronal debris, the type of insult, the state of the BBB, and the presence or absence of an immune challenge triggering the immune adaptive response (Villoslada et al., 2008). Although a sustained inflammatory response certainly can be detrimental to the CNS, increasing evidence indicate that microglial cells have a beneficial function by clearing debris and possibly promoting repair (Rivest, 2009). Many studies have shown that microglial cells are attracted to amyloid-β deposits in tissue from both human and transgenic mouse models that develop Alzheimer's disease (AD)-like alterations (Simard et al., 2006). In addition, Raivich et al. found that the levels of microglial cell activation were reliable correlates of the neuronal cell loss that occurs over time following facial nerve axotomy (Raivich et al., 1998; Raivich et al., 2003). Moreover, microglia have been shown to express elevated levels of brain-derived neurotrophic factor (BDNF) (Batchelor et al., 1999). Conversely, the neuroprotective effects of glial derived neurotrophic factor (GDNF) against excitotoxicity involve microglial cell activation in the CA3 region of the hippocampus (Boscia et al., 2009).

In wild-type and RAG1-KO mice treated with KA, the activation of microglial cells was selectively restricted to regions of the hippocampal formation where neuronal cell loss had occurred. In particular, the lack of $CD3^+$ T cells led to aggravated neurodegeneration in the KA-injected hippocampus, notably in the CA3a,b area and in the granule cell layer of the dentate gyrus, resulting eventually in complete destruction of the ipsilateral hippocampus, a feature never seen in wild-type mice. This massive destruction was brought about by neutrophils and

was mirrored by strong microglial activation reflecting exactly the entity of the damage.

Atrophied neurons are more difficult to detect due to their decreased ability to uptake standard counterstains (i.e., Cresyl violet), therefore, assessments using counts of activated microglial cells, which depict dying neurons being engulfed by phagocytic microglia, provide an accurate picture of the status of neurons after KA injection (Raivich et al., 1998). Here, we used a similar approach based on densitometric measurements of CD68-IR to indirectly measure the severity of neurodegeneration in KA-treated mice. This approach was justified by the fact that in all cases examined, there was a perfect overlap between the presence of pyknotic neurons and activated microglial cells, as seen by CD68 (as well as CD11b, Iba1, Gr-1, and F4/80) immunostaining.

This close relationship was taken as evidence that neuronal death is a consequence of microglial cell activation. In particular, expression of tissue plasminogen activator (tPA), a serine protease, by activated microglial cells has been implicated in neurodegeneration induced by stroke and KA excitotoxicity (Tsirka et al., 1995; Wang et al., 1998; Cinelli et al., 2001). However, in our hands, tPA-knockout mice are not protected against intra-hippocampal KA injection (Fritschy, unpublished). Furthermore, Siao et al. (Siao et al., 2003) demonstrated that microglia activation after intra-hippocampal KA injection depends on tPA release from injured neurons. Additional evidence in our study against a role of microglial cells in triggering neuronal death is the fact that the aggravated neurodegeneration in RAG1-KO mice is entirely dependent on neutrophil infiltration, as shown with anti-Gr-1 neutralizing antibodies (see Fig. 3.2). Therefore, in this model, we conclude that activated microglia are not the cell death executors; rather, they might promote repair by removing debris and be neuroprotective by limiting neutrophil action and possibly even phagocytosing them. In fact when microglial cells encounter compromised cells, they can act as antigen presenting cells and they can also remove sick or dying cells through the process of phagocytosis.

Clear support for this conclusion was provided by the analysis of the granule cell layer of the dentate gyrus; normally after KA injection the granule cells start to

disperse while the surrounding microglial cells remain in a “resting” state. Microglial cells are randomly arranged in the hilus and molecular layer and concentrated on the hilar and molecular layer borders of the granule cell layer, where they commonly display a fusiform morphology instead of a multipolar shape (Shapiro et al., 2009). When granule cells of the dentate gyrus are affected and unable to undergo dispersion, as seen after partial macrophage depletion, microglial cells become “alerted” and acquire an intermediate morphology between “resting” and “activated” (Figure 3.12). Finally, granule cell degeneration leads to pronounced microglial cell activation, possibly to limit the damage by phagocytosing the debris. The absence of microglia activation in the granule cell layer of KA-treated wild-type mice stands in contrast with the very prominent astrogliosis occurring in the dentate gyrus, which has been postulated to contribute to epileptogenesis via increased expression and function of adenosine kinase (Fedele et al., 2005).

Blood-born macrophages infiltrate the molecular layer of the lesioned hippocampus

Using F4/80 antibody, a marker of macrophages and microglial cells, we could observe the presence of large, macrophage-like, cells selectively in the dentate gyrus. Given the accumulation in the KA injected hippocampus of activated resident microglia, which are the native immune occupants of the CNS, the recruitment of additional infiltrating monocytes from the peripheral blood seems puzzling. In the absence of a marker allowing to discriminate between macrophages and microglial cells, evidence for their origin (periphery, perivascular macrophages, or microglia) was thought by pharmacological intervention. In addition, a key question was whether the infiltrating monocyte-derived macrophages contribute to repair, or represent an unavoidable detrimental response. Collectively, our results show that the population of infiltrating monocyte-derived macrophages is functionally distinct from the inflammatory resident microglia and is essential for granule cell survival in the lesioned hippocampus.

The proof that these cells are monocytes/macrophages from the blood and lymphoid system and not resident microglia or perivascular macrophages, is based on the results of the following experiments: (1) preventing entry of blood mononuclear cells into the brain; using anti α_4 integrin mAb; (2) depletion of peripheral monocytes/macrophages, using clodronate liposomes and 3) morphological analysis of macrophages compared to microglial cells. As examined 14 days post-KA in wild-type mice, the depletion of peripheral monocytes/macrophages had no effect on the lesion in CA1-CA3, but resulted in partial degeneration and decreased dispersion of dentate granule cells. Most strikingly, the reduced number of F4/80$^+$ macrophages in the dentate gyrus correlated locally with the extent of neuronal damage. Clodronate liposome treatment caused a massive reduction of F4/80$^+$ macrophages in the dentate gyrus, and replicated the granule cell degeneration and reduced dispersion seen in the previous experiment. In addition, macrophages could be detected in the meninges (data not shown), supporting our hypothesis of their blood-born origin.

The converse possibility, namely that at least part of the activated microglial cells observed in KA-injured hippocampus could originate from the periphery, was not examined in our study. However, Mildner et al. (Mildner et al., 2007) have demonstrated that recruitment of circulating Ly-6ChiCCR21 monocytes to lesioned brain areas and their differentiation into microglial cells only occur effectively upon pre-conditioning of the brain by total body irradiation.

Altogether, these results indicate that circulating monocytes penetrate into brain parenchyma following KA-induced lesion; they selectively localize in the dentate gyrus, where they exert a protective role on granule cells and facilitate their dispersion. Therefore, activation of innate immunity and brain entry of mononuclear phagocytes contribute to the pathophysiology of TLE; unexpectedly by providing protection against neurodegeneration.

Moreover, macrophages were not seen in the contralateral hippocampus, where no granule cell layer dispersion occurs or anywhere else in the brain. The effect of macrophage recruitment is local and only related to the cytoarchitectural changes occurring in the lesioned hippocampus.

The distinction between microglia and macrophages is always critical because they express identical cell surface markers reflecting their common origin. However, the level of expression can be different, as seen here with F4/80, which labels microglia with less intensity than infiltrating macrophages. Despite having the same monocytic origin, microglial cells and macrophages encompass a wide range of phenotypically and functionally distinct subpopulations (Soulet and Rivest, 2008). Indeed, in our experiments, microglial cells and macrophages exhibited clearly distinctive morphology. In particular, macrophages have a larger body, often are elongated, and their processes are fewer and thicker compared to ramified microglial cells with long and slender branches in the resting state or with a "bushy" appearance in the active state.

The role of macrophages in epilepsy is not well understood. Recent data from Schwartz et al. (Schwartz et al., 1999) related to spinal cord injury have shown that the spatial organization of infiltrating myeloid progenitors around the lesion site has a direct impact on functional indices of recovery following spinal cord injury; in another study, this group has elegantly shown that infiltrating monocyte-derived macrophages mediate a function essential for repair that cannot be provided by resident microglial cells during SCI (Shechter et al., 2009). Therefore, we speculate that the presence of macrophages in the molecular layer is beneficial for the survival of granule cells and might even promote their dispersion. These macrophages could release some trophic factors allowing granule cell survival and dispersion after KA injection. The precise mechanism of action is unclear; granule cell dispersion depends on TrkB receptor activation during the acute phase of epileptogenesis (Inoue et al., 1998) and on disrupted Reelin signaling during the latent and chronic phase after KA injection (Haas et al., 2002; Haas and Frotscher, 2009), but additional factors remain to be identified. Recently, a spectrum of activation has been described for macrophages, consisting of 2 main subgroups: inflammatory macrophages (M1) and alternatively activated macrophages (M2a, -b or –c). Each subgroup is characterized by a distinct profile of gene expression, and accordingly, each mediates and modulates different functions (Nahrendorf et al., 2007). In this respect, M1 macrophages express TNFα and iNOS and have a proteolytic activity,

while M2 macrophages possess important immunomodulatory and tissue repair and remodeling properties (Martinez et al., 2009).

Exacerbated KA-induced neurodegeneration in RAG1-KO mice is mediated by a massive infiltration of Gr-1$^+$neutrophils

The infiltration of Gr-1$^+$ neutrophils in the KA-lesioned hippocampus of RAG1-KO mice was unexpected, since these cells were never observed in wild-type mice. These data strongly suggest that neutrophils are responsible for the extensive neurodegeneration occurring during the chronic phase.

During the first 10 days after injection, the KA-induced hippocampal lesion was largely comparable in wild-type and RAG1-KO mice, indicating that the excitotoxic effects of KA were not influenced by the mutation. This conclusion is further supported by the fact that RAG2-KO mice also were similar to RAG1, despite the fact that the RAG2 gene is not expressed in the brain. Overall, however, RAG1-KO mice appeared more sensitive to KA and the dose injected had to be reduced.

Immunostaining for Gr-1, performed primarily to detect neutrophils, revealed unexpected differences between wild-type and RAG1-KO mice. In the latter, only neutrophils were seen, with negligible background in brain sections, whereas in wild-type mice Gr-1-IR also faintly labeled microglia, notably in lesioned tissue. In control experiments (unpublished), Gr-1 staining of cultured microglia was moderate in both genotypes, indicating that the difference seen *in vivo* is not related to lack of Gr-1 in RAG1-KO microglial cells. Interestingly, however, upon suppression of neutrophil infiltration, Gr-1 staining in RAG1-KO mice also labeled activated microglial cells, suggesting suppression of Gr-1 expression in microglia by infiltrating neutrophils.

Neutrophils were first detected in brain parenchyma of RAG1-KO mice around 10 days post-KA; signs of markedly increased neurodegeneration appeared shortly thereafter. In animals analyzed at 28 days post-KA, almost complete destruction of the hippocampus along with massive microglial cell activation were evident. The neutralization of neutrophils by repeated administration of anti-Gr-1 IgGs provided compelling evidence that these cells are directly responsible for the

aggravated damage seen in RAG1-KO mice. Indeed, the depletion of neutrophils during the second week after KA treatment in immunodeficient mice was sufficient to revert the severity and pattern of the lesion to those seen in wild-type mice (see Fig. 3.2). Importantly, neutrophil depletion in wild-type mice did not cause any changes either in the cytoarchitecture of the hippocampal formation and /or T cell recruitment compared to mice treated with KA only, indicating that peripheral neutrophils play no detectable role in the progression of the lesion during the latent phase. These findings stand at odds with the conclusions of Fabene et al. (Fabene et al., 2008) who showed that anti-Gr-1 treatment suppressed SE and reduced SRS in the pilocarpine mouse model. This difference is likely due to the fact that pilocarpine itself alters BBB permeability and causes an array of effects on peripheral immune cells (see next section).

Abundant evidence exists that extravasation of leukocytes into the injured tissue and inflammatory responses are mounted within the CNS after cerebral ischemia and SCI (Neumann et al., 2008; Stirling et al., 2009). However, in these models, a robust neutrophil response is induced acutely; within 6-24 hours. Moreover post-ischemic inflammation comprises together with neutrophil infiltration, strong microglial cell activation along with expression of pro-inflammatory cytokines and chemokines, adhesion molecules, and other inflammatory mediators (Dirnagl et al., 1999; Feuerstein and Wang, 2001). It is suggested that activated neutrophils contribute to tissue damage by release of oxygen radicals, proteases, and pro-inflammatory cytokines (Barone et al., 1991).

Moreover, *in vivo* studies strongly correlate the degree of neutrophil infiltration to the size of the neuronal damage (Beray-Berthat et al., 2003; Weston et al., 2007). Another study reported a positive correlation between the intensity of myeloperoxidase staining, a hallmark of neutrophil activity, and the degree of neuronal damage in the area of ischemia (Matsuo et al., 1994). This finding supports the view that neutrophils are critically involved in the progress of post-ischemic neuronal damage. As evidence, experimental strategies to suppress neutrophil infiltration into the injured brain parenchyma are neuroprotective (Beray-Berthat et al., 2003; Miljkovic-Lolic et al., 2003), whereas Neumann et al.

(Neumann et al., 2008) demonstrated in an *ex vivo* model of neuroinflammation that microglial cells were effective in phagocytosing invading neutrophils.

Similarly, high resolution confocal laser scanning microscopy analysis of neutrophil-microglia interactions in KA-treated tissue showed that microglia establish direct contact with neutrophils and even engulf them entirely, suggesting phagocytosis in the inflamed tissue.

Altogether, our results demonstrate that in the absence of T cell-mediated adaptive immunity, cells of the innate immunity like neutrophils can invade the lesioned hippocampus and aggravate the long-term degeneration of the epileptic hippocampus. Therefore, the integrity of the immune system is critical for the pathogenesis of TLE and the interplay between innate and adaptive immunity is a crucial point associated with the neuronal damage occurring in our model of epilepsy.

Leukocyte-endothelial interaction as a key factor of immune cell infiltration in the injured brain parenchyma

CNS inflammation is associated with breakdown of the BBB, and BBB leakage has been implicated both in the induction of seizures and in the progression to epilepsy (Seiffert et al., 2004; Marchi et al., 2007a). Leukocyte recruitment is a hallmark of and a point of therapeutic intervention in tissue inflammation (Ransohoff et al., 2003; Luster et al., 2005) but a role for leukocyte-endothelial interactions in seizure pathogenesis is not well understood. Fabene et al. (Fabene et al., 2008) challenged traditional concepts and provided compelling evidence that a key epileptogenic process may actually begin in the blood vessels. They used the pilocarpine mouse model of SE to determine whether leukocyte-endothelial interactions are altered by SE and contribute to chronic seizure pathogenesis and epilepsy. After pilocarpine administration, these researchers noticed increased expression of cell adhesion molecules (specifically VCAM-1, P-selectin, E-selectin) in brain blood vessels, which are important mediators for leukocyte extravasation during inflammatory processes. They demonstrated that SE does not occur in wild-type mice pretreated with an anti-α_4 integrin antibody,

which prevent the adhesion of leukocytes to VCAM-1 on endothelium. These findings indicate that seizure activity is associated with leukocytic inflammatory changes in the CNS vasculature in the pilocarpine mouse model of TLE.

In our experiments, we used anti-α_4 integrin and clodronate liposome treatments in wild-type and RAG1-KO KA-treated mice in order to interfere with the intra-parenchymal infiltration of lymphocytes and macrophages, respectively. Interestingly, the outcome of the two treatments was very similar, albeit causing opposite between the two genotypes. Thus, the KA-induced lesion was overall more pronounced in wild-type mice, whereas the severe neurodegeneration usually seen in RAG1-KO mice was prevented. As discussed above, these effects were explained by absence of neutrophils and concomitant suppression of neuroprotective action by macrophages. However, control experiments using an isotype antibody (for α_4 integrin) and empty liposomes (clodronate liposomes) are needed to validate our data.

The widespread effects of anti-α_4 integrin treatment on neutrophil and macrophage infiltration into the KA-treated hippocampus corroborate reports that these cells rely on similar interactions with vascular endothelial cells as lymphocytes (Johnston and Kubes, 1999). However, we can not exclude that anti-α_4 integrin mAb treatment interefered with neutrophil recruitment through other mechanisms. More unexpected was the finding that clodronate liposome treatment not only depleted macrophages but also interfered with neutrophil recruitment in RAG1-KO mice. The nature of this interference is not clear, especially since macrophages are also reduced in number in the dentate gyrus of RAG1-KO mice infiltrated with neutrophils. We speculate that the depletion of macrophages in the periphery of immunodeficient mice might affect signals and soluble mediators involved in the recruitment of neutrophils.

Since adhesion molecules are only minimally expressed in naive mice and given the fact that antibodies to not act in the absence of its target protein, the results obtained by Fabene et al. (Fabene et al., 2008) indicate that VCAM-1 is likely up-regulated before the onset of SE, possibly by pilocarpine itself. Immunohistochemical analysis of endothelial adhesion molecules (VCAM-1 and ICAM-1) in wild-type and RAG1-KO after KA injection revealed strongly increased

expression along brain blood vessels in the lesioned hippocampus, but no detectable differences between genotypes (unpublished results). Therefore, like systemic pilocarpine, KA injection is likely to cause a transient increase in BBB permeability.

The existence of a latent phase of epileptogenesis in KA-treated mice depends on the integrity of $CD3^+$ T cell-mediated adaptive immunity

To complement our morphological data and provide insight into their functional significance, we investigated whether activation of the adaptive and innate immunity contributes to epileptogenesis and onset of SRS in this mouse model of TLE. According to Fabene et al. (Fabene et al., 2008), seizure activity is associated with leukocytic inflammatory changes in the CNS vasculature and blockade or deficiency of leukocyte adhesion mechanisms effectively prevents the occurrence of SRS. A limitation in our mouse model is that we were not able to test the effect of anti-Gr-1, anti-α_4 integrin, and clodronate liposome treatment on seizure activity, notably in RAG1-KO mice, because the combined intra-hippocampal injection of KA, electrode implantation/EEG recording, and recurrent systemic administration of antibodies/liposomes would not have been tolerated by these immunodeficient mice.

To overcome this problem we investigated epileptogenesis in different lines of immunodeficient mice from five different genotypes, in addition to wild-type mice (C57BL/6J, RAG1-KO, RAG2-KO Balb/C and C57BL/6, β2-microglobulin-KO, MHC II-KO), focusing on the functional relevance of leukocyte infiltration into the KA-treated hippocampus. As reported previously for NMRI mice (Riban et al., 2002), the appearance of paroxysmal discharges in C57BL/6J mice occurred after a 2 weeks latent period suggesting that a critical period of reorganization of hippocampal circuits is needed in order to lead to the onset of recurrent seizures. Strikingly, characteristic hippocampal paroxysmal discharges were recorded already during the recording session in RAG1- and RAG2-KO mice, as early as 2 days post-KA injection, indicating a dramatic shortening of the latent phase.

These results suggest that the existence of a latent phase of epileptogenesis is related to the integrity of the adaptive immune system in this TLE model. Deletion of the RAG1 gene is sufficient for curtailing the latent phase, even though this mutation selectively affects maturation of lymphocytes. Furthermore, these results suggest that synaptic reorganization in the lesioned hippocampus, notably mossy fiber sprouting (Bouilleret et al., 1999), is not necessary for the emergence and expression of hippocampal paroxysmal discharges. Intrahippocampal EEG recordings of mice lacking a subset of $CD3^+$ T cells ($CD4^+$ T cells in MHC II-KO and $CD8^+$ T cells in β2-microglobulin-KO) were analyzed to understand which of these two cell populations is implicated in the abolition of the latent phase. Surprisingly, a subset of MHC II-KO mice are resistant to seizures and the others show few seizures, but already at day 2 post-KA; in addition, β2m-KO mice also exhibit premature seizure onset, but their frequency decreased over time.

The interpretation of these results is complicated by the fact that MHC II-KO and β2-microglobulin-KO mice cannot be considered simply as lacking a subset of T cells. Rather, multiple cytokines and chemokines produced by $CD4^+$ and $CD8^+$ cells, respectively that influence the maturation and production of other cells types are lacking, as well. Furthermore, the role of MHC class II molecules, which are expressed for instance on dendritic cells, microglial cells, and macrophages is not known in the context of epileptogenesis. Understanding which soluble factors, cytokines and chemokines, are produced either in wild-type or RAG1-KO mice and that are responsible for the leukocyte recruitment detected in these genotypes after KA-injection, would unravel new aspect and faces of the role of inflammatory mechanisms in temporal lobe epilepsy.

Chemokine and cytokine expression

Several inflammatory mediators, such as pro-inflammatory cytokines/chemokines as a hallmark of brain inflammation, are expressed in activated glial cells in various experimental models of seizures and in human epilepsies (Vezzani et al., 2008). For instance, experimental data on limbic seizures in rodents (Vezzani et al., 2002) showed that limbic seizures rapidly and transiently enhance IL-1β, IL-6,

and TNFα mRNA in the hippocampus with a peak effect at 6 h after SE; immunoreactivity of the various cytokines was increased in glial cells.

Here, we used Luminex xMAP technology in order to understand which kind of cytokines or chemokines is implicated as a driving force behind leukocyte recruitment to the hippocampus and microglial cell activation. Despite the fact that the Luminex xMap technology is very sensitive to detect multiple analytes in a single sample, this biochemical approach was limited in our hands to determine which cytokines might be implicated in the pathological changes observed in the TLE model, and in particular, in the exceptionally rapid epileptogenesis occurring in RAG1-KO mice, because information about appropriate time-points for analysis is not available. We detected IL-1α, IL-1β, MIP-1α, IL-10, IL-17, MCP-1, IL-6, KC and VEGF in hippocampal tissue homogenates but overall there was no significant difference between the different time-points analyzed and genotypes. Interestingly, differences in basal cytokines expression level between genotypes, notably in IL-1β, MIP1-α, IL-17, IL-6 and KC were abolished at the two time-points examined in the ipsilateral, KA-injected hippocampus. However, we cannot exclude that major changes in expression of these mediators might have occurred earlier or was missed in our samples for technical reasons.

The absence of modulation of MCP-1, which is a key mediator of macrophage recruitment to the site of injury, and KC, which is involved in chemotaxis and activation of neutrophils, underscore the likelihood that earlier time-points should be examined in this model for understanding the mechanisms underlying macrophage and neutrophil recruitment into the lesioned hippocampal formation.

IL-6 affects neuromodulation and also plays a protective role against various noxious conditions. Biber et al. have demonstrated that IL-6 increases the expression and function of the neuronal adenosine A_1 receptor, with relevant consequences to synaptic transmission and neuroprotection (Biber et al., 2008). Our TLE mouse model is characterized by a profound and essentially irreversible loss in the pyramidal cell layer of CA1-CA3, therefore G protein coupled receptor like the neuronal A_1 receptor most likely disappeared completely in these areas and therefore were not able to respond to neuromodulators like IL-6. It has been

shown that rapid and long-term alterations of hippocampal $GABA_B$ receptors occur in the KA mouse model of TLE; in particular, a striking finding was the almost complete and irreversible loss of $GABA_B$ receptor subunit staining in the KA-lesioned areas within 24 hours of injection (Straessle et al., 2003).

Proposed model for the role of leukocyte trafficking in the KA mouse model

The KA mouse model of TLE was used in these studies because it mimics major pathophysiological features of MTLE (degeneration in CA1 and hilar neurons, extensive astrogliosis, and occurrence of focal SRS after a latent phase of epileptogenesis). The recruitment of T cells in the lesioned hippocampus along with microglial cell activation represent here neuroprotective factors aiming to protect the hippocampal formation from further damage: T cell by excluding neutrophil infiltration and microglial cells by phagocyting the debris of dying neurons. Indeed, the absence of T cells in immunodeficient mice aggravates the long-term degeneration of the epileptic hippocampus because it allows invasion of the lesioned hippocampus by neutrophils. Furthermore, circulating monocytes-macrophages penetrate into brain parenchyma following KA-induced lesion; they selectively localize in the dentate gyrus, where they exert a protective role on granule cells and facilitate their dispersion. None of these events influences the pattern and time-course of neurodegeneration caused by KA in CA1, CA3c, and the hilus. However, this damage likely contributes to a local inflammation affecting vascular endothelial cells, thereby allowing cellular interactions required for brain infiltration. Based on the presence of leukocytes in tissue resected from patients with intractable MTLE, a similar cascade of events might be operant and contribute to the long term preservation of the dentate gyrus and CA3a,b areas.

Future directions

Our results have immediate consequences for studies of the pathophysiology of TLE, mechanisms of epileptogenesis, and design of therapeutic strategies. In particular, leukocyte recruitment is a hallmark of and a point of therapeutic

intervention in tissue inflammation, but the role for innate and adaptive immune cells in seizures pathogenesis has not been explored.

The results of our pharmacological interventions to prevent neutrophil and macrophage infiltration into the KA-lesioned hippocampal formation need to be consolidated by a set of control experiments, in particular using non-immunogenic isotype-specific mAbs to control for the effects of anti-Gr-1 and anti-α4 integrin neutralization. This second control will be crucial to determine whether blockade of neutrophil infiltration upon anti-α4 integrin treatment was due to non-specific effects of the mAb. Likewise, mice treated with "empty" liposomes will need to be analyzed to demonstrate the specificity of the clodronate effects.

Our present EEG recordings in the various lines of immunodeficient mice show the occurrence of hippocampal paroxysmal discharges already at day 2 post-KA injection. It is known that immune responses in the CNS are a critical first line defense against injury but how this could be correlated with the onset of hippocampal paroxysmal discharges is not clear. It would be of major interest to understand which specific immune cell populations are involved in the process of epileptogenesis and to explore the consequences of acute immunosuppression during KA-induced SE on the timing of seizure onset in wild-type mice.

For the first question, a possible approach is represented by adoptive transfer of $CD4^+$ and or $CD8^+$ T cells in immunodeficient mice in the TLE model. The goal would be to understand which one of the immune cell populations is involved in the abolition of the latent phase normally seen in wild-type mice after KA injection. However, we have to keep in mind that the immune system comprizes numerous cell populations and soluble factors (chemokines and cytokines) that interact together and influence their own environment. The transfer of a specific cell population in immunodeficient mice along with all the cytokines and chemokines they release represents more than introducing only the cell population by itself. The second question could be addressed by using immune-suppressant drug therapy during the early latent phase while daily monitoring seizure activity.

It is clear that a better understanding of the role of microglia, macrophages and lymphocytes in the brain during epilepsy is required. Moreover, we have to unravel the mechanisms by which these cells are recruited in a more efficient manner without having side effects associated with their inflammatory characteristics. It is also crucial to unravel how macrophages selectively infiltrate into the lesioned hippocampus and provide essential support for granule cell survival. In particular, definite proof that peripheral monocytes/macrophages migrate in the dentate gyrus after KA injection could be provided by adoptive transfer of monocytes expressing eGFP. Furthermore, the precise time sequence of lymphocyte and macrophage infiltration during the latent phase, especially in relation to VEGF-mediated compromission of BBB permeability, should be determined to better understand the early mechanisms involved in these processes.

Ultimately, the recognition that inflammation might be beneficial under specific circumstances implies that appropriate therapy targeting specific immunomodulators holds great potential to limit CNS injury and degeneration across a variety of disorders, including those not classically associated with inflammation, such epilepsy. Therefore, better understanding of the intricate relationships between innate and adaptive immunity is a prerequisite for moving into this promising new field of pharmacology.

References

(1993) Guidelines for epidemiologic studies on epilepsy. Commission on Epidemiology and Prognosis, International League Against Epilepsy. Epilepsia 34:592-596.
Alexander C, Rietschel ET (2001) Bacterial lipopolysaccharides and innate immunity. J Endotoxin Res 7:167-202.
Aloisi F, Serafini B, Adorini L (2000) Glia-T cell dialogue. J Neuroimmunol 107:111-117.
Antonucci F, Bozzi Y, Caleo M (2009) Intrahippocampal infusion of botulinum neurotoxin E (BoNT/E) reduces spontaneous recurrent seizures in a mouse model of mesial temporal lobe epilepsy. Epilepsia 50:963-966.
Antonucci F, Di Garbo A, Novelli E, Manno I, Sartucci F, Bozzi Y, Caleo M (2008) Botulinum neurotoxin E (BoNT/E) reduces CA1 neuron loss and granule cell dispersion, with no effects on chronic seizures, in a mouse model of temporal lobe epilepsy. Exp Neurol 210:388-401.
Arabadzisz D, Antal K, Parpan F, Emri Z, Fritschy JM (2005) Epileptogenesis and chronic seizures in a mouse model of temporal lobe epilepsy are associated with distinct EEG patterns and selective neurochemical alterations in the contralateral hippocampus. Exp Neurol 194:76-90.
Barone FC, Hillegass LM, Price WJ, White RF, Lee EV, Feuerstein GZ, Sarau HM, Clark RK, Griswold DE (1991) Polymorphonuclear leukocyte infiltration into cerebral focal ischemic tissue: myeloperoxidase activity assay and histologic verification. J Neurosci Res 29:336-345.
Batchelor PE, Liberatore GT, Wong JY, Porritt MJ, Frerichs F, Donnan GA, Howells DW (1999) Activated macrophages and microglia induce dopaminergic sprouting in the injured striatum and express brain-derived neurotrophic factor and glial cell line-derived neurotrophic factor. J Neurosci 19:1708-1716.
Beray-Berthat V, Croci N, Plotkine M, Margaill I (2003) Polymorphonuclear neutrophils contribute to infarction and oxidative stress in the cortex but not in the striatum after ischemia-reperfusion in rats. Brain Res 987:32-38.
Biber K, Pinto-Duarte A, Wittendorp MC, Dolga AM, Fernandes CC, Von Frijtag Drabbe Kunzel J, Keijser JN, de Vries R, Ijzerman AP, Ribeiro JA, Eisel U, Sebastiao AM, Boddeke HW (2008) Interleukin-6 upregulates neuronal adenosine A1 receptors: implications for neuromodulation and neuroprotection. Neuropsychopharmacology 33:2237-2250.
Block ML, Zecca L, Hong JS (2007) Microglia-mediated neurotoxicity: uncovering the molecular mechanisms. Nat Rev Neurosci 8:57-69.
Boison D (2006) Adenosine kinase, epilepsy and stroke: mechanisms and therapies. Trends Pharmacol Sci 27:652-658.
Boscia F, Esposito CL, Di Crisci A, de Franciscis V, Annunziato L, Cerchia L (2009) GDNF selectively induces microglial activation and neuronal survival in CA1/CA3 hippocampal regions exposed to NMDA insult through Ret/ERK signalling. PLoS One 4:e6486.
Bouilleret V, Loup F, Kiener T, Marescaux C, Fritschy JM (2000) Early loss of interneurons and delayed subunit-specific changes in GABA(A)-receptor expression in a mouse model of mesial temporal lobe epilepsy. Hippocampus 10:305-324.

Bouilleret V, Ridoux V, Depaulis A, Marescaux C, Nehlig A, Le Gal La Salle G (1999) Recurrent seizures and hippocampal sclerosis following intrahippocampal kainate injection in adult mice: electroencephalography, histopathology and synaptic reorganization similar to mesial temporal lobe epilepsy. Neuroscience 89:717-729.

Browne TR, Holmes GL (2001) Epilepsy. N Engl J Med 344:1145-1151.

Bulloch K, Miller MM, Gal-Toth J, Milner TA, Gottfried-Blackmore A, Waters EM, Kaunzner UW, Liu K, Lindquist R, Nussenzweig MC, Steinman RM, McEwen BS (2008) CD11c/EYFP transgene illuminates a discrete network of dendritic cells within the embryonic, neonatal, adult, and injured mouse brain. J Comp Neurol 508:687-710.

Byram SC, Carson MJ, DeBoy CA, Serpe CJ, Sanders VM, Jones KJ (2004) CD4-positive T cell-mediated neuroprotection requires dual compartment antigen presentation. J Neurosci 24:4333-4339.

Cacheaux LP, Ivens S, David Y, Lakhter AJ, Bar-Klein G, Shapira M, Heinemann U, Friedman A, Kaufer D (2009) Transcriptome profiling reveals TGF-beta signaling involvement in epileptogenesis. J Neurosci 29:8927-8935.

Cavalheiro EA, Leite JP, Bortolotto ZA, Turski WA, Ikonomidou C, Turski L (1991) Long-term effects of pilocarpine in rats: structural damage of the brain triggers kindling and spontaneous recurrent seizures. Epilepsia 32:778-782.

Chun JJ, Schatz DG, Oettinger MA, Jaenisch R, Baltimore D (1991) The recombination activating gene-1 (RAG-1) transcript is present in the murine central nervous system. Cell 64:189-200.

Cinelli P, Madani R, Tsuzuki N, Vallet P, Arras M, Zhao CN, Osterwalder T, Rulicke T, Sonderegger P (2001) Neuroserpin, a neuroprotective factor in focal ischemic stroke. Mol Cell Neurosci 18:443-457.

Colmers WF, El Bahh B (2003) Neuropeptide Y and Epilepsy. Epilepsy Curr 3:53-58.

de Lanerolle NC, Lee TS (2005) New facets of the neuropathology and molecular profile of human temporal lobe epilepsy. Epilepsy Behav 7:190-203.

Deckers CL, Knoester PD, de Haan GJ, Keyser A, Renier WO, Hekster YA (2003) Selection criteria for the clinical use of the newer antiepileptic drugs. CNS Drugs 17:405-421.

Dirnagl U, Iadecola C, Moskowitz MA (1999) Pathobiology of ischaemic stroke: an integrated view. Trends Neurosci 22:391-397.

Dugladze T, Vida I, Tort AB, Gross A, Otahal J, Heinemann U, Kopell NJ, Gloveli T (2007) Impaired hippocampal rhythmogenesis in a mouse model of mesial temporal lobe epilepsy. Proc Natl Acad Sci U S A 104:17530-17535.

Engelhardt B (2008) Immune cell entry into the central nervous system: involvement of adhesion molecules and chemokines. J Neurol Sci 274:23-26.

Fabene PF, Navarro MG, Martinello M, Rossi B, Merigo F, Ottoboni L, Bach S, Angiari S, Benati D, Chakir A, Zanetti L, Schio F, Osculati A, Marzola P, Nicolato E, Homeister JW, Xia L, Lowe JB, McEver RP, Osculati F, Sbarbati A, Butcher EC, Constantin G (2008) A role for leukocyte-endothelial adhesion mechanisms in epilepsy. Nat Med 14:1377-1383.

Fedele DE, Gouder N, Guttinger M, Gabernet L, Scheurer L, Rulicke T, Crestani F, Boison D (2005) Astrogliosis in epilepsy leads to overexpression of adenosine kinase, resulting in seizure aggravation. Brain 128:2383-2395.

Feuerstein GZ, Wang X (2001) Inflammation and stroke: benefits without harm? Arch Neurol 58:672-674.

Fritschy JM, Mohler H (1995) GABAA-receptor heterogeneity in the adult rat brain: differential regional and cellular distribution of seven major subunits. J Comp Neurol 359:154-194.

Gibson RM, Rothwell NJ, Le Feuvre RA (2004) CNS injury: the role of the cytokine IL-1. Vet J 168:230-237.

Gouder N, Fritschy JM, Boison D (2003) Seizure suppression by adenosine A1 receptor activation in a mouse model of pharmacoresistant epilepsy. Epilepsia 44:877-885.

Gouder N, Scheurer L, Fritschy JM, Boison D (2004) Overexpression of adenosine kinase in epileptic hippocampus contributes to epileptogenesis. J Neurosci 24:692-701.

Goverman J (2009) Autoimmune T cell responses in the central nervous system. Nat Rev Immunol 9:393-407.

Ha GK, Huang Z, Streit WJ, Petitto JM (2006) Endogenous T lymphocytes and microglial reactivity in the axotomized facial motor nucleus of mice: effect of genetic background and the RAG2 gene. J Neuroimmunol 172:1-8.

Ha GK, Parikh S, Huang Z, Petitto JM (2008) Influence of injury severity on the rate and magnitude of the T lymphocyte and neuronal response to facial nerve axotomy. J Neuroimmunol 199:18-23.

Haas CA, Frotscher M (2009) Reelin deficiency causes granule cell dispersion in epilepsy. Exp Brain Res.

Haas CA, Dudeck O, Kirsch M, Huszka C, Kann G, Pollak S, Zentner J, Frotscher M (2002) Role for reelin in the development of granule cell dispersion in temporal lobe epilepsy. J Neurosci 22:5797-5802.

Hanisch UK, Kettenmann H (2007) Microglia: active sensor and versatile effector cells in the normal and pathologic brain. Nat Neurosci 10:1387-1394.

Henry CJ, Huang Y, Wynne A, Hanke M, Himler J, Bailey MT, Sheridan JF, Godbout JP (2008) Minocycline attenuates lipopolysaccharide (LPS)-induced neuroinflammation, sickness behavior, and anhedonia. J Neuroinflammation 5:15.

Heppner FL, Greter M, Marino D, Falsig J, Raivich G, Hovelmeyer N, Waisman A, Rulicke T, Prinz M, Priller J, Becher B, Aguzzi A (2005) Experimental autoimmune encephalomyelitis repressed by microglial paralysis. Nat Med 11:146-152.

Ibbotson GC, Doig C, Kaur J, Gill V, Ostrovsky L, Fairhead T, Kubes P (2001) Functional alpha4-integrin: a newly identified pathway of neutrophil recruitment in critically ill septic patients. Nat Med 7:465-470.

Inoue T, Hirai H, Onteniente B, Suzuki F (1998) Correlated long-term increase of brain-derived neurotrophic factor and Trk B proteins in enlarged granule cells of mouse hippocampus after kainic acid injection. Neuroscience 86:723-728.

Jack C, Ruffini F, Bar-Or A, Antel JP (2005) Microglia and multiple sclerosis. J Neurosci Res 81:363-373.
Jankowsky JL, Patterson PH (2001) The role of cytokines and growth factors in seizures and their sequelae. Prog Neurobiol 63:125-149.
Johnston B, Kubes P (1999) The alpha4-integrin: an alternative pathway for neutrophil recruitment? Immunol Today 20:545-550.
Kettenmann H, Verkhratsky A (2008) Neuroglia: the 150 years after. Trends Neurosci 31:653-659.
Kim SU, de Vellis J (2005) Microglia in health and disease. J Neurosci Res 81:302-313.
Kotter MR, Zhao C, van Rooijen N, Franklin RJ (2005) Macrophage-depletion induced impairment of experimental CNS remyelination is associated with a reduced oligodendrocyte progenitor cell response and altered growth factor expression. Neurobiol Dis 18:166-175.
Le Duigou C, Bouilleret V, Miles R (2008) Epileptiform activities in slices of hippocampus from mice after intra-hippocampal injection of kainic acid. J Physiol 586:4891-4904.
Le Duigou C, Wittner L, Danglot L, Miles R (2005) Effects of focal injection of kainic acid into the mouse hippocampus in vitro and ex vivo. J Physiol 569:833-847.
Ledergerber D, Fritschy JM, Kralic JE (2006) Impairment of dentate gyrus neuronal progenitor cell differentiation in a mouse model of temporal lobe epilepsy. Exp Neurol 199:130-142.
Loscher W (2002) Current status and future directions in the pharmacotherapy of epilepsy. Trends Pharmacol Sci 23:113-118.
Loup F, Wieser HG, Yonekawa Y, Aguzzi A, Fritschy JM (2000) Selective alterations in GABAA receptor subtypes in human temporal lobe epilepsy. J Neurosci 20:5401-5419.
Luster AD, Alon R, von Andrian UH (2005) Immune cell migration in inflammation: present and future therapeutic targets. Nat Immunol 6:1182-1190.
Marchi N, Oby E, Batra A, Uva L, De Curtis M, Hernandez N, Van Boxel-Dezaire A, Najm I, Janigro D (2007a) In vivo and in vitro effects of pilocarpine: relevance to ictogenesis. Epilepsia 48:1934-1946.
Marchi N, Angelov L, Masaryk T, Fazio V, Granata T, Hernandez N, Hallene K, Diglaw T, Franic L, Najm I, Janigro D (2007b) Seizure-promoting effect of blood-brain barrier disruption. Epilepsia 48:732-742.
Martinez FO, Helming L, Gordon S (2009) Alternative activation of macrophages: an immunologic functional perspective. Annu Rev Immunol 27:451-483.
Martino G, Hartung HP (1999) Immunopathogenesis of multiple sclerosis: the role of T cells. Curr Opin Neurol 12:309-321.
Matsuo Y, Onodera H, Shiga Y, Nakamura M, Ninomiya M, Kihara T, Kogure K (1994) Correlation between myeloperoxidase-quantified neutrophil accumulation and ischemic brain injury in the rat. Effects of neutrophil depletion. Stroke 25:1469-1475.
Mildner A, Schmidt H, Nitsche M, Merkler D, Hanisch UK, Mack M, Heikenwalder M, Bruck W, Priller J, Prinz M (2007) Microglia in the adult brain arise from

Ly-6ChiCCR2+ monocytes only under defined host conditions. Nat Neurosci 10:1544-1553.

Miljkovic-Lolic M, Silbergleit R, Fiskum G, Rosenthal RE (2003) Neuroprotective effects of hyperbaric oxygen treatment in experimental focal cerebral ischemia are associated with reduced brain leukocyte myeloperoxidase activity. Brain Res 971:90-94.

Mombaerts P, Iacomini J, Johnson RS, Herrup K, Tonegawa S, Papaioannou VE (1992) RAG-1-deficient mice have no mature B and T lymphocytes. Cell 68:869-877.

Muller WA (2009) Mechanisms of transendothelial migration of leukocytes. Circ Res 105:223-230.

Nahrendorf M, Swirski FK, Aikawa E, Stangenberg L, Wurdinger T, Figueiredo JL, Libby P, Weissleder R, Pittet MJ (2007) The healing myocardium sequentially mobilizes two monocyte subsets with divergent and complementary functions. J Exp Med 204:3037-3047.

Nau R, Bruck W (2002) Neuronal injury in bacterial meningitis: mechanisms and implications for therapy. Trends Neurosci 25:38-45.

Neumann J, Sauerzweig S, Ronicke R, Gunzer F, Dinkel K, Ullrich O, Gunzer M, Reymann KG (2008) Microglia cells protect neurons by direct engulfment of invading neutrophil granulocytes: a new mechanism of CNS immune privilege. J Neurosci 28:5965-5975.

Nguyen MD, Julien JP, Rivest S (2002) Innate immunity: the missing link in neuroprotection and neurodegeneration? Nat Rev Neurosci 3:216-227.

Oby E, Janigro D (2006) The blood-brain barrier and epilepsy. Epilepsia 47:1761-1774.

Owens T, Tran E, Hassan-Zahraee M, Krakowski M (1998) Immune cell entry to the CNS--a focus for immunoregulation of EAE. Res Immunol 149:781-789; discussion 844-786, 855-760.

Raivich G, Jones LL, Kloss CU, Werner A, Neumann H, Kreutzberg GW (1998) Immune surveillance in the injured nervous system: T-lymphocytes invade the axotomized mouse facial motor nucleus and aggregate around sites of neuronal degeneration. J Neurosci 18:5804-5816.

Raivich G, Bohatschek M, Werner A, Jones LL, Galiano M, Kloss CU, Zhu XZ, Pfeffer K, Liu ZQ (2003) Lymphocyte infiltration in the injured brain: role of proinflammatory cytokines. J Neurosci Res 72:726-733.

Ransohoff RM, Kivisakk P, Kidd G (2003) Three or more routes for leukocyte migration into the central nervous system. Nat Rev Immunol 3:569-581.

Ravizza T, Vezzani A (2006) Status epilepticus induces time-dependent neuronal and astrocytic expression of interleukin-1 receptor type I in the rat limbic system. Neuroscience 137:301-308.

Ravizza T, Gagliardi B, Noe F, Boer K, Aronica E, Vezzani A (2008) Innate and adaptive immunity during epileptogenesis and spontaneous seizures: evidence from experimental models and human temporal lobe epilepsy. Neurobiol Dis 29:142-160.

Riban V, Bouilleret V, Pham-Le BT, Fritschy JM, Marescaux C, Depaulis A (2002) Evolution of hippocampal epileptic activity during the development of

hippocampal sclerosis in a mouse model of temporal lobe epilepsy. Neuroscience 112:101-111.
Rivest S (2009) Regulation of innate immune responses in the brain. Nat Rev Immunol 9:429-439.
Schauwecker PE (2000) Seizure-induced neuronal death is associated with induction of c-Jun N-terminal kinase and is dependent on genetic background. Brain Res 884:116-128.
Schauwecker PE (2003) Genetic basis of kainate-induced excitotoxicity in mice: phenotypic modulation of seizure-induced cell death. Epilepsy Res 55:201-210.
Schauwecker PE, Steward O (1997) Genetic determinants of susceptibility to excitotoxic cell death: implications for gene targeting approaches. Proc Natl Acad Sci U S A 94:4103-4108.
Schwartz M (2001) Protective autoimmunity as a T-cell response to central nervous system trauma: prospects for therapeutic vaccines. Prog Neurobiol 65:489-496.
Schwartz M, Moalem G, Leibowitz-Amit R, Cohen IR (1999) Innate and adaptive immune responses can be beneficial for CNS repair. Trends Neurosci 22:295-299.
Seiffert E, Dreier JP, Ivens S, Bechmann I, Tomkins O, Heinemann U, Friedman A (2004) Lasting blood-brain barrier disruption induces epileptic focus in the rat somatosensory cortex. J Neurosci 24:7829-7836.
Serpe CJ, Kohm AP, Huppenbauer CB, Sanders VM, Jones KJ (1999) Exacerbation of facial motoneuron loss after facial nerve transection in severe combined immunodeficient (scid) mice. J Neurosci 19:RC7.
Shaftel SS, Carlson TJ, Olschowka JA, Kyrkanides S, Matousek SB, O'Banion MK (2007) Chronic interleukin-1beta expression in mouse brain leads to leukocyte infiltration and neutrophil-independent blood brain barrier permeability without overt neurodegeneration. J Neurosci 27:9301-9309.
Shapiro LA, Perez ZD, Foresti ML, Arisi GM, Ribak CE (2009) Morphological and ultrastructural features of Iba1-immunolabeled microglial cells in the hippocampal dentate gyrus. Brain Res 1266:29-36.
Shechter R, London A, Varol C, Raposo C, Cusimano M, Yovel G, Rolls A, Mack M, Pluchino S, Martino G, Jung S, Schwartz M (2009) Infiltrating blood-derived macrophages are vital cells playing an anti-inflammatory role in recovery from spinal cord injury in mice. PLoS Med 6:e1000113.
Siao CJ, Fernandez SR, Tsirka SE (2003) Cell type-specific roles for tissue plasminogen activator released by neurons or microglia after excitotoxic injury. J Neurosci 23:3234-3242.
Silverman AJ, Sutherland AK, Wilhelm M, Silver R (2000) Mast cells migrate from blood to brain. J Neurosci 20:401-408.
Simard AR, Soulet D, Gowing G, Julien JP, Rivest S (2006) Bone marrow-derived microglia play a critical role in restricting senile plaque formation in Alzheimer's disease. Neuron 49:489-502.
Sisodiya SM (2003) Mechanisms of antiepileptic drug resistance. Curr Opin Neurol 16:197-201.

Soranzo N, Goldstein DB, Sisodiya SM (2005) The role of common variation in drug transporter genes in refractory epilepsy. Expert Opin Pharmacother 6:1305-1312.

Soulet D, Rivest S (2008) Microglia. Curr Biol 18:R506-508.

Spanopoulou E, Cortes P, Shih C, Huang CM, Silver DP, Svec P, Baltimore D (1995) Localization, interaction, and RNA binding properties of the V(D)J recombination-activating proteins RAG1 and RAG2. Immunity 3:715-726.

Stirling DP, Liu S, Kubes P, Yong VW (2009) Depletion of Ly6G/Gr-1 leukocytes after spinal cord injury in mice alters wound healing and worsens neurological outcome. J Neurosci 29:753-764.

Straessle A, Loup F, Arabadzisz D, Ohning GV, Fritschy JM (2003) Rapid and long-term alterations of hippocampal GABAB receptors in a mouse model of temporal lobe epilepsy. Eur J Neurosci 18:2213-2226.

Suidan GL, Dickerson JW, Chen Y, McDole JR, Tripathi P, Pirko I, Seroogy KB, Johnson AJ (2010) CD8 T cell-initiated vascular endothelial growth factor expression promotes central nervous system vascular permeability under neuroinflammatory conditions. J Immunol 184:1031-1040.

Suzuki F, Junier MP, Guilhem D, Sorensen JC, Onteniente B (1995) Morphogenetic effect of kainate on adult hippocampal neurons associated with a prolonged expression of brain-derived neurotrophic factor. Neuroscience 64:665-674.

Tambuyzer BR, Ponsaerts P, Nouwen EJ (2009) Microglia: gatekeepers of central nervous system immunology. J Leukoc Biol 85:352-370.

Thom M (2004) Recent advances in the neuropathology of focal lesions in epilepsy. Expert Rev Neurother 4:973-984.

Tsirka SE, Gualandris A, Amaral DG, Strickland S (1995) Excitotoxin-induced neuronal degeneration and seizure are mediated by tissue plasminogen activator. Nature 377:340-344.

van Gassen KL, de Wit M, Koerkamp MJ, Rensen MG, van Rijen PC, Holstege FC, Lindhout D, de Graan PN (2008) Possible role of the innate immunity in temporal lobe epilepsy. Epilepsia 49:1055-1065.

van Vliet EA, da Costa Araujo S, Redeker S, van Schaik R, Aronica E, Gorter JA (2007) Blood-brain barrier leakage may lead to progression of temporal lobe epilepsy. Brain 130:521-534.

Vezzani A (2004) Brain Inflammation and Seizures. Epilepsy Curr 4:73-75.

Vezzani A (2005) Inflammation and epilepsy. Epilepsy Curr 5:1-6.

Vezzani A, Granata T (2005) Brain inflammation in epilepsy: experimental and clinical evidence. Epilepsia 46:1724-1743.

Vezzani A, Janigro D (2009) Leukocyte-endothelial adhesion mechanisms in epilepsy: cheers and jeers. Epilepsy Curr 9:118-121.

Vezzani A, Ravizza T, Balosso S, Aronica E (2008) Glia as a source of cytokines: implications for neuronal excitability and survival. Epilepsia 49 Suppl 2:24-32.

Vezzani A, Moneta D, Richichi C, Aliprandi M, Burrows SJ, Ravizza T, Perego C, De Simoni MG (2002) Functional role of inflammatory cytokines and antiinflammatory molecules in seizures and epileptogenesis. Epilepsia 43 Suppl 5:30-35.

Villoslada P, Moreno B, Melero I, Pablos JL, Martino G, Uccelli A, Montalban X, Avila J, Rivest S, Acarin L, Appel S, Khoury SJ, McGeer P, Ferrer I, Delgado M, Obeso J, Schwartz M (2008) Immunotherapy for neurological diseases. Clin Immunol 128:294-305.

Wang YF, Tsirka SE, Strickland S, Stieg PE, Soriano SG, Lipton SA (1998) Tissue plasminogen activator (tPA) increases neuronal damage after focal cerebral ischemia in wild-type and tPA-deficient mice. Nat Med 4:228-231.

Weston RM, Jones NM, Jarrott B, Callaway JK (2007) Inflammatory cell infiltration after endothelin-1-induced cerebral ischemia: histochemical and myeloperoxidase correlation with temporal changes in brain injury. J Cereb Blood Flow Metab 27:100-114.

Williams KC, Hickey WF (2002) Central nervous system damage, monocytes and macrophages, and neurological disorders in AIDS. Annu Rev Neurosci 25:537-562.

Yang I, Han SJ, Kaur G, Crane C, Parsa AT (2009) The role of microglia in central nervous system immunity and glioma immunology. J Clin Neurosci.

Yong VW, Rivest S (2009) Taking advantage of the systemic immune system to cure brain diseases. Neuron 64:55-60.

Ziv Y, Ron N, Butovsky O, Landa G, Sudai E, Greenberg N, Cohen H, Kipnis J, Schwartz M (2006) Immune cells contribute to the maintenance of neurogenesis and spatial learning abilities in adulthood. Nat Neurosci 9:268-275.

Abbreviations

ACSF	artificial cerebrospinal fluid
AED	antiepileptic drug
BBB	blood-brain barrier
β2m	β2-microglobulin
CA	cornu ammonis, part of the hippocampus proper
CD	cluster of differentiation
CNS	central nervous system
contra	contralateral
CXCR	CXC chemokine receptor
DG	dentate gyrus, part of the hippocampal formation
EEG	electroencephalography
GCL	granule cell layer of the dentate gyrus
G-CSF	granulocyte colony stimulating factor
GM-CSF	granulocyte-macrophage colony stimulating factor
HL	hilus, part of the hippocampal formation
HS	hippocampal sclerosis
ICAM	intercellular cell adhesion molecule
Ig	immunoglobulin
IL	interleukin
i.p.	intraperitoneal
ipsi	ipsilateral
INFγ	interferon gamma
IR	immunoreactivity
i.v.	intravenously
KA	kainic acid
KC	keratinocyte-derived chemokine
KO	knock-out
LIF	leukemia inhibitory factor
LTLE	lateral temporal lobe epilepsy

MCP	monocyte chemotactic protein
MIP	macrophage inflammatory protein
MHC	major histocompatibility complex
MS	multiple sclerosis
MTLE	mesial temporal lobe epilepsy
NaCl	sodium chloride
RAG	recombination activating gene
SCI	spinal cord injury
SE	status epilepticus
SO	stratum oriens
SP	stratum pyramidale
SRS	spontaneous recurrent seizures
SR	stratum radiatum
TLE	temporal lobe epilepsy
TNF	tumor necrosis factor
VCAM	vascular endothelial cell adhesion molecule
VEGF	vascular endothelial growth factor
WT	wild-type

Curriculum Vitae

Surname:	ZATTONI
First name:	Michela
Date of birth:	1st of March 1979
Place of origin:	Bolzano, Italia

Education

08.2006- present	PhD thesis: Department of Neurosurgery, University Hospital Zurich, Zurich, Switzerland Supervision: Prof. Dr. Jean-Marc Fritschy, Prof. Dr. Karl Frei Founding: Neuroscience Center Zurich (ZNZ), Swiss League Against Epilepsy
10.2005-08.2006	Staff Research Associate - Department of Anesthesiology, University of California San Diego, La Jolla, CA 92037 USA. Supervision: Prof. Tony Yaksh
06.2004-10.2005	Research scholar - The Burnham Institute, La Jolla, CA 92037, USA. Supervision: Prof. Giovanni Paternostro
10.1998-12.2003	Master of Science in medical Biotechnology Facoltà di Medicina e Chirurgia dell'Università degli Studi di Modena e Reggio Emilia, Italia. Final mark 110/110 cum laudae Thesis: 'Role of the transcription factor CCAAT/Enhancer Binding Protein-alpha in myeloid progenitors transformed from the oncoprotein BCR/ABL'.

	Supervision: Prof. Bruno Calabretta Research work for the thesis: Department of Microbiology and Immunology, Thomas Jefferson University, Kimmel Cancer Center, Philadelphia**,** PA, USA**.**
	Supervision: Prof. Bruno Calabretta
09.1993-07.1998	Maturità scientifica, Liceo scientifico E. Torricelli, Bolzano (BZ), Italia

List of publications

Original publications

Differential role of spinal p38a and b MAPK in inflammation-induced hyperalgesia and spinal COX-2 expression. Bethany L. Fitzsimmons[1], Michela Zattoni[1#], Camilla I. Svensson[^], Joanne Steinauer**,** Xiao-Ying Hua and Tony L. Yaksh (2009 in preparation)

Svensson CI, **Zattoni M**, Serhan CN (2007) Lipoxins and aspirin-triggered lipoxin inhibit inflammatory pain process. J Exp Med. 204(2):245-252.

Ferrari-Amorotti G, Keeshan K, **Zattoni M**, Guerzoni C, Iotti G, Cattelani S, Donato NJ, Calabretta B (2006) Leukemogenesis induced by wild-type and STI571-resistant BCR/ABL is potently suppressed by C/EBPalpha. Blood 108(4):1353-1362.

Abstracts for posters

Swiss Society for Neuroscience NCCR "Neural Plasticity and Repair" Swiss Multiple Sclerosis Society, March 9-10, 2007, University of Berne

Impact of inflammatory cytokines on astrocytic glutamate transporters and glutamine synthetase and their role in temporal lobe epilepsy.

***Zattoni M**, Lachos J, Wieser HG, Yonekawa Y, Frei K. (2007)*

6th FENS Forum of European Neuroscience, Geneva, Switzerland July 12-16, 2008

Immune system and epilepsy: is there a crucial interaction?

***Zattoni M**, Fritschy JM and Frei K. (2008)*

Annual meeting 2008 of the Swiss Society of Experimental Pharmacology, University of Zurich, Switzerland August 29, 2008

Immune system and epilepsy: is there a crucial interaction?

***Zattoni M**, Fritschy JM and Frei K. (Version 2) (2008)*

Swiss Society for Neuroscience, SSN Annual Meeting 2009, University of Fribourg, Switzerland 14th of March 2009

What is the role of leukocytes during epileptogenesis?

***Zattoni M**, Mura ML, Frei K. and Fritschy JM.*

Society for Neuroscience SfN Chicago October 17-21, 2009

Absence of T-cells aggravates epileptogenesis and neurodegeneration in a mouse model of temporal lobe epilepsy (TLE)

***Zattoni M**, Mura ML, Fritschy JM. and Frei K.*

Abstract for talk

Spring hippocampal research conference, Verona, Italy, 14-19 June 2009

Contribution of CD3-positive T-cells to seizures and epileptogenesis.

ACKNOWLEDGEMENTS

My warm and sincere thank goes to all the people that supported me to accomplish my PhD thesis. To all those, who helped me in the difficult moments, who advised, believed in me and made this experience a great life experience.

I would like to thank Prof. Karl Frei who gave me the opportunity to come to Zurich, to work in his group and doing my PhD. Thanks for all the advice and for having always believed in me.

My sincere gratitude goes to Prof. Jean-Marc Fritschy who gave me the opportunity to join his admirable group. “Grazie mille” for your great supervision, for always having time for me, even during crazy and busy periods. Thanks for all the advice, for teaching me every day something new about the extraordinary field of neuroscience.

Thanks to all the members of the lab (past and present), the Fritschy group, not only for scientific support but also for the great and friendly atmosphere in and outside of the lab. Danke Martina for teaching me the kainate injection and electrodes implantation; it was a great start.

A special and warm thanks to Ako, Ale, Mari and Mary, my Swiss-Japanese-Italian-Kenyan friends for sharing good and bad moments, but especially for being my friends. You girls are the best.

Many thanks to Francine, my first master student; it was a pleasure to work with you; you are an eager student and a very friendly person.

Big thanks go to my husband Raffaele; who supported, encouraged and advised me throughout these years; it was fundamental having you beside me for the achievement of my goals.

Furthermore, I thank my family (mamma, papa’ and sister); you are always there for me; you supported me throughout my whole life and made it possible that I could freely choose the direction of my own life.